



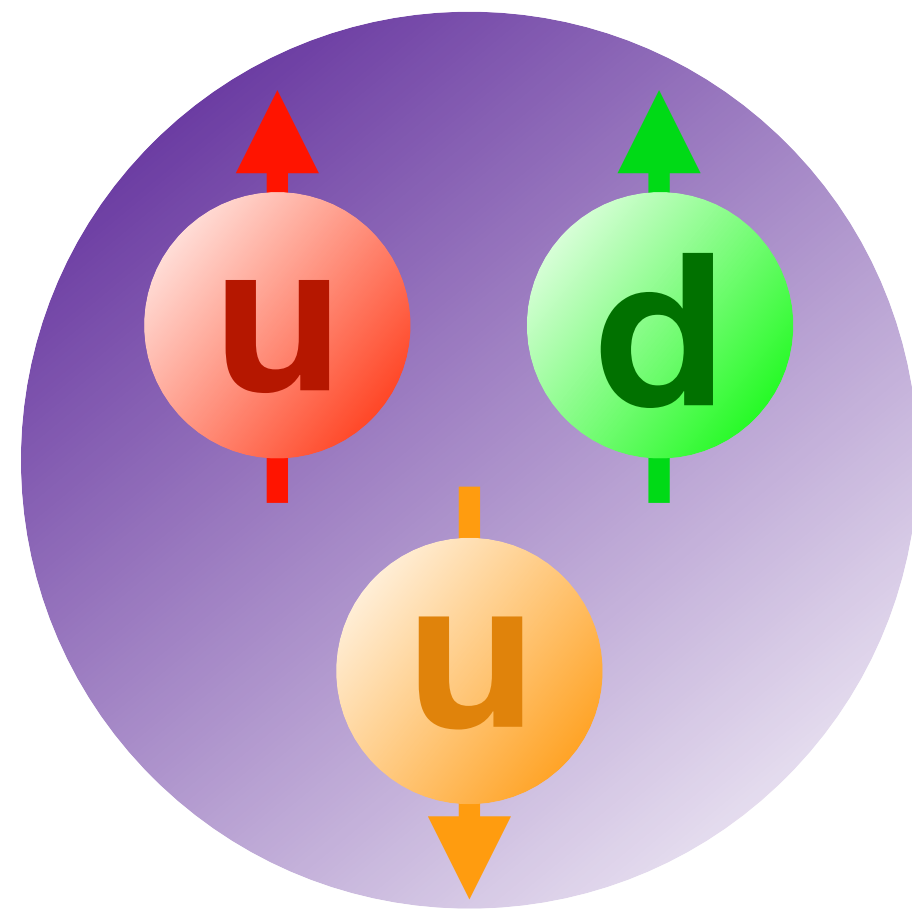
Upcoming Measurements of the $N \rightarrow \Delta$ Transition Form Factors at Jefferson Lab

Low-q workshop, Island of Crete, Greece, May 19 2023

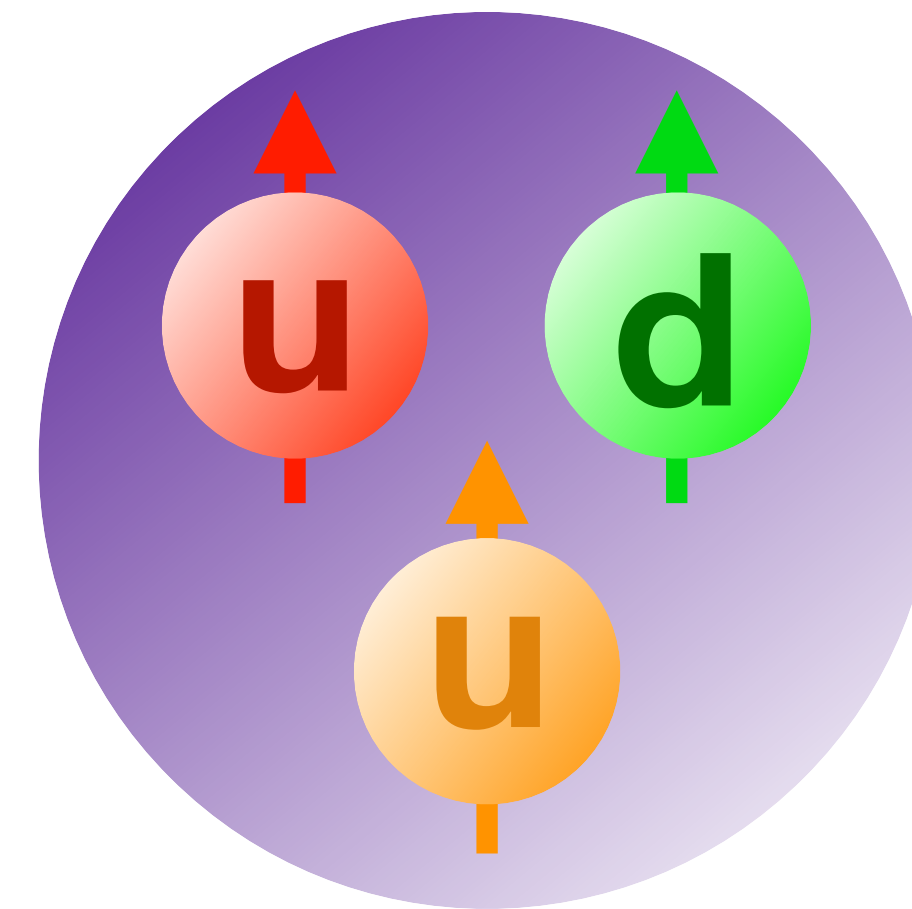
Michael Paolone, New Mexico State University

The N- Δ transition

Proton (938 MeV)



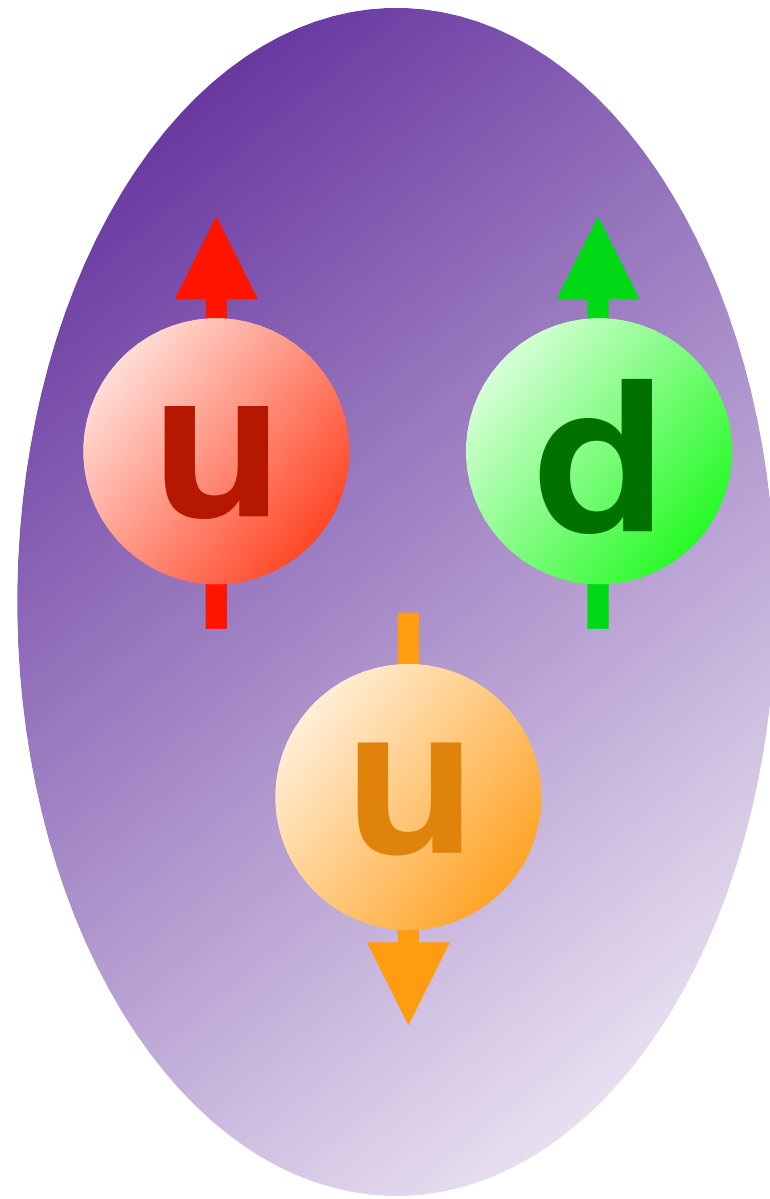
Delta (1232 MeV)



**The dominant transition from proton to delta involves a dipole (M1) transition
(spherical S-wave proton WF \rightarrow spherical S-wave Delta WF)**

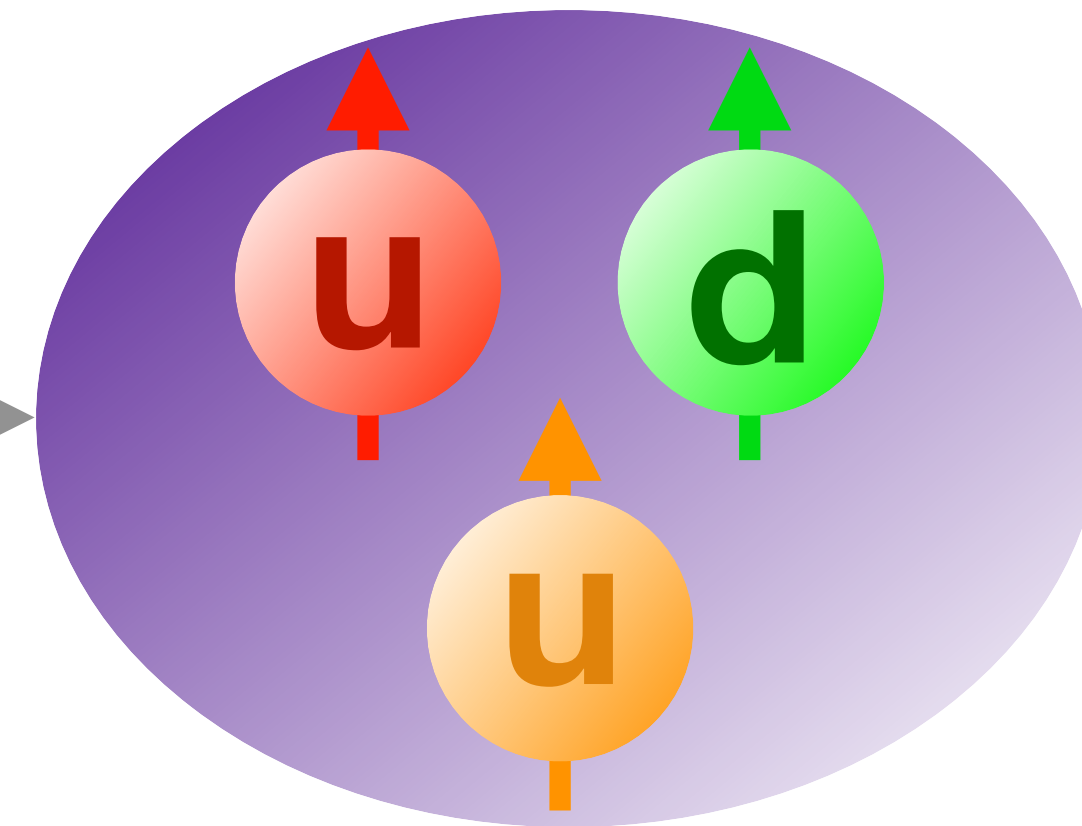

The N- Δ transition

Proton (938 MeV)



Delta (1232 MeV)

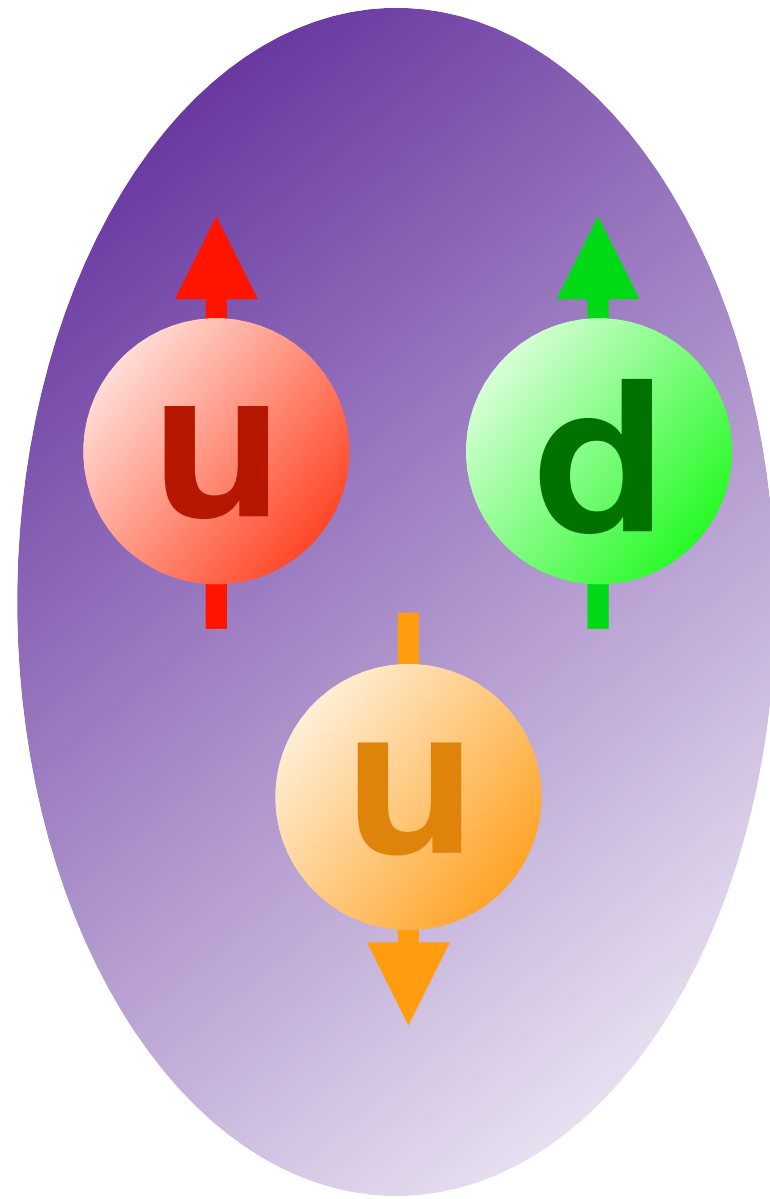
γ^* , E2, C2



**There also exists a quadrupole (E2 or C2) transition from proton to delta.
(The quadrupole amplitudes are associated with the existence of non-spherical
components in the proton and Delta WF)**

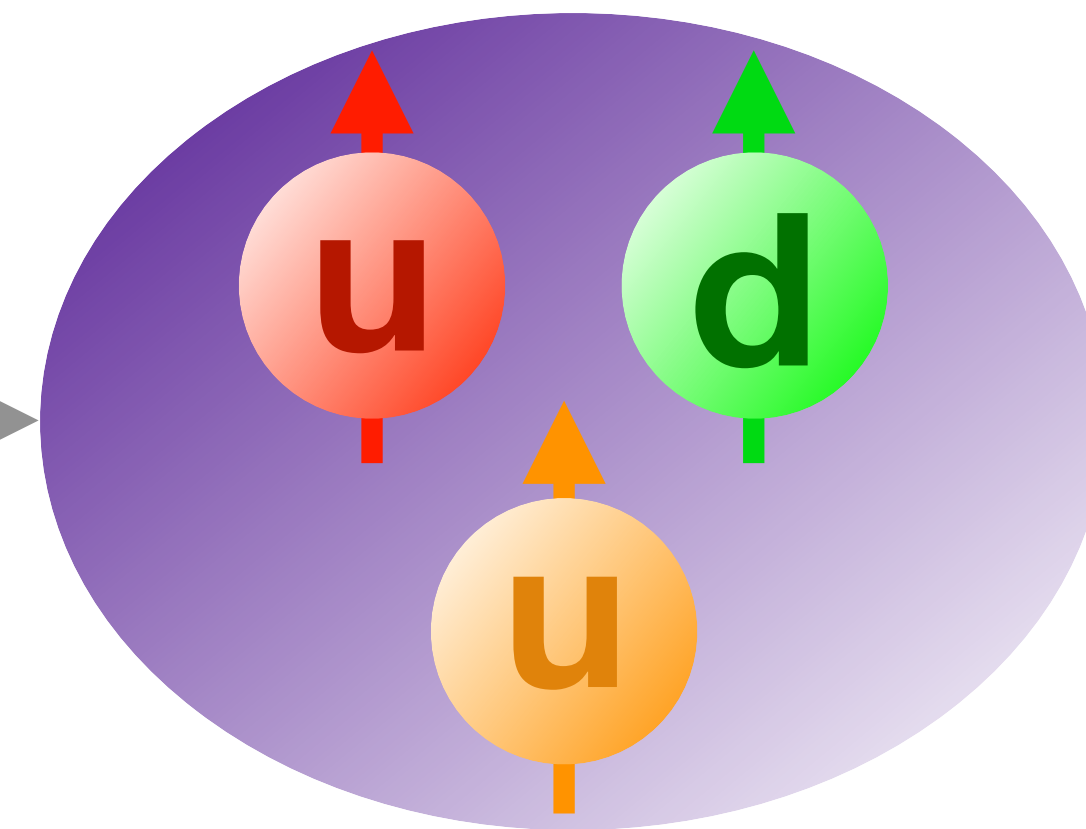
The N - Δ transition

Proton (938 MeV)



Delta (1232 MeV)

γ^* , E2, C2



There also exists a quadrupole (E2 or C2) transition from proton to delta.
(The quadrupole amplitudes are associated with the existence of non-spherical components in the proton and Delta WF)

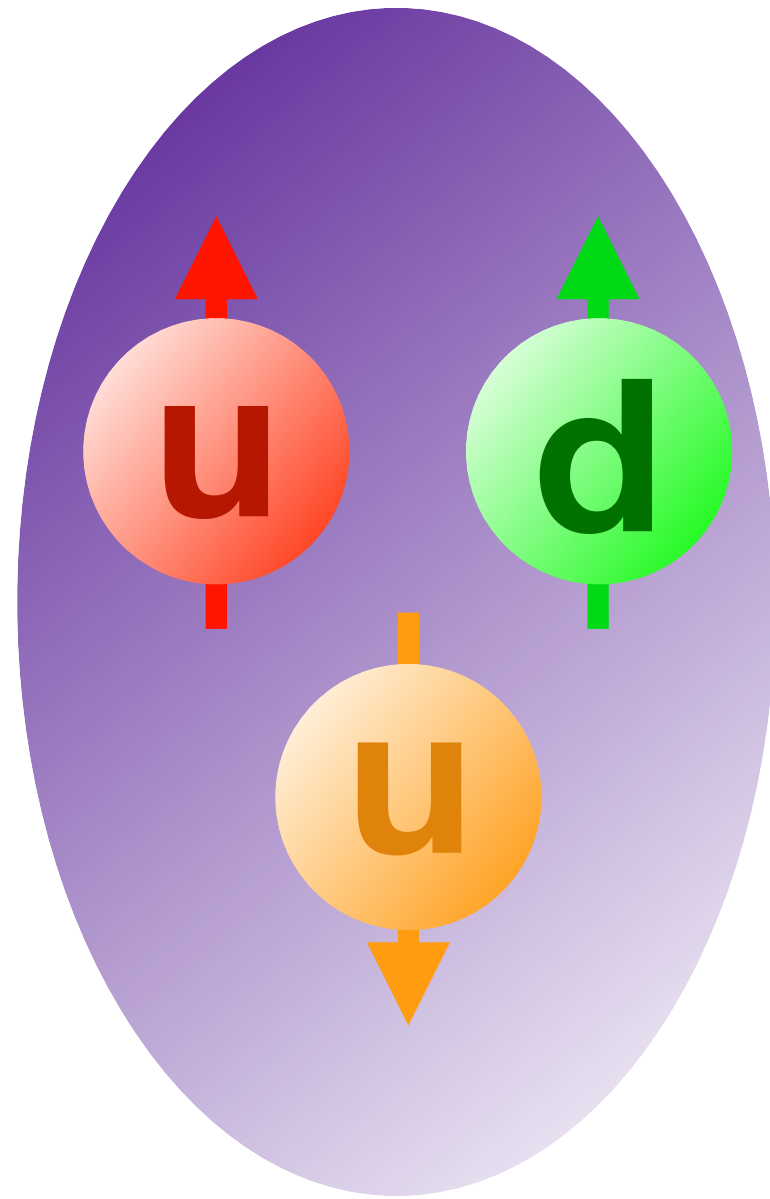
The quadrupole to dipole ratio (**E2/M1** or **C2/M1**) is non-zero... Why?

Electric-Quadrupole to **M**agnetic-Dipole **R**atio = **EMR** = **E2/M1**

Coulomb-Quadrupole to **M**agnetic-Dipole **R**atio = **CMR** = **C2/M1**

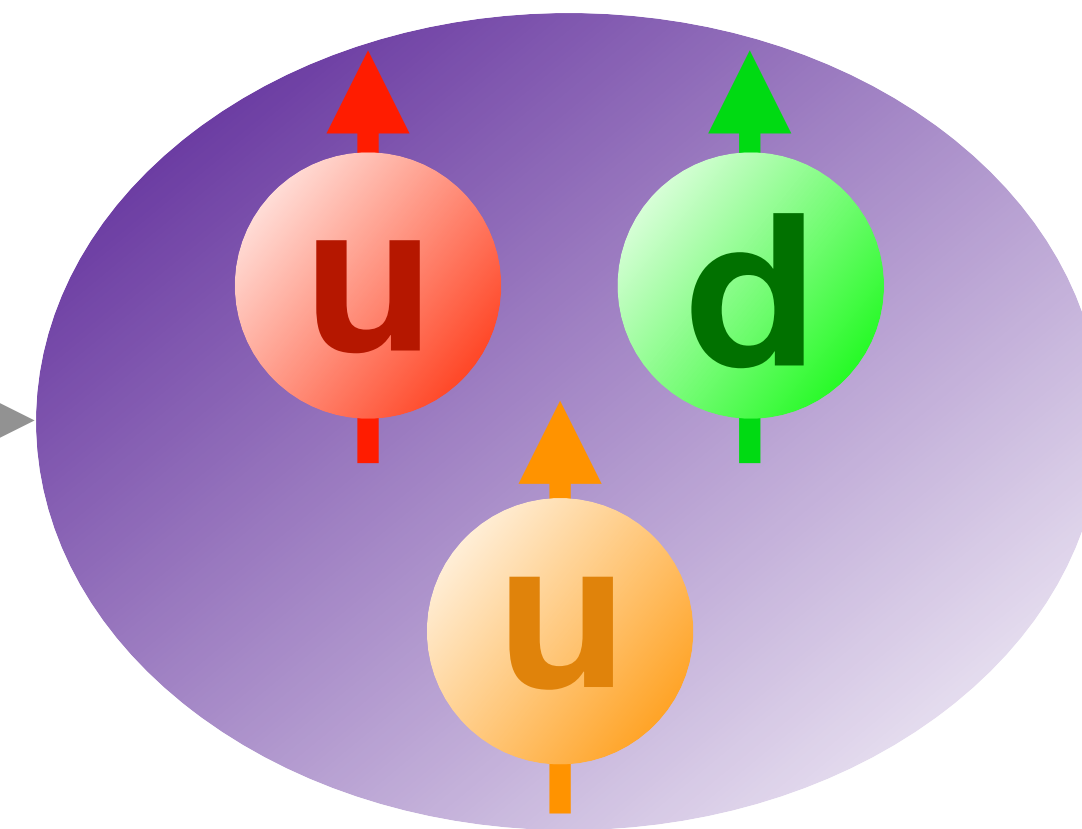
The N - Δ transition

Proton (938 MeV)



Delta (1232 MeV)

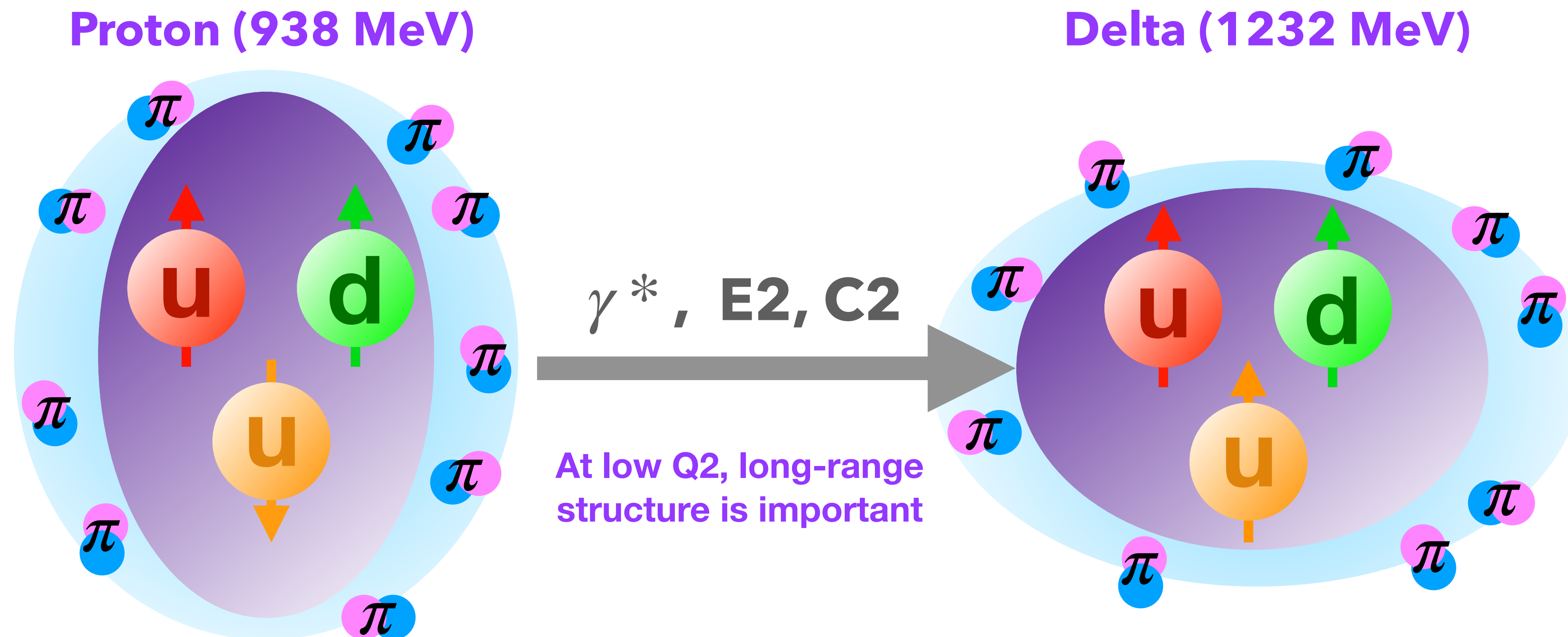
γ^* , E2, C2



There also exists a quadrupole (E2 or C2) transition from proton to delta.
(The quadrupole amplitudes are associated with the existence of non-spherical components in the proton and Delta WF)

The quadrupole to dipole ratio (**E2/M1** or **C2/M1**) is non-zero... **Why?**
Non-central (tensor) interactions between quarks can account for some of the spherical deviation, but not all...

The N - Δ transition



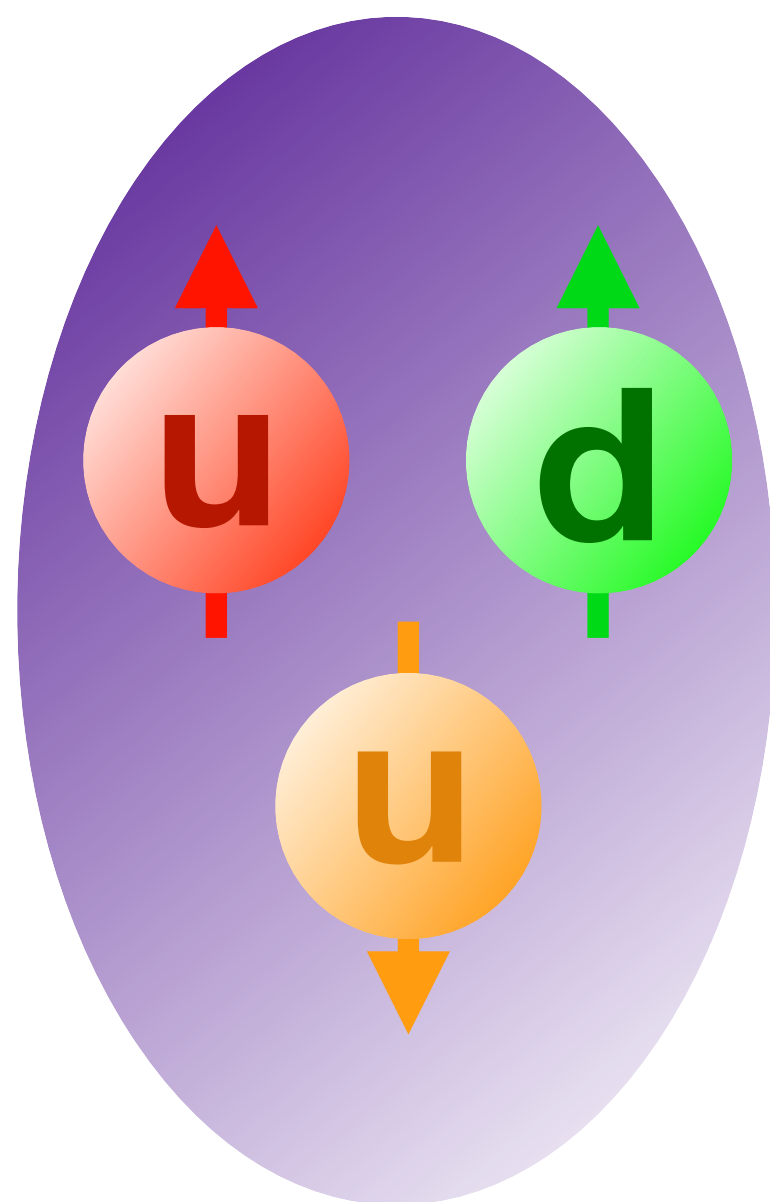
There also exists a quadrupole (E2 or C2) transition from proton to delta.
(The quadrupole amplitudes are associated with the existence of non-spherical components in the proton and Delta WF)

The quadrupole to dipole ratio (**E2/M1** or **C2/M1**) is non-zero... **Why?**

At low Q^2 , the dynamics of a meson cloud are important to describe the structure of the nucleon.

The N - Δ transition

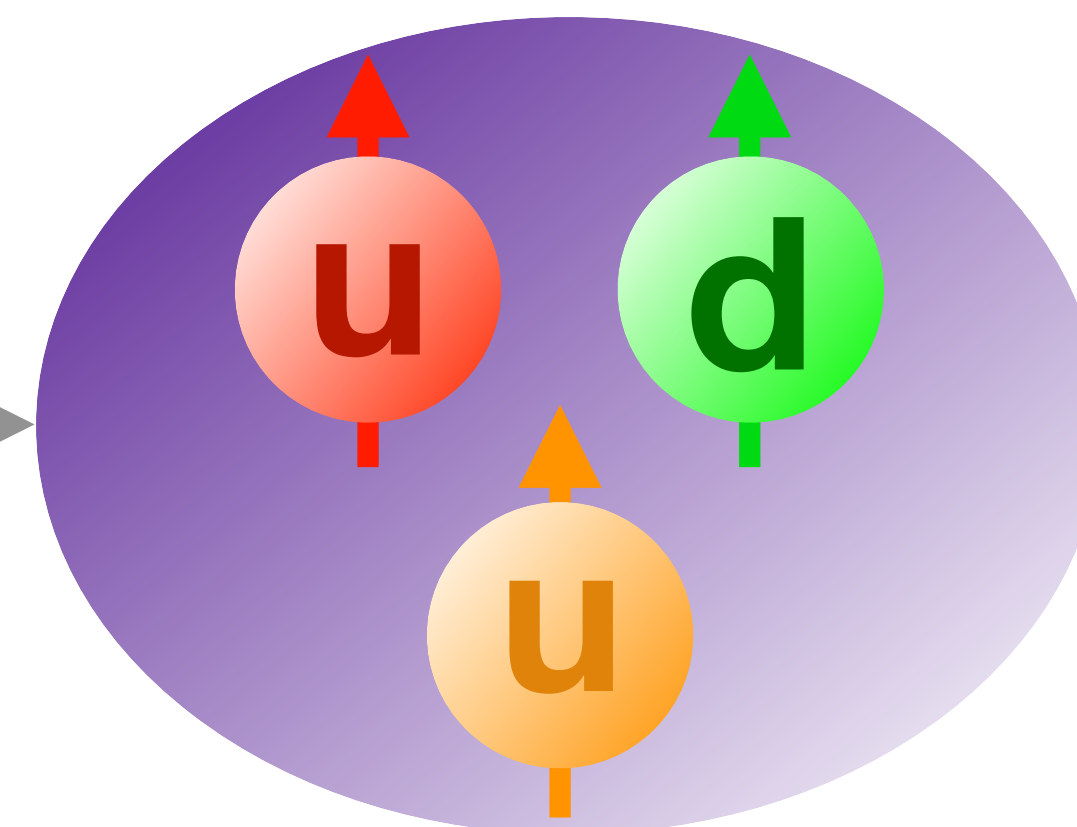
Proton (938 MeV)



Delta (1232 MeV)

γ^* , E2, C2

Large Q^2 , pQCD predicts
EMR $\rightarrow +1$, CMR \rightarrow constant

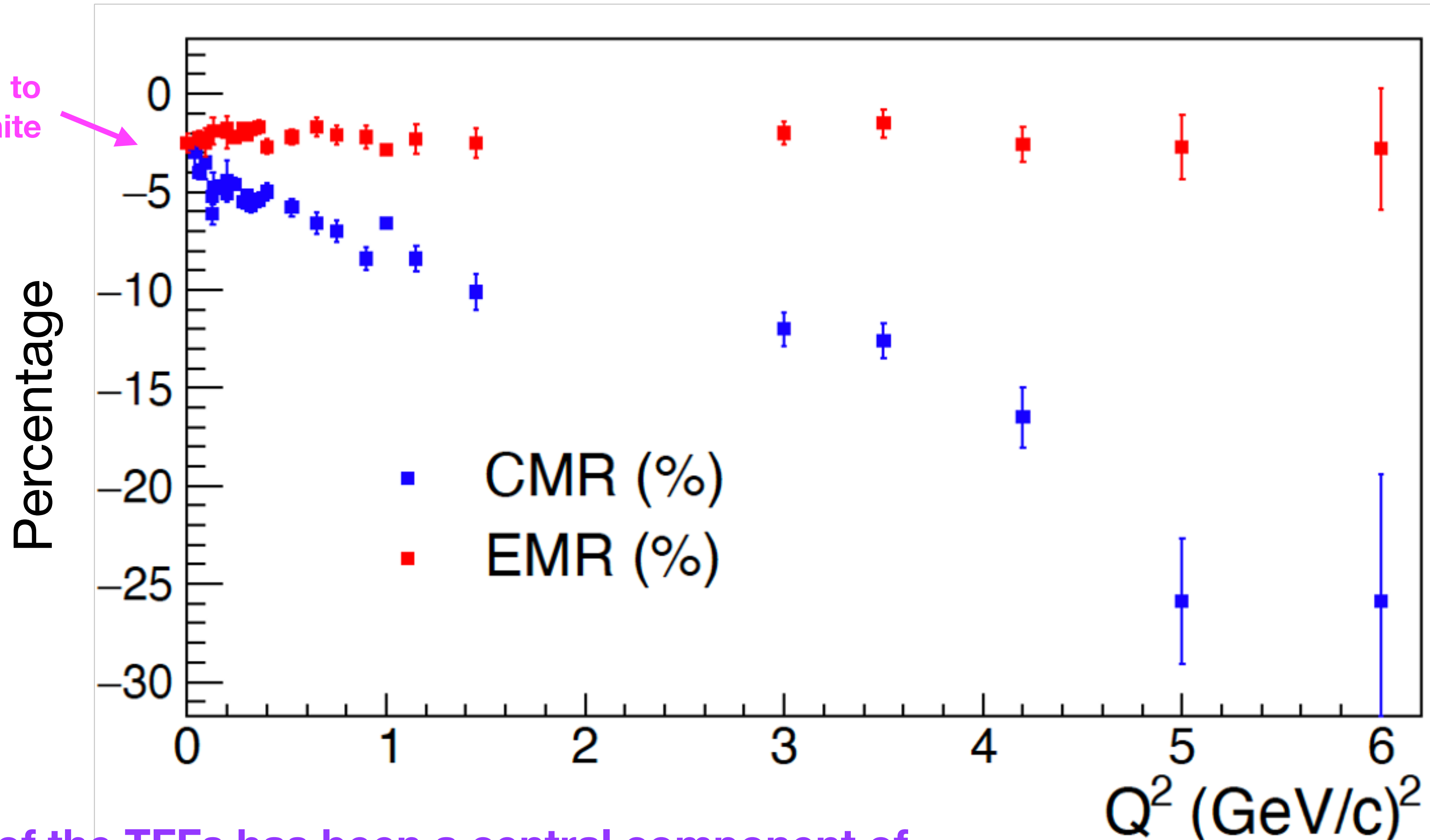


There also exists a quadrupole (E2 or C2) transition from proton to delta.
(The quadrupole amplitudes are associated with the existence of non-spherical components in the proton and Delta WF)

The quadrupole to dipole ratio (**E2/M1** or **C2/M1**) is non-zero... **Why?**
At high Q^2 , perturbative calculations should become more reliable and helicity conserving amplitudes are expected to dominate.

World data and status of TFFs

CMR & EMR predicted to converge at a small finite value as $Q^2 \rightarrow 0$

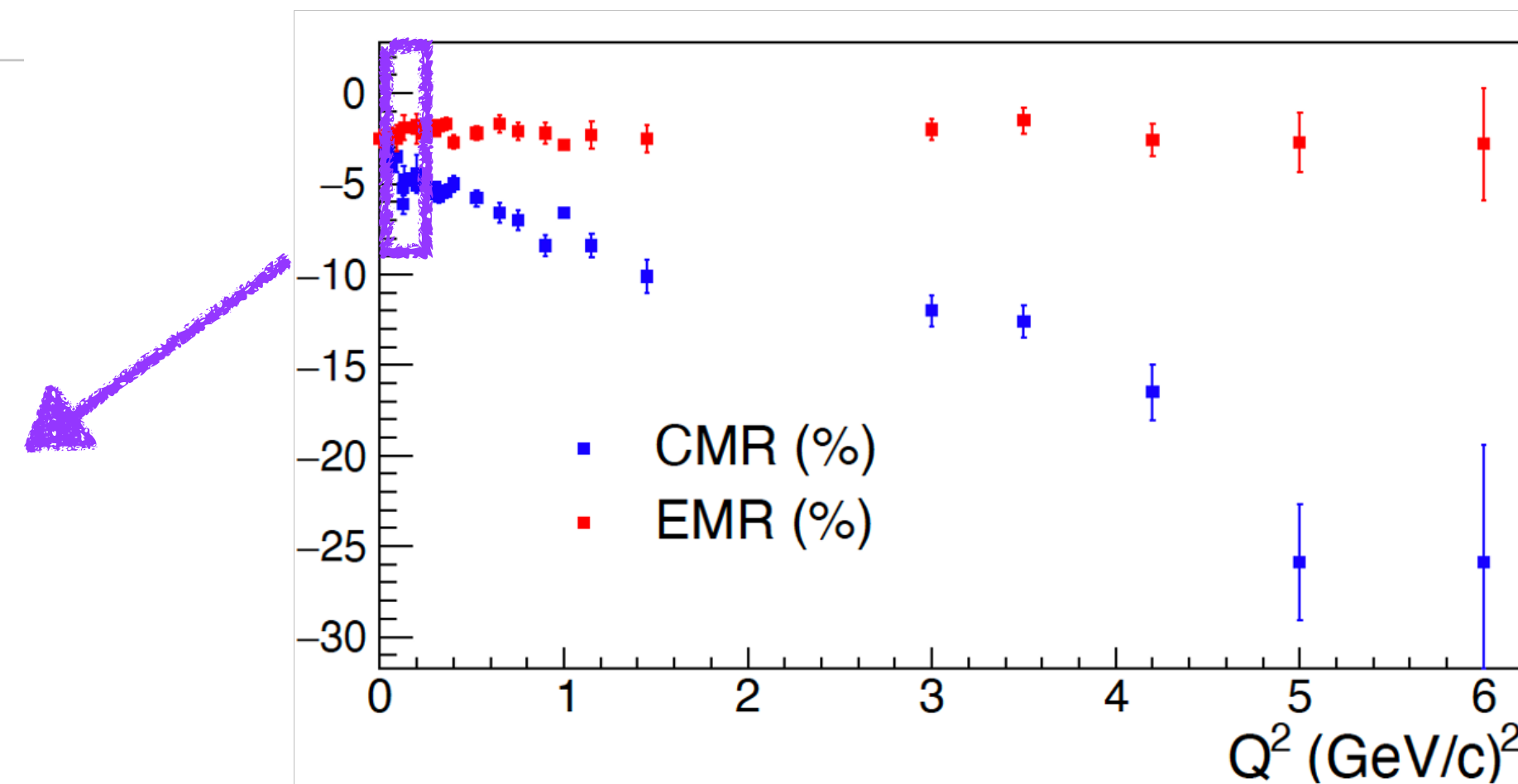
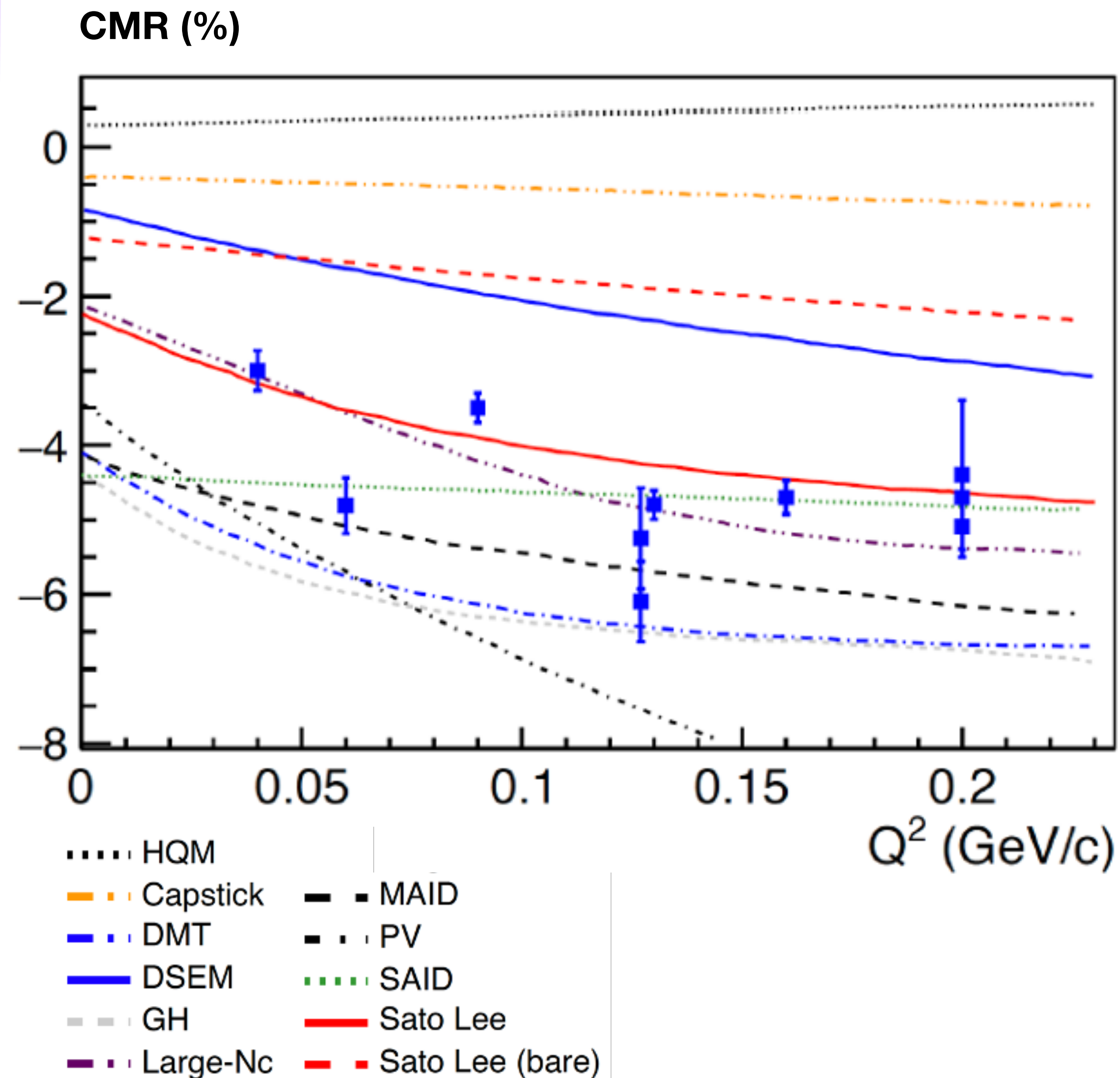


Extraction of the TFFs has been a central component of Jlab's experimental program:

(Most of these measurements are from JLab Halls A, B, and C)

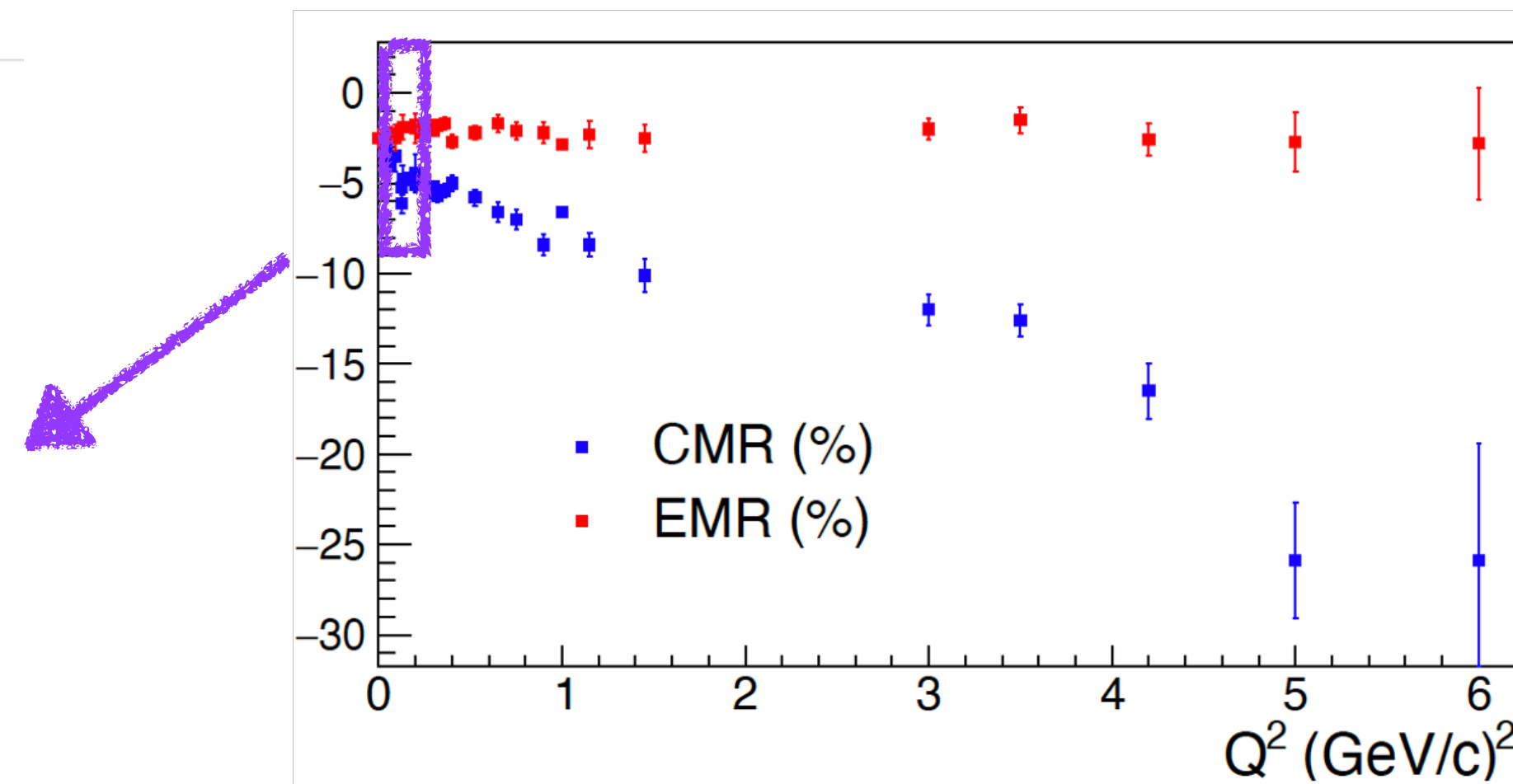
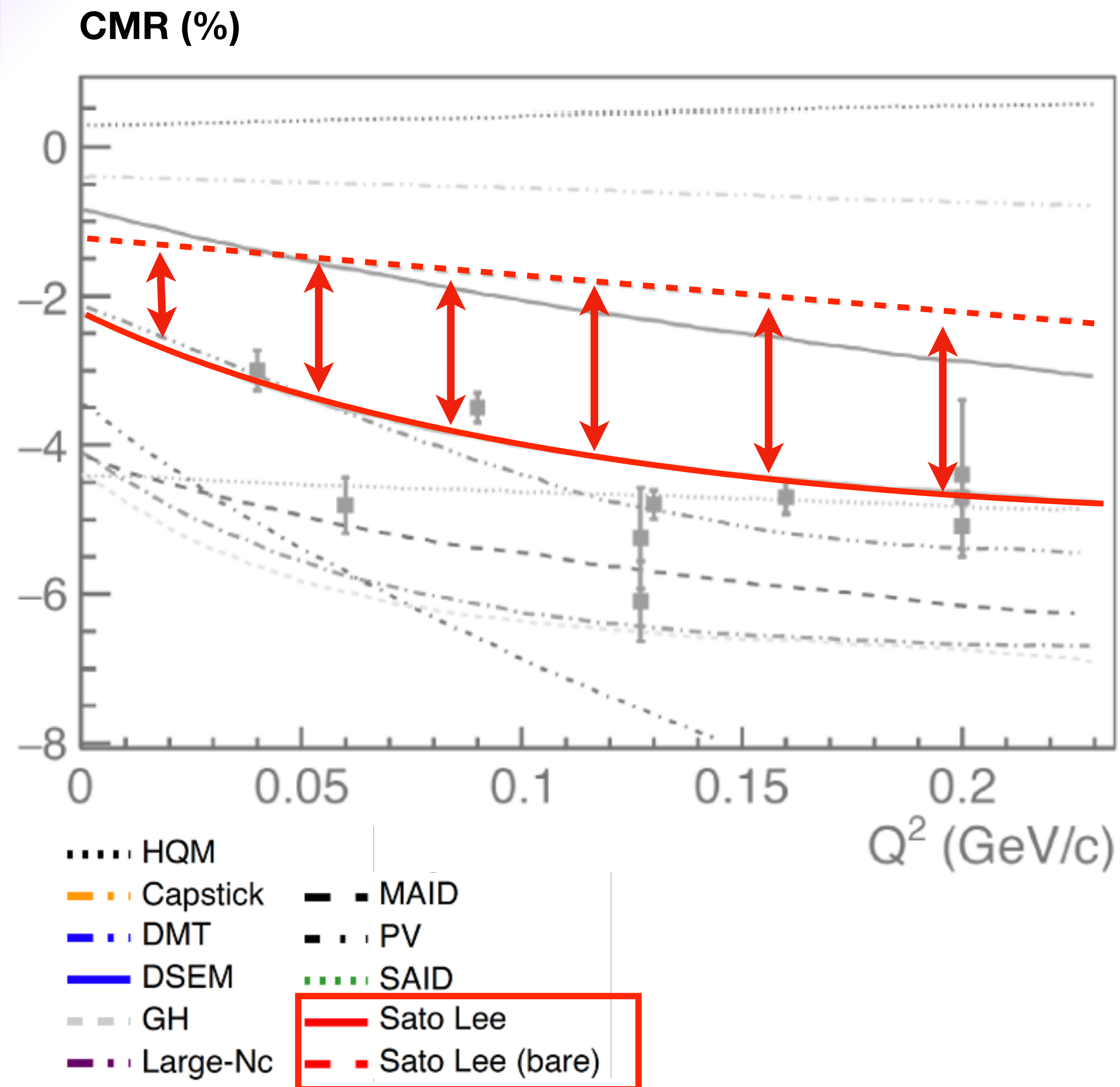
At large Q^2 , no direct indication of EMR \rightarrow 100% and CMR \rightarrow constant (predicted in pQCD regime)

Low Q^2 N - Δ transition form factors



- Low Q^2 landscape is an important region to measure:
 - Mesonic cloud effects are predicted to be:
 - dominant in explaining the magnitude of the TFFs
 - changing most rapidly over all Q^2
 - Provides an excellent test bed for ChEFT and LQCD calculations
 - Relates the excitation mechanism to spatial information of the proton and the Delta.
 - Tests the predicted convergence of EMR and CMR as $Q^2 \rightarrow 0$.
 - Sparsely measured region.

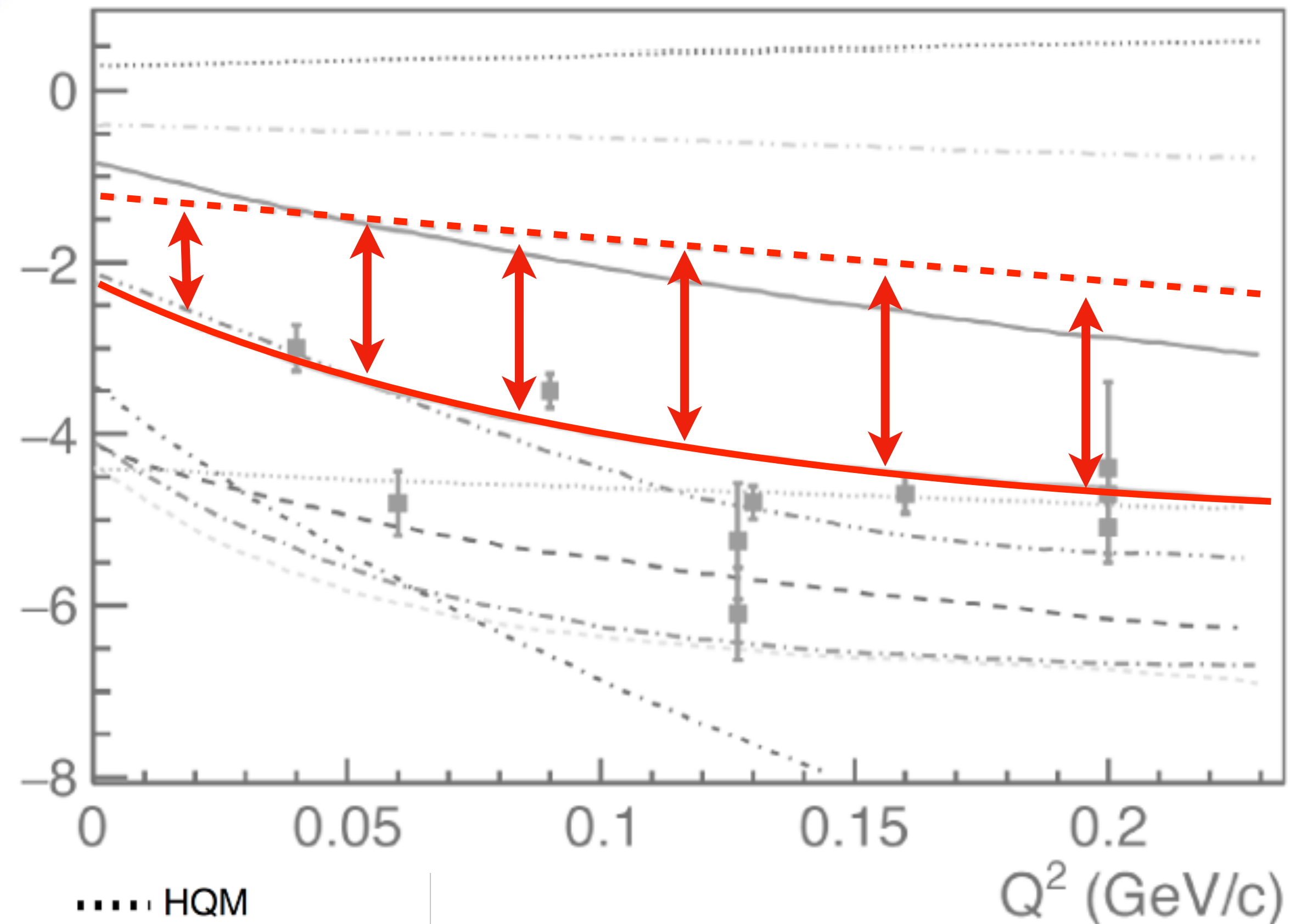
Low Q^2 N - Δ transition form factors



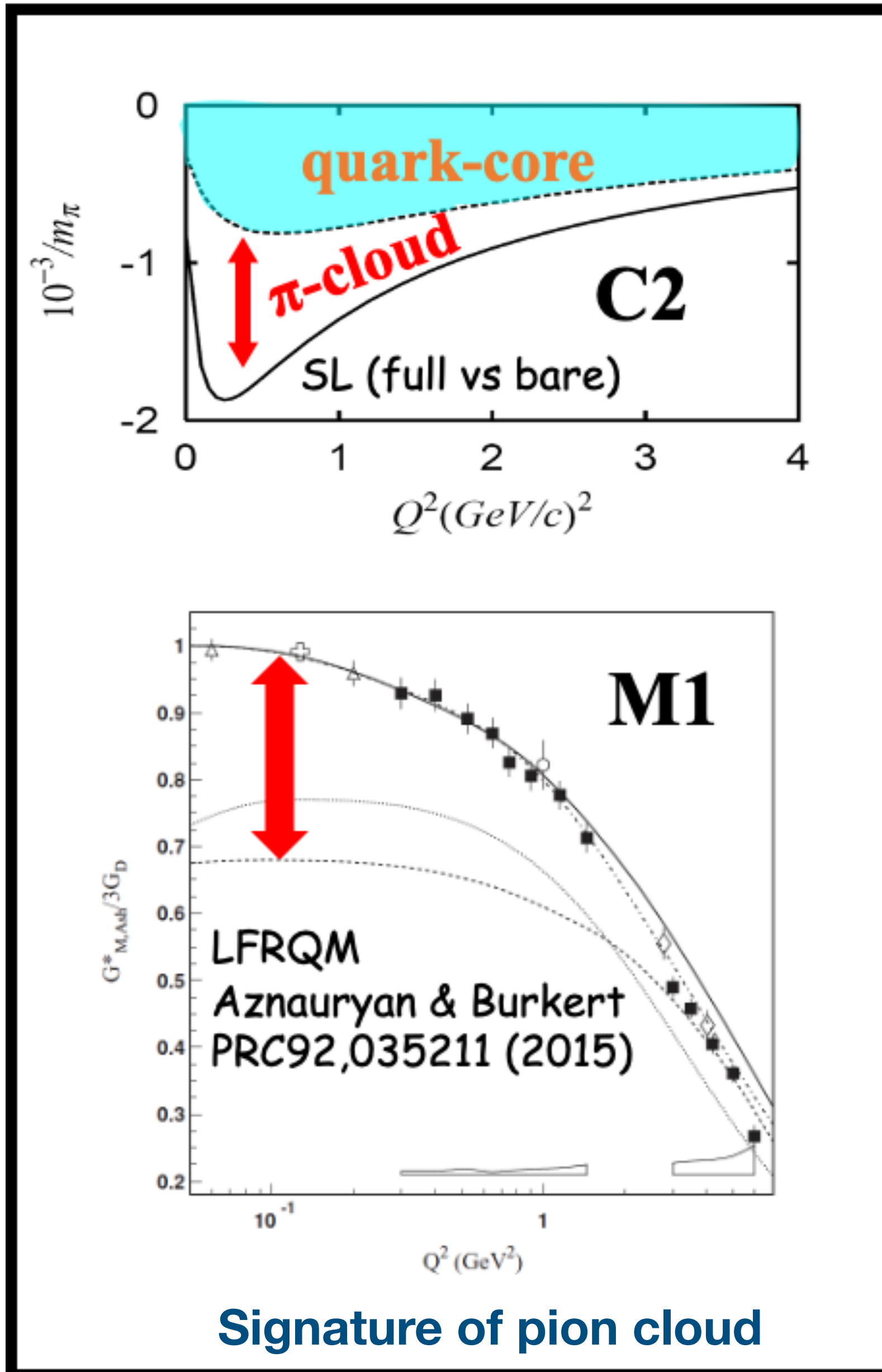
- Low Q^2 landscape is an important region to measure:
 - Mesonic cloud effects are predicted to be:
 - dominant in explaining the magnitude of the TFFs
 - changing most rapidly over all Q^2
 - Provides an excellent test bed for ChEFT and LQCD calculations
 - Relates the excitation mechanism to spatial information of the proton and the Delta.
 - Tests the predicted convergence of EMR and CMR as $Q^2 \rightarrow 0$.
 - Sparsely measured region.

Low Q^2 N - Δ transition form factors

CMR (%)



..... HQM
 - - - Capstick
 - - - DMT
 - - - DSEM
 - - - GH
 - - - Large-Nc
 - - - MAID
 - - - PV
 - - - SAID
 - - - Sato Lee
 - - - Sato Lee (bare)

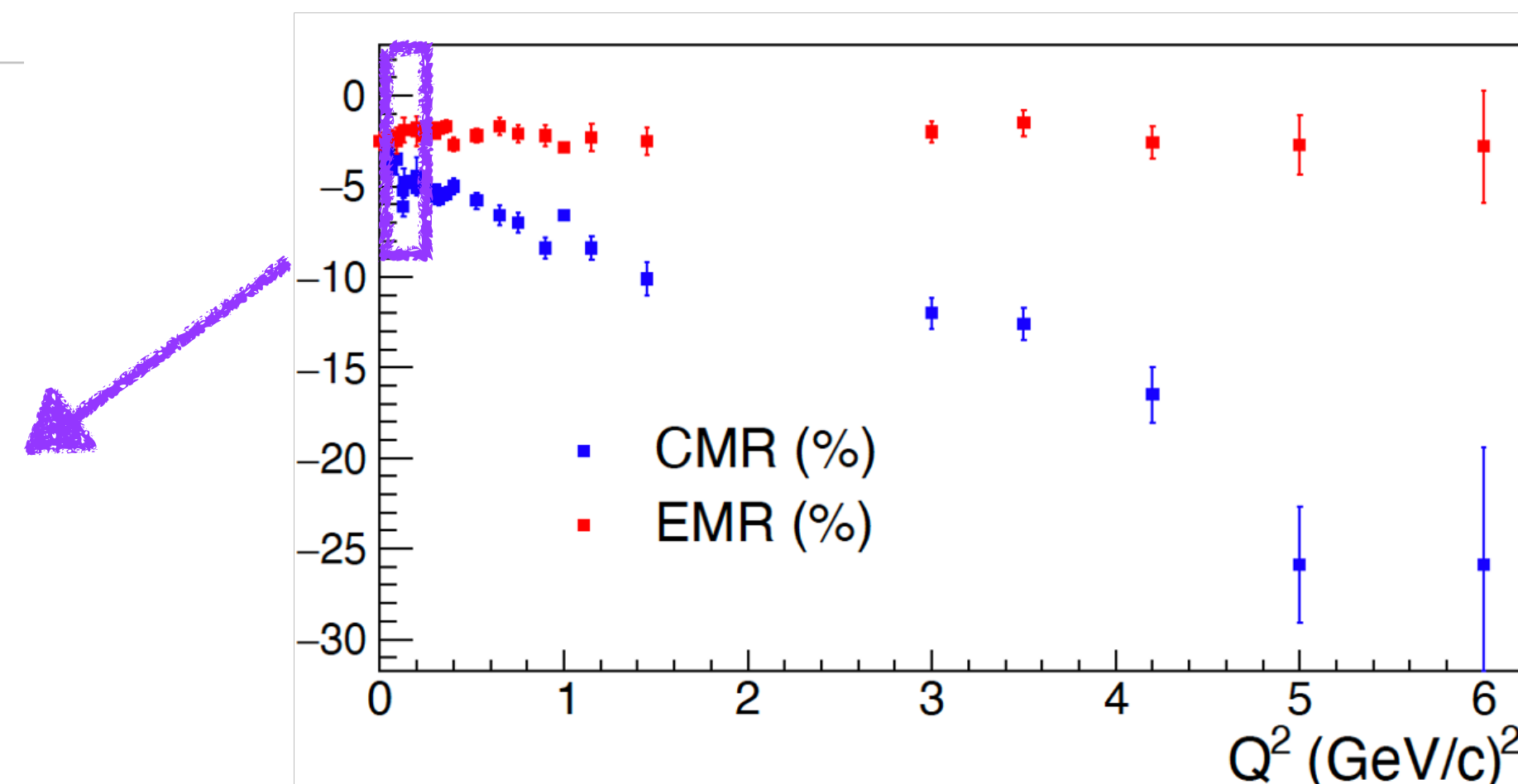
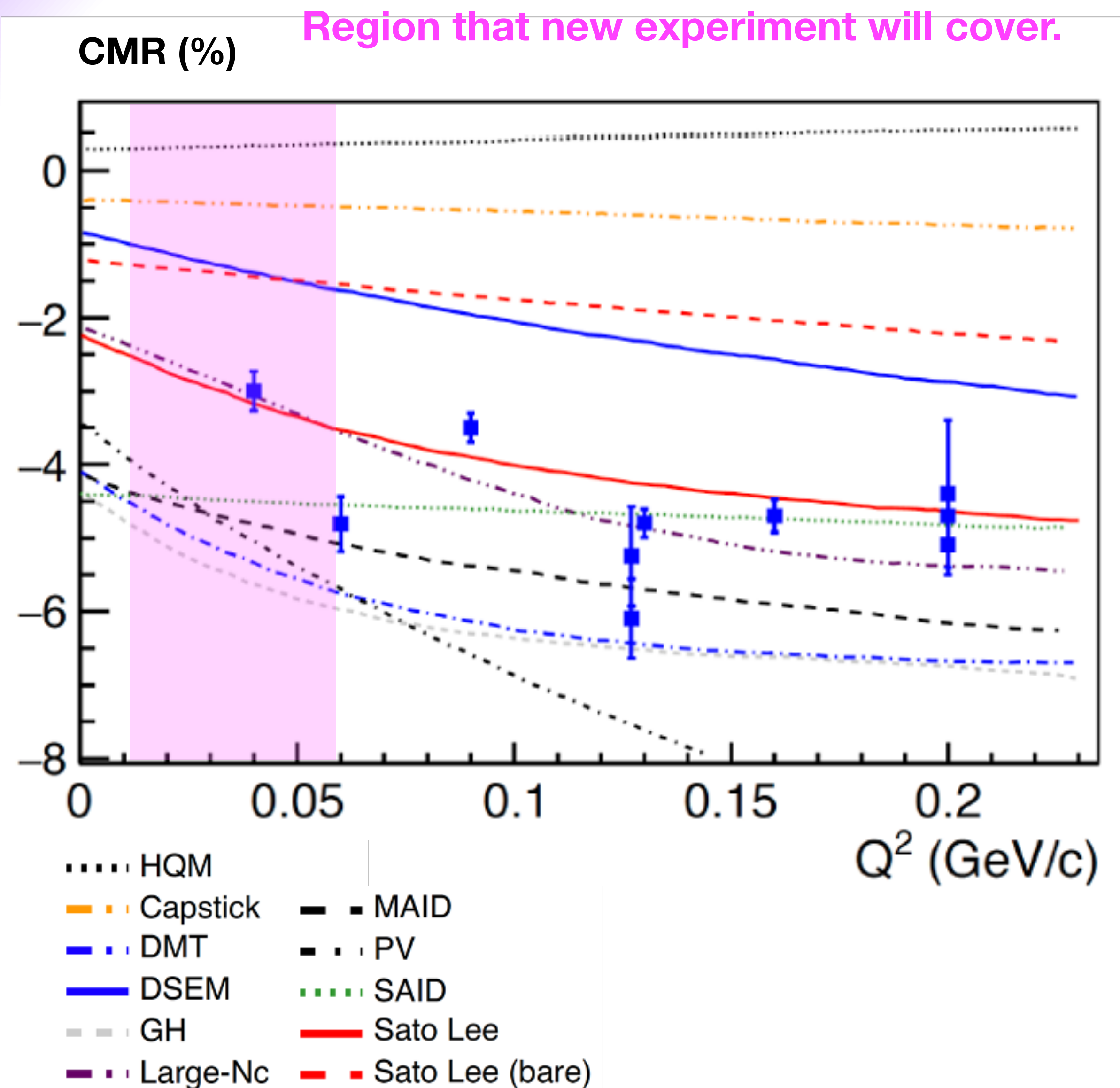


Dominant role of mesonic d.o.f. at large distance scale:

Mesonic cloud $\sim 50\%$ of the quadrupole amplitude magnitude & $1/3$ of the magnetic dipole strength

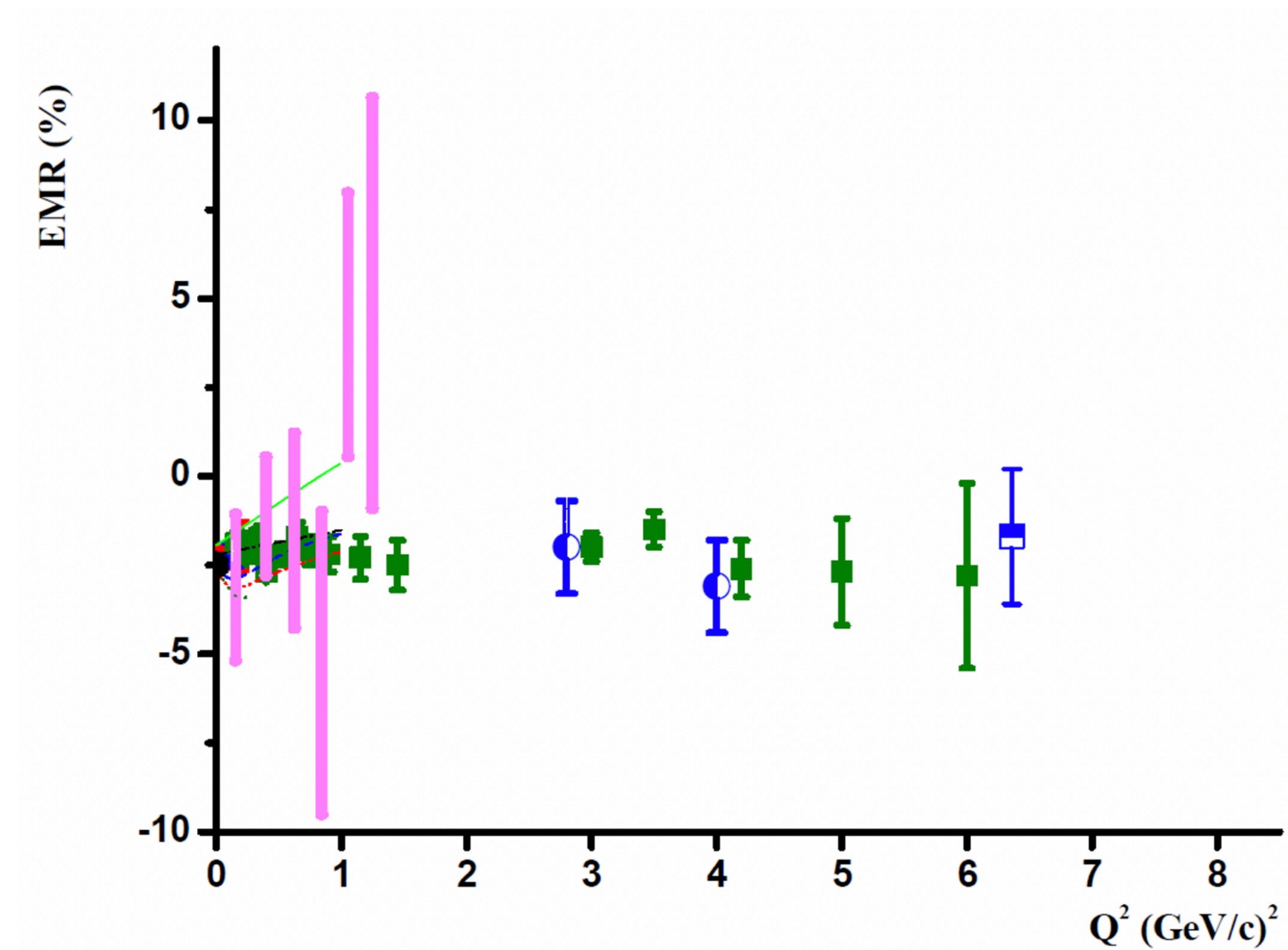
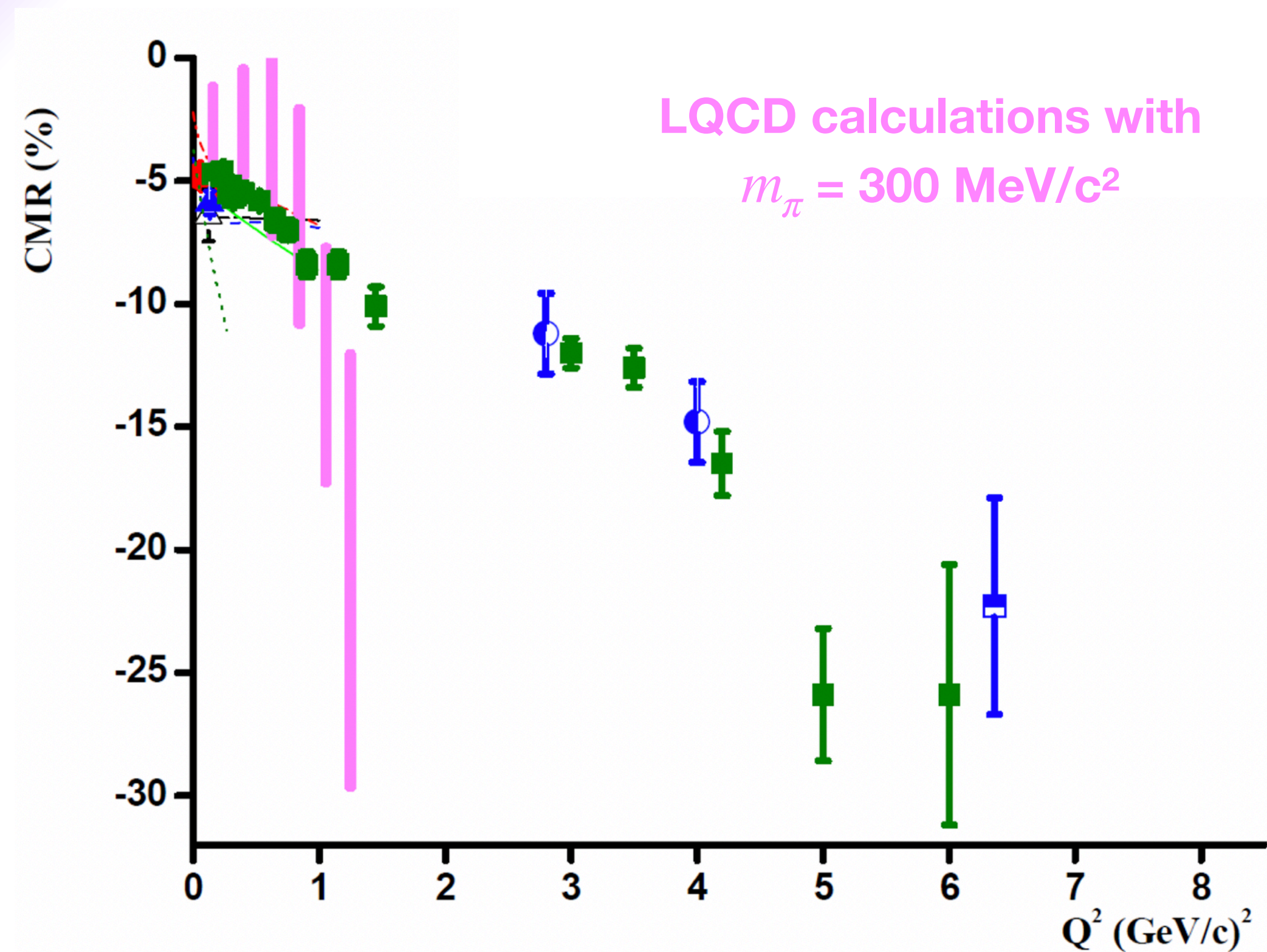
Signature of pion cloud

Low Q^2 N - Δ transition form factors



- Low Q^2 landscape is an important region to measure:
 - Mesonic cloud effects are predicted to be:
 - dominant in explaining the magnitude of the TFFs
 - changing most rapidly over all Q^2
 - Provides an excellent test bed for ChEFT and LQCD calculations
 - Relates the excitation mechanism to spatial information of the proton and the Delta.
 - Tests the predicted convergence of EMR and CMR as $Q^2 \rightarrow 0$.
 - Sparsely measured region.

Lattice Calculations



- Updated LQCD calculations are in progress → new calculations will have a physical pion mass and uncertainties comparable to experiment.
- Extended Twisted mass collaboration results expected within 2 years.
- Efforts are partly motivated to understand baryon structure for neutrino scattering.
- Low Q^2 data will provide a precision benchmark for LQCD calculations.

What can we say about the geometry (shape) of the nucleon?

...an issue since the 80's

● What is the "shape" of the nucleon?

- Is it spherically symmetric or deformed?
 - If deformed, what is the origin of the deformation?
- Exactly how are shape and structure related?

● How can one explore shape?

- Quadrupole moment of the ground state is identically 0 for a spin 1/2 system.
 - Pure proton scattering without spin excitation can't give you any information.
- The only isolated spin-excitation resonance of the proton is the $\Delta^+(1232)$.

● A more comprehensive review can be found at:

- C. Alexandrou, C. Papanicolas, M. Vanderhaeghen,
 - "*The shape of hadrons*", Rev. Mod. Phys. 84, 1231 (2012)
- A. Bernstein, C. Papanicolas
 - "*Overview: The shape of hadrons*" , AIP Conf. Proc. 904, 1 (2007)

Imaging the Δ and the N - Δ transition

Empirical transverse charge transition densities

Eur. Phys. J. Special Topics 198, 141 (2011)

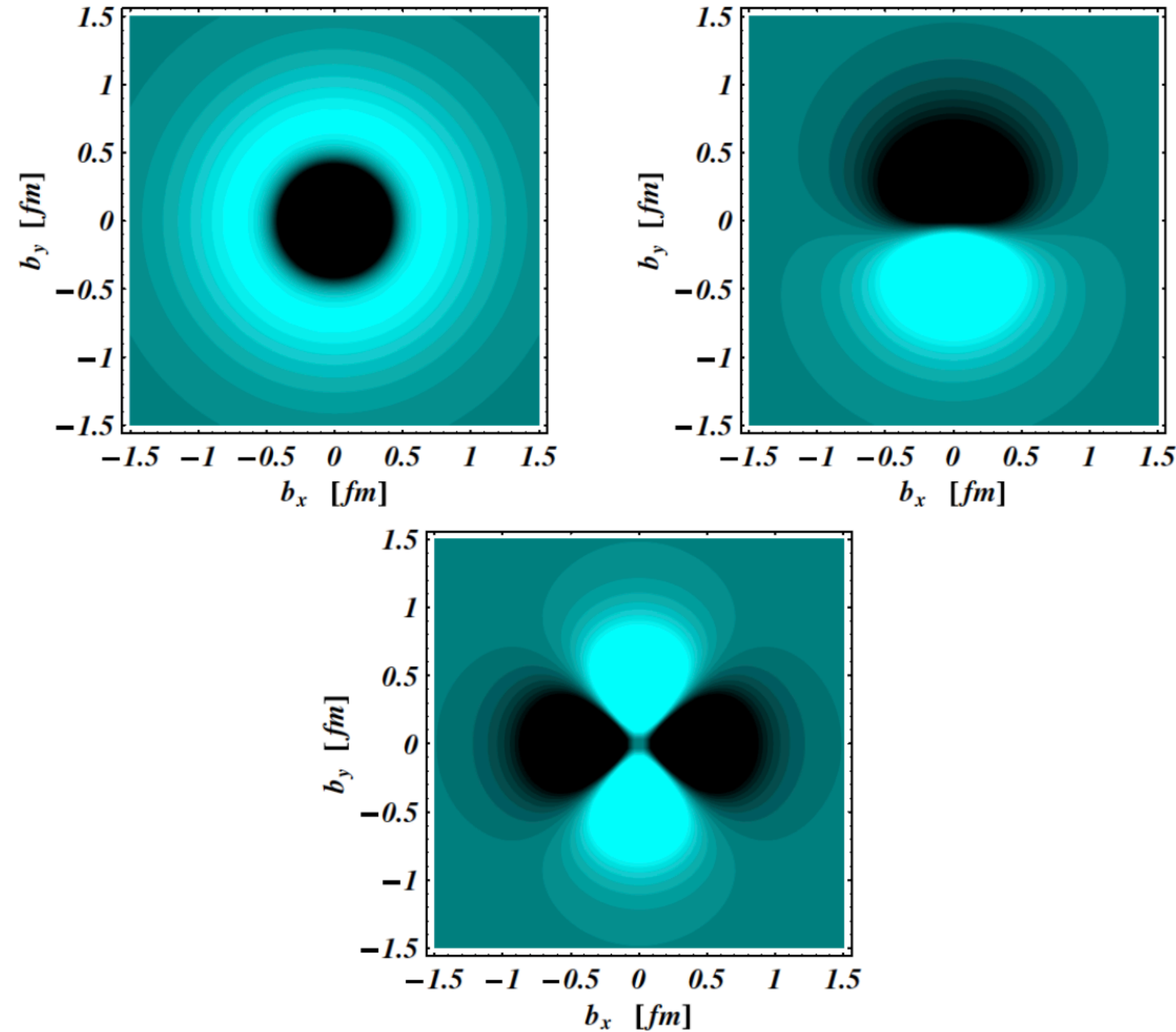


Fig. 18. Quark transverse charge density corresponding to the $p \rightarrow \Delta(1232)P_{33}$ e.m. transition. Upper left panel: p and Δ are in a light-front helicity $+1/2$ state ($\rho_0^{pP_{33}}$). Upper right panel: p and Δ are polarized along the x -axis ($\rho_T^{pP_{33}}$) as in Fig. 14. The lower panel shows the quadrupole pattern, whose contribution to the polarized transition density is very small due to the weak $E2/C2$ admixtures in the $N\Delta$ transition and practically invisible in the upper right panel. The light (dark) regions correspond to positive (negative) densities. For the $p \rightarrow P_{33}(1232)$ e.m. transition FFs, we use the MAID2007 parametrization.

Probing hadron wave functions in Lattice QCD

Phys. Rev. D. 66, 094503 (2002)

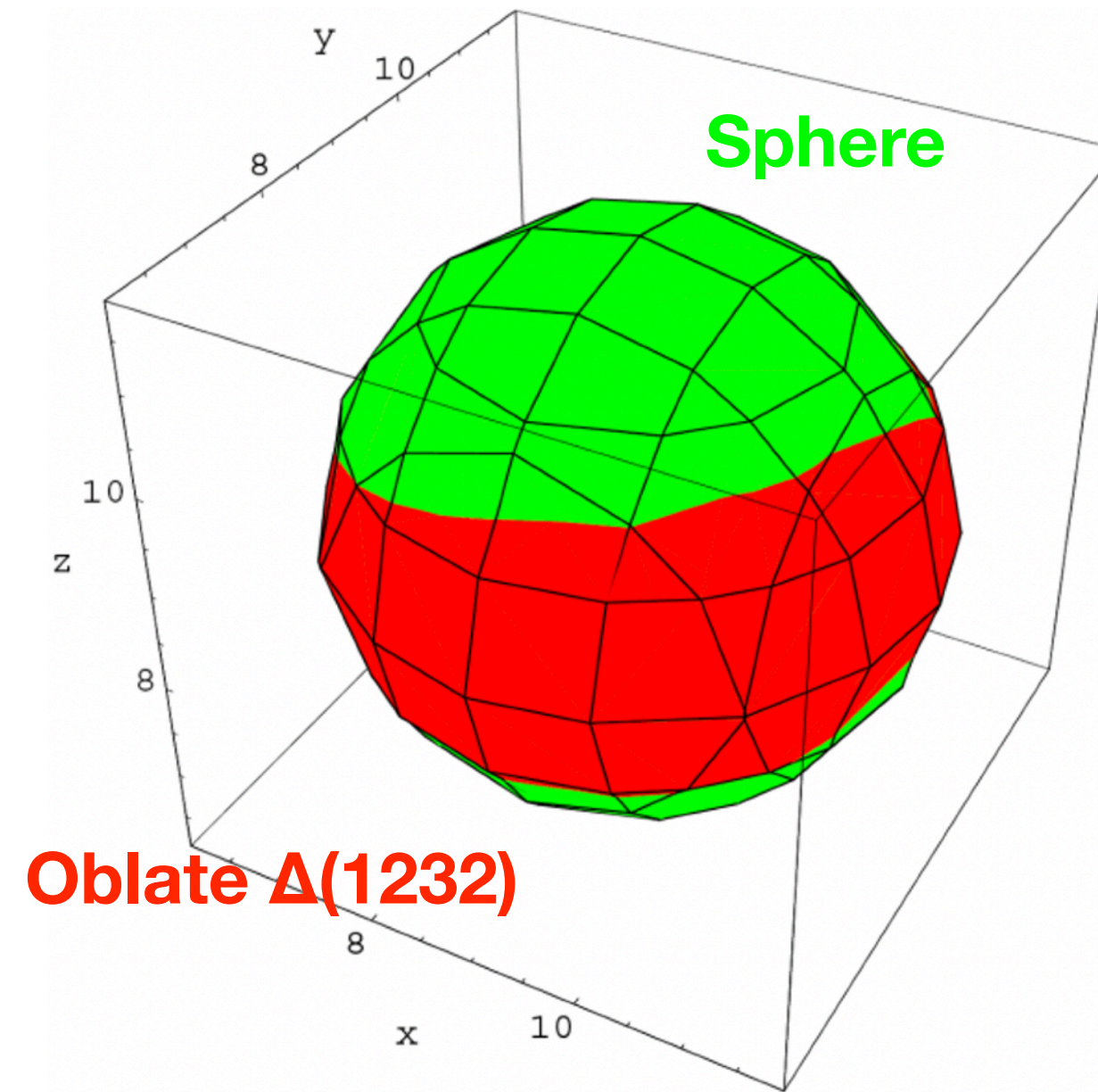


FIG. 18. Three-dimensional contour plot of the correlator (black): upper for the ρ state with 0 spin projection (cigar shape) and lower for the Δ^+ state with $+3/2$ (slightly oblate) spin projection for two dynamical quarks at $\kappa = 0.156$. Values of the correlator (0.5 for the ρ , 0.8 for the Δ^+) were chosen to show large distances but avoid finite-size effects. We have included for comparison the contour of a sphere (grey).

Lattice QCD: Quark transverse charge density in $\Delta^+(1232)$

Phys. Rev. D. 79, 014507 (2009)

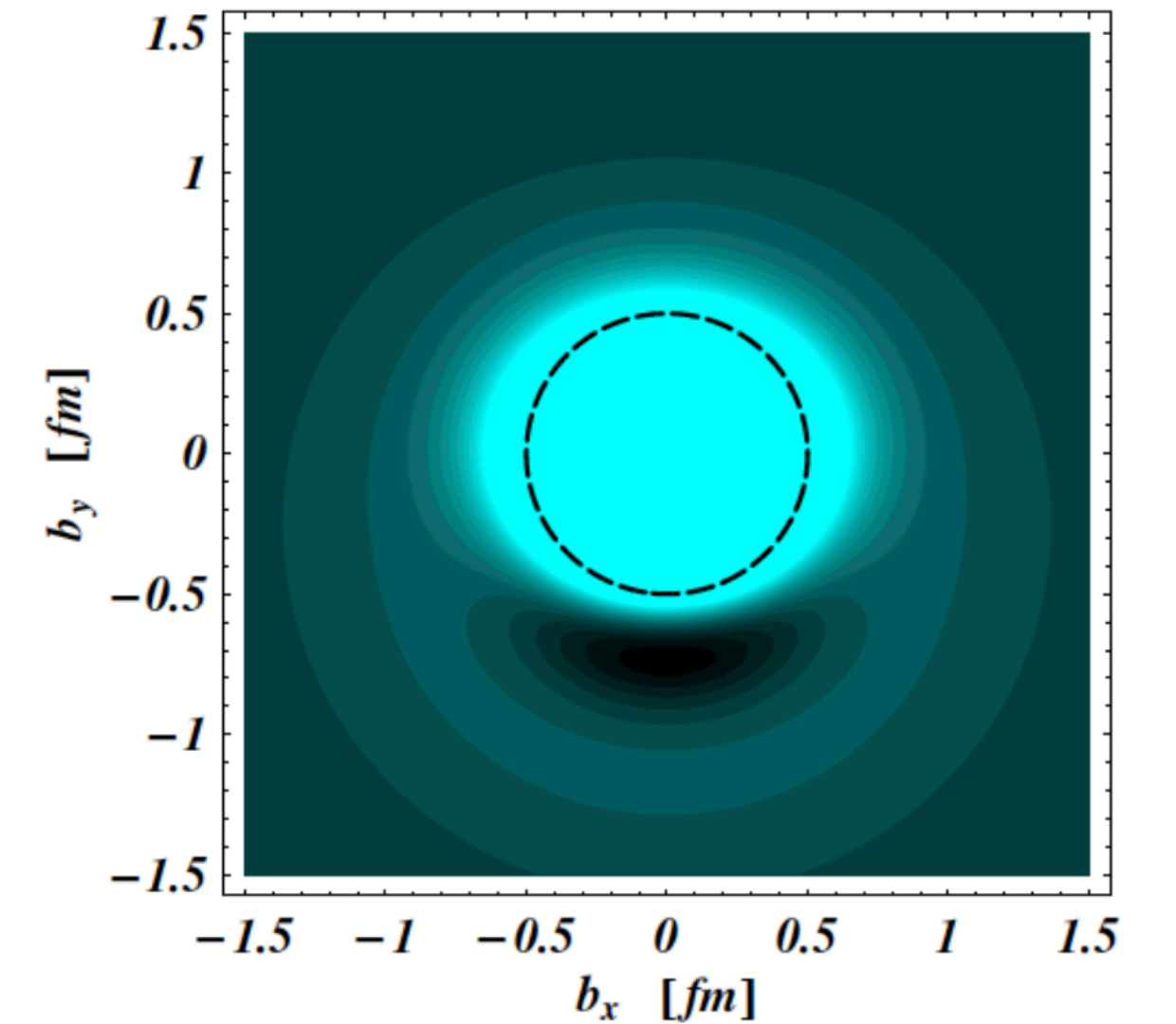


FIG. 10: Lattice QCD results for the quark transverse charge density $\rho_T^{\Delta^+ \frac{3}{2}}$ in a $\Delta^+(1232)$ which is polarized along the positive x -axis. The light (dark) regions correspond to the largest (smallest) values of the density. In order to see the deformation more clearly, a circle of radius 0.5 fm is drawn for comparison. The density is obtained from quenched lattice QCD results at $m_\pi = 410$ MeV for the Δ e.m. FFs [48].

Connections to the neutron structure

- There are long-known relations between the TFFs and the neutron FFs.

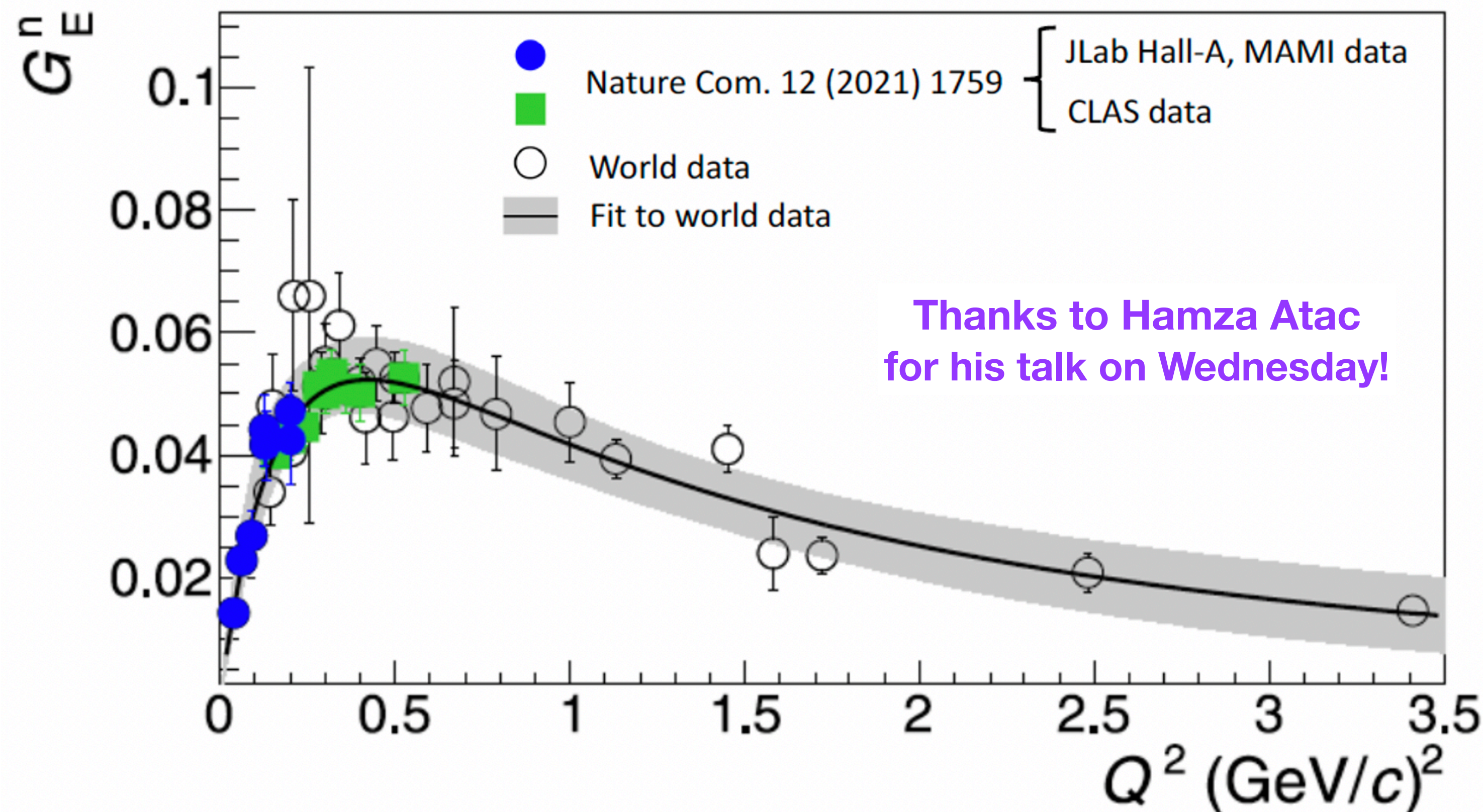
- Pascalutsa, V. & Vanderhaeghen, M. : Phys. Rev. D 76 (2007) [Large-Nc]

- Grabmayr, P. & Buchmann, A. J. : Phys. Rev. Lett. 86 (2001) [CQM + 2-body currents]

- G_E^n extraction from TFFs show strong agreement with world data.

- Allows access to low- Q^2 region where direct measurement of G_E^n is difficult.

- The relations receive theoretical corrections that can be analyzed and confronted with experimental data e.g. they can be analyzed in a theoretical framework that combines ChPT with the $1/N_c$ expansion.



Impact on other domains of nuclear physics

- Generalized polarizabilities (GPs) of the proton:

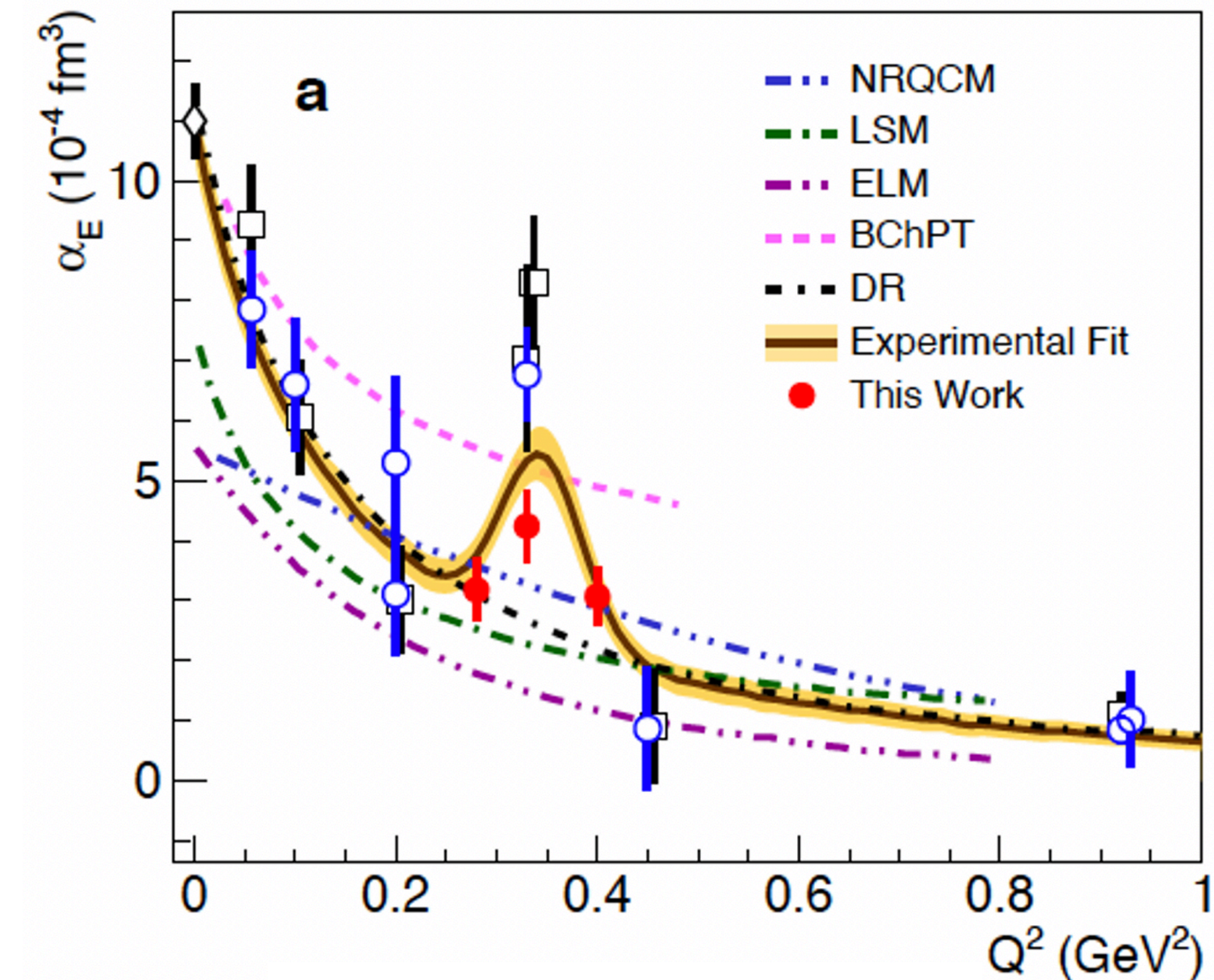
- The TFFs enter as an input in the VCS cross section over the Δ resonance region – their precise knowledge is necessary for the precise extraction of the GPs from the measured cross sections

- Physics of interest:

- Electric polarizability puzzle
- Interplay of paramagnetism & diamagnetism in the proton
- Extraction of the polarizability radii and imaging of the induced polarization density.

- Neutrino oscillation studies and neutrino-nucleus scattering

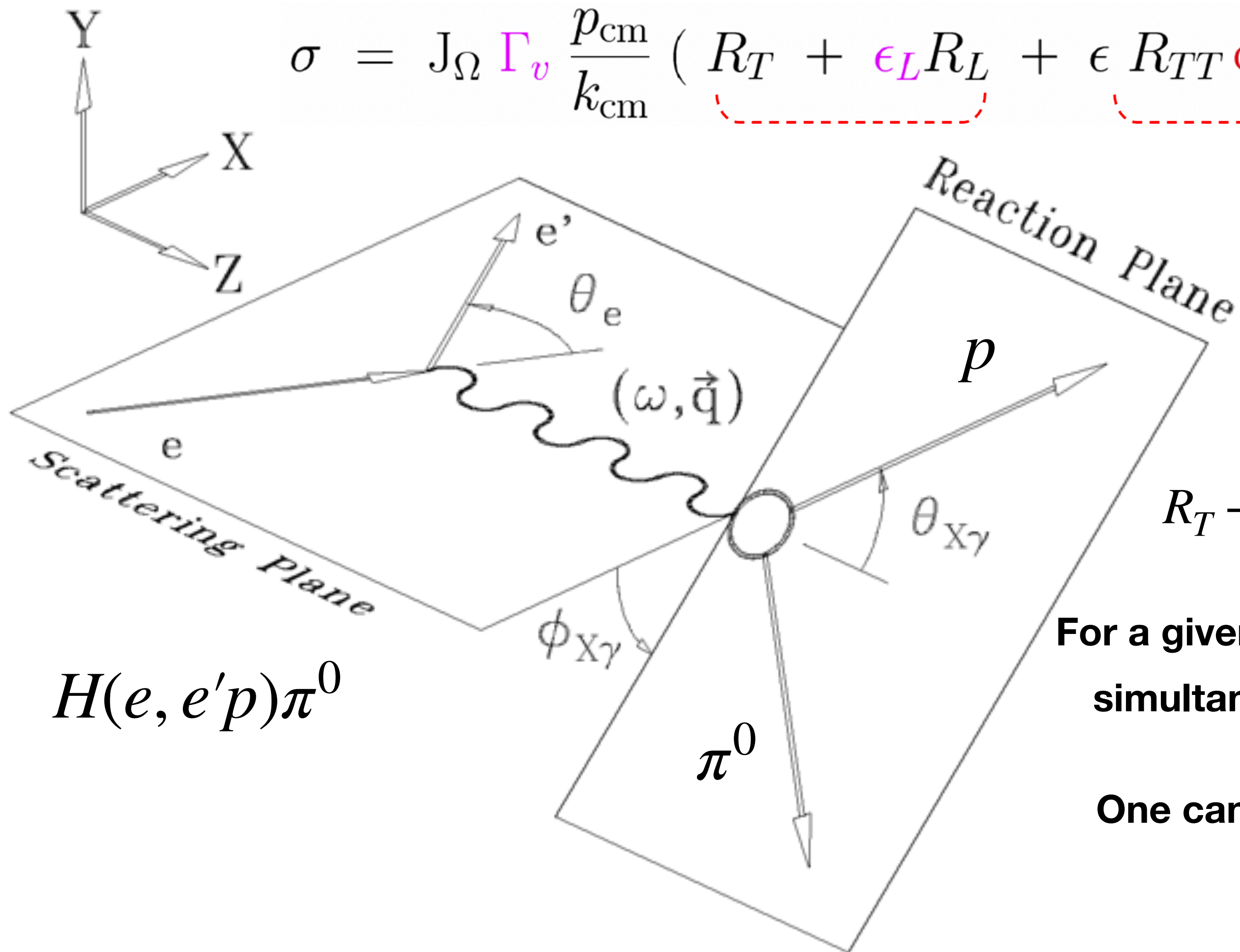
- Dominant source of systematic error: uncertainties in neutrino-nucleus reaction cross sections in the nucleon-resonance region.



Thanks to Nikos Sparveris
for his talk on Monday!

Experimental Methodology

$$\sigma = J_{\Omega} \Gamma_v \frac{p_{\text{cm}}}{k_{\text{cm}}} \left(\underbrace{R_T + \epsilon_L R_L}_{\text{}} + \underbrace{\epsilon R_{TT} \cos 2\phi_{X\gamma}}_{\text{}} - \underbrace{v_{LT} R_{LT} \cos \phi_{X\gamma}}_{\text{}} \right)$$



$$R_T + R_L, R_{TT}, R_{LT} = f(A(W, Q^2), g(\theta_{X\gamma}))$$

For a given $\theta_{X\gamma}$, one can measure at least 3 $\phi_{X\gamma}$ to simultaneously extract $R_T + R_L, R_{TT}$ and R_{LT} .

One can then scan $\theta_{X\gamma}$ to extract the relevant amplitudes $A(W, Q^2)$.

Experimental Methodology

$$R_{TT} = 3 \sin^2 \theta (E2 M1 + M1^2 + \dots \Sigma_{\text{background}})$$

$$R_{LT} = -6 \cos \theta \sin \theta (C2 M1 + \dots \Sigma_{\text{background}})$$

$$R_T + R_L = M1^2 + \dots \Sigma_{\text{background}}$$

$R_{TT} \rightarrow$ sensitive to the **EMR**

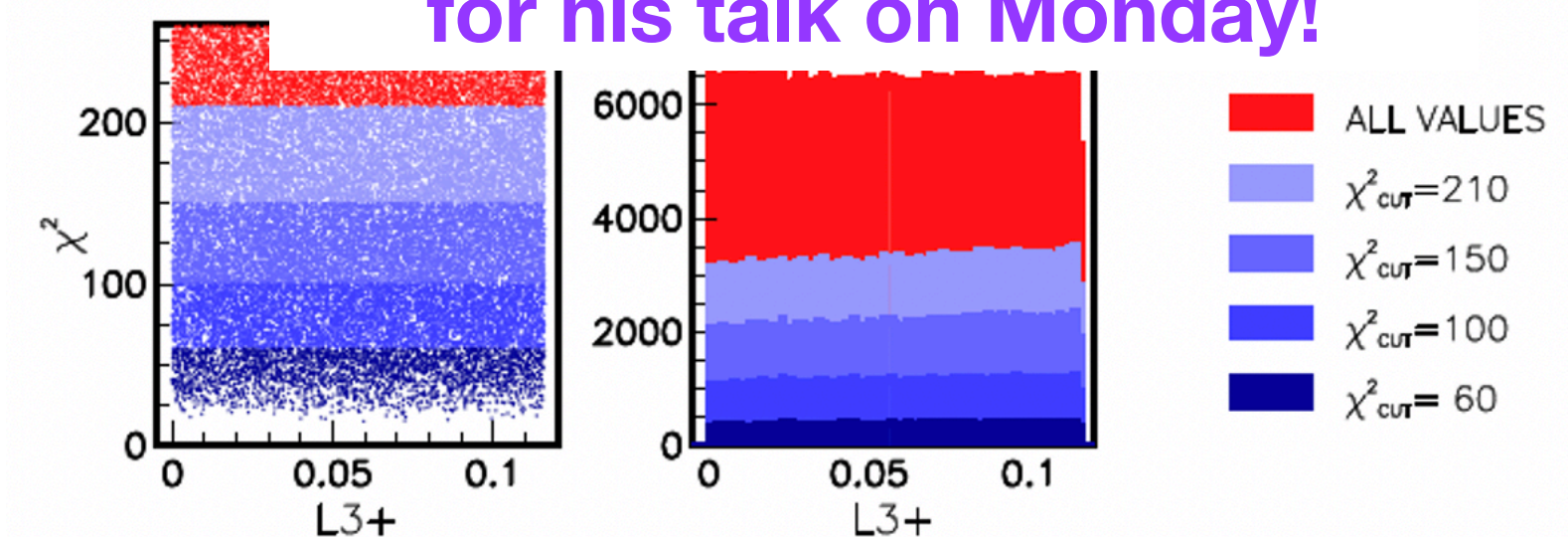
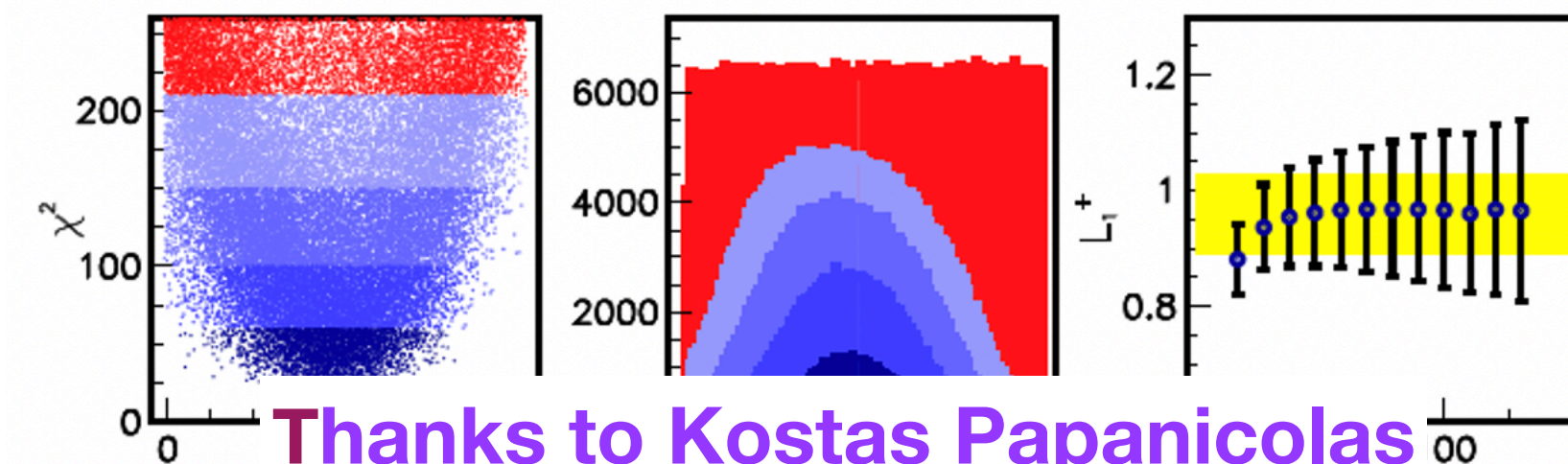
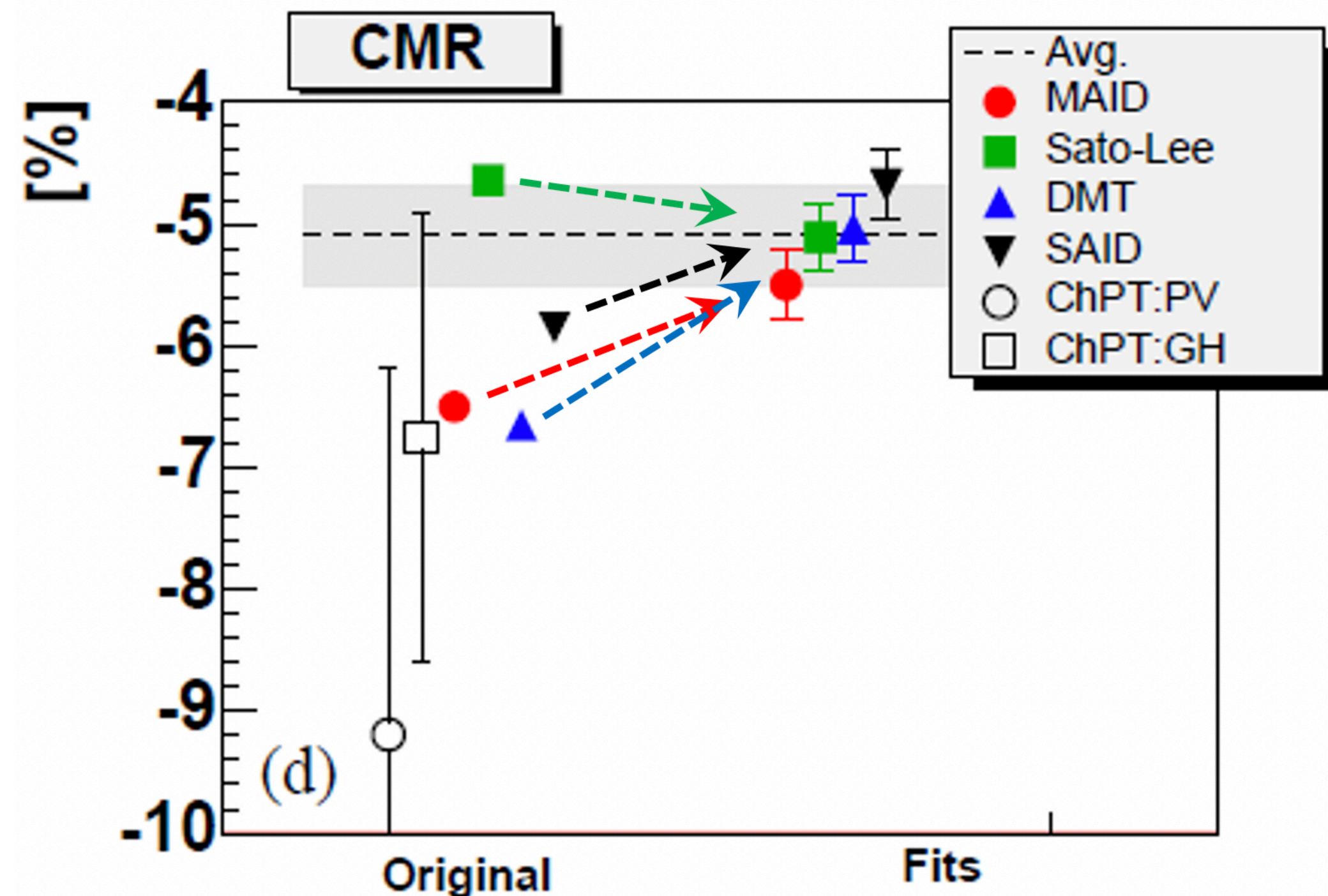
$R_{LT} \rightarrow$ sensitive to the **CMR**

$R_T + R_L \rightarrow$ sensitive to **M1**

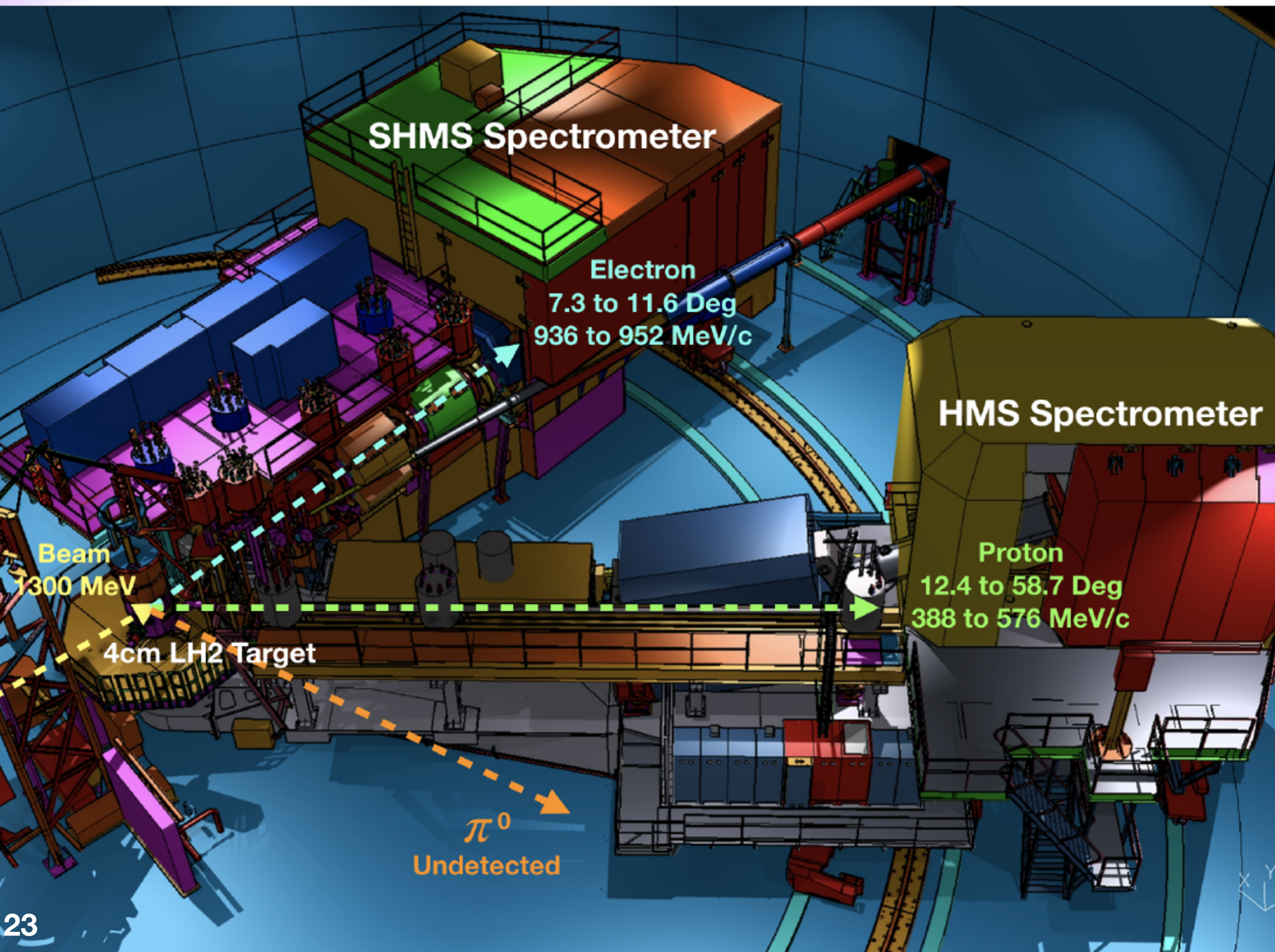
Fit parameterized models to data

and/or

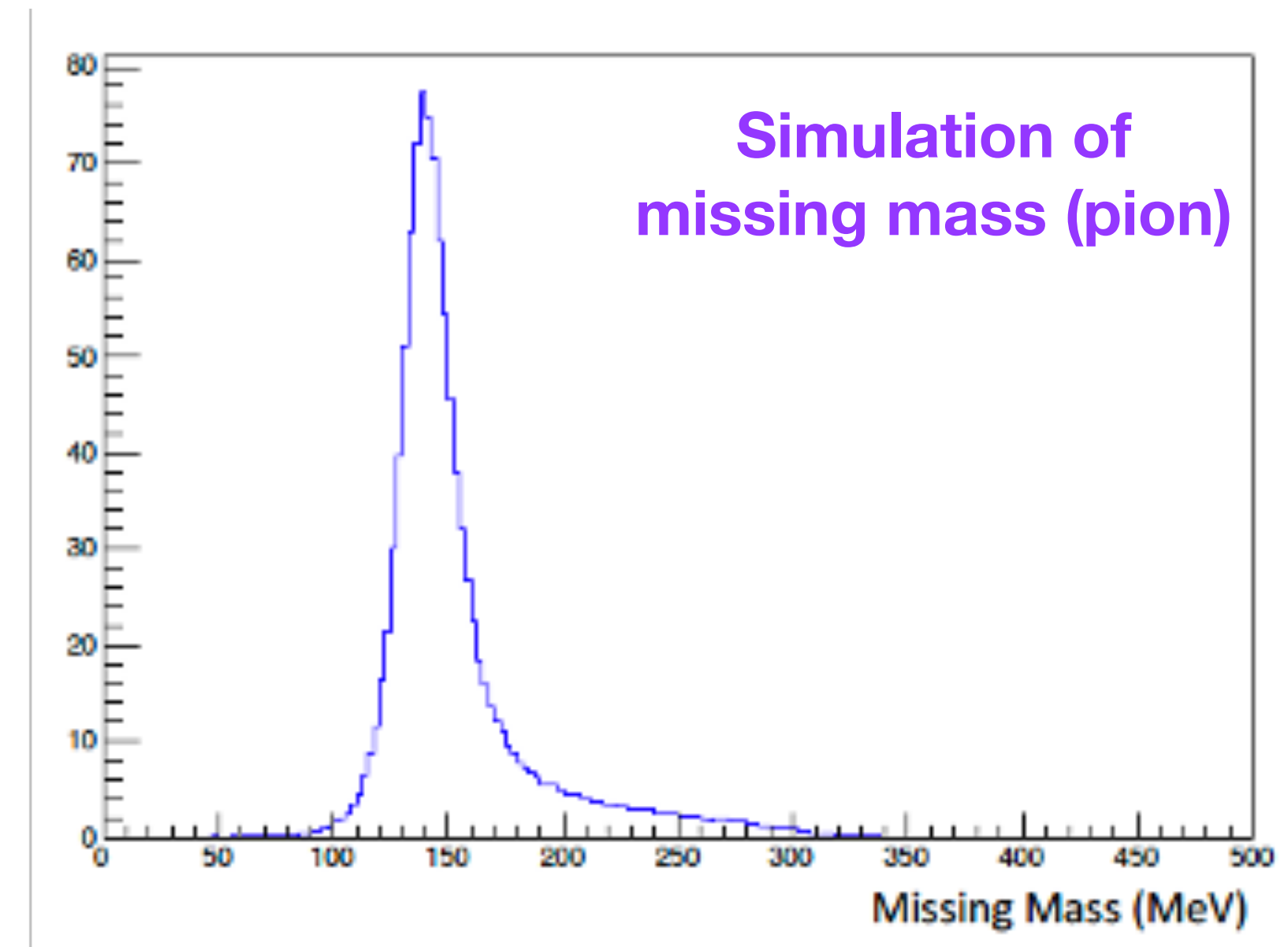
Use model independent statistical methods to identify and determine with maximal precision parameters that are sensitive to the data:
AMIAS (Eur. Phys. J. A 56 (2020) 10, 270)



Proposed to PAC49 and PAC50: low- Q^2 TFF measurements in Hall-C



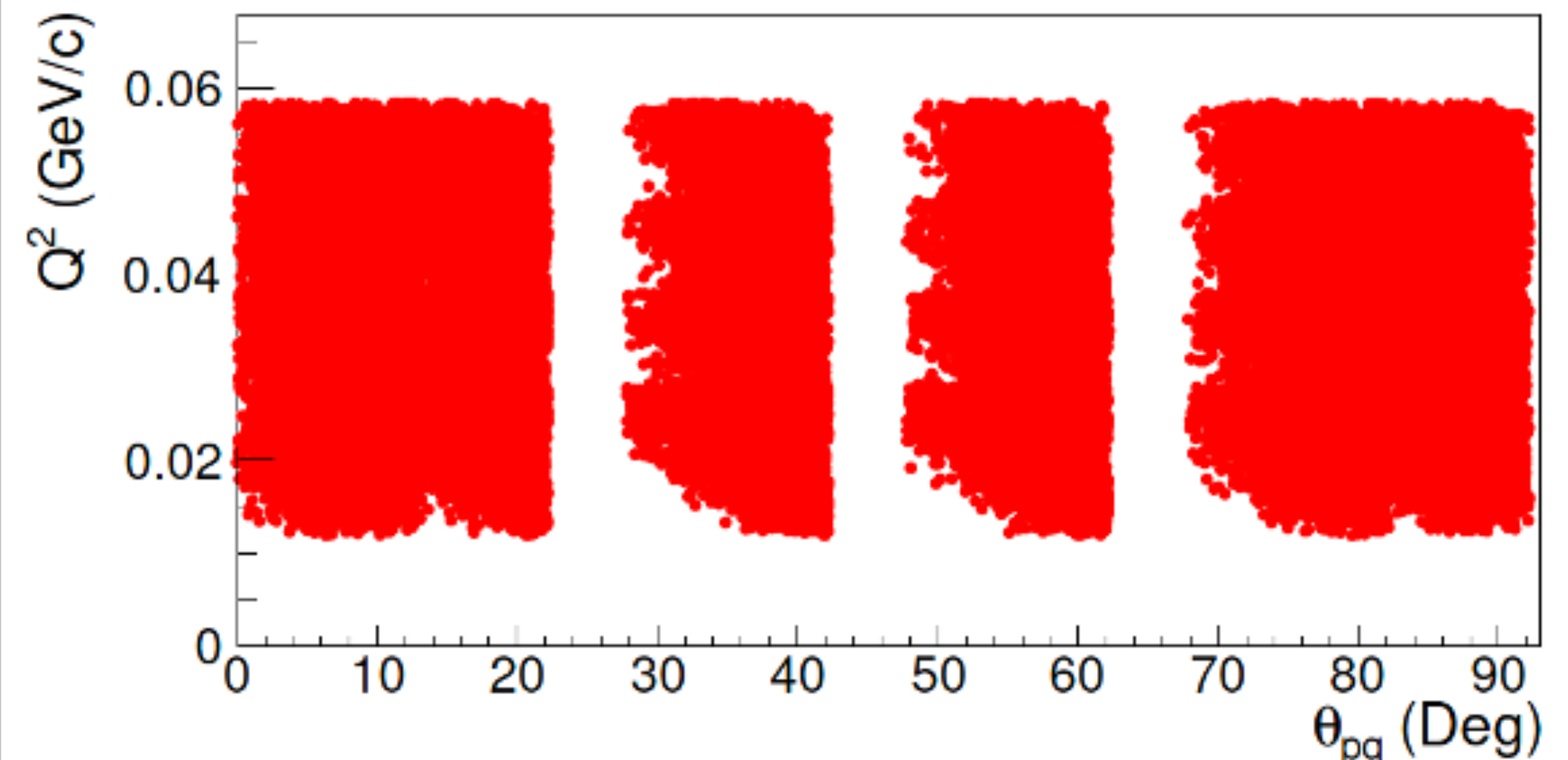
- Standard Hall-C equipment
 - 1300 MeV electron beam
 - Detect proton and electron in coincidence
 - Reconstruct pion from missing mass.



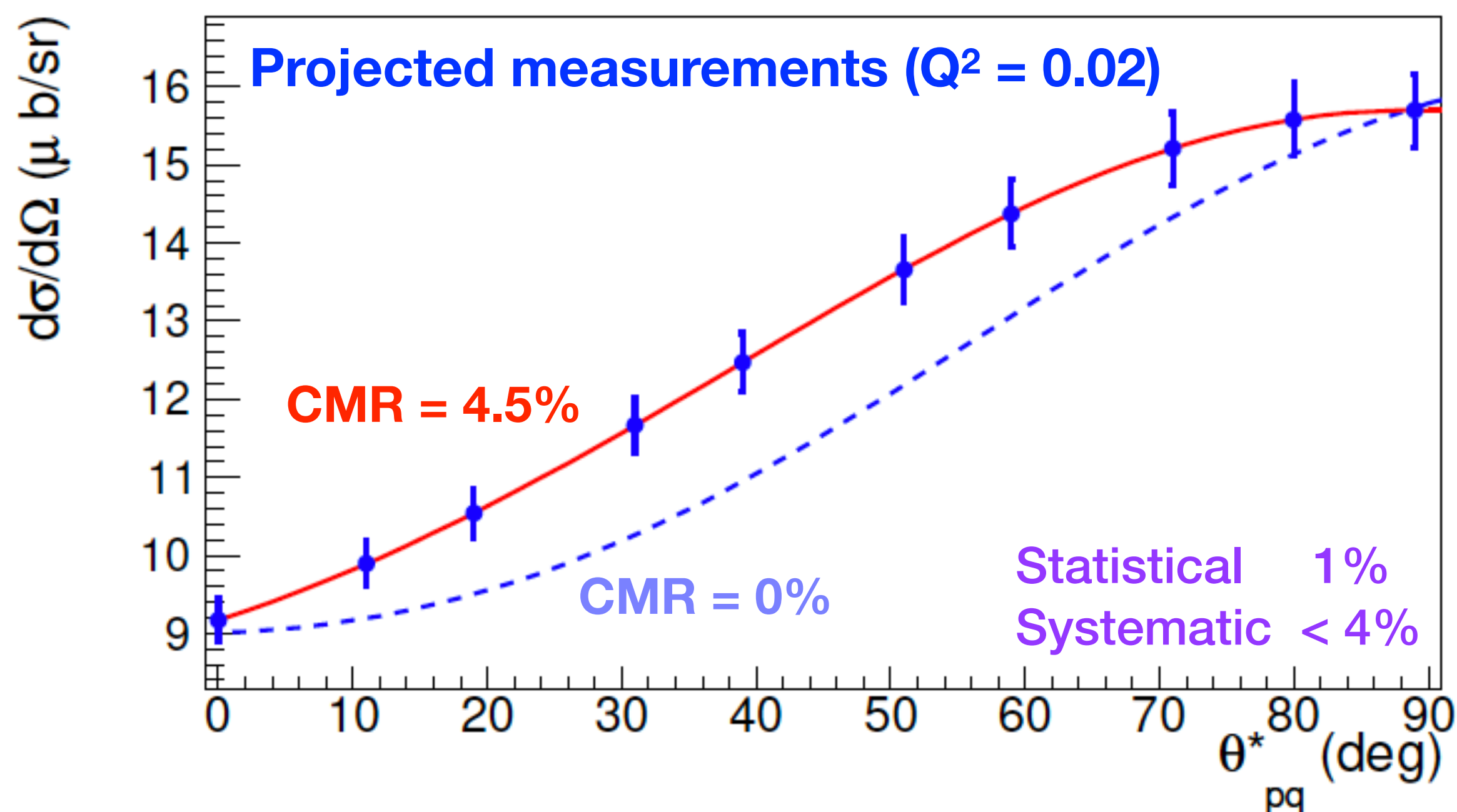
Measurement Settings

Setting	SHMS θ (deg)	SHMS P (MeV/c)	HMS θ (deg)	HMS P (MeV/c)	S/N	Time (hrs)
1a	7.29	952.26	18.77	532.53	2	7
2a			25.17	527.72	2	7
3a			33.7	506.61	3.2	6
4a			42.15	469.66	4.3	5
5a			50.44	418.56	4.9	5
6a			54.47	388.38	4.9	5
7a			12.37	527.72	2.7	6
1b	8.95	946.93	22.01	547.54	1.2	6
2b			28.24	542.61	1.4	6
3b			36.52	520.95	2.5	5
4b			44.64	483.08	3.4	4
5b			52.68	430.78	3.7	4
6b			56.53	399.92	3.5	4
7b			12.46	535.98	1.6	5
1c	10.37	941.61	24.40	562.00	1.5	9
2c			30.47	556.95	1.9	9
3c			38.52	534.79	3.5	6
4c			46.47	496.06	4.4	6
5c			54.17	442.64	4.8	6
6c			57.85	411.16	4.8	6
7c			12.69	543.24	2	6
1d	11.63	936.28	26.24	575.96	1.8	12
2d			32.16	570.80	2.5	11
3d			40.01	548.17	4.5	8
4d			47.73	508.64	5.5	8
5d			55.18	454.17	6.9	7
6d			58.71	422.13	6	8
7d			12.47	548.17	2.1	10

- Cover a Q^2 range of 0.015 to 0.055 (GeV/c)²
 - 28 arm configurations
 - Coverage for 9 Q^2 bins.
 - 8 days production
 - 3 days other (dummy, calibration, etc..)

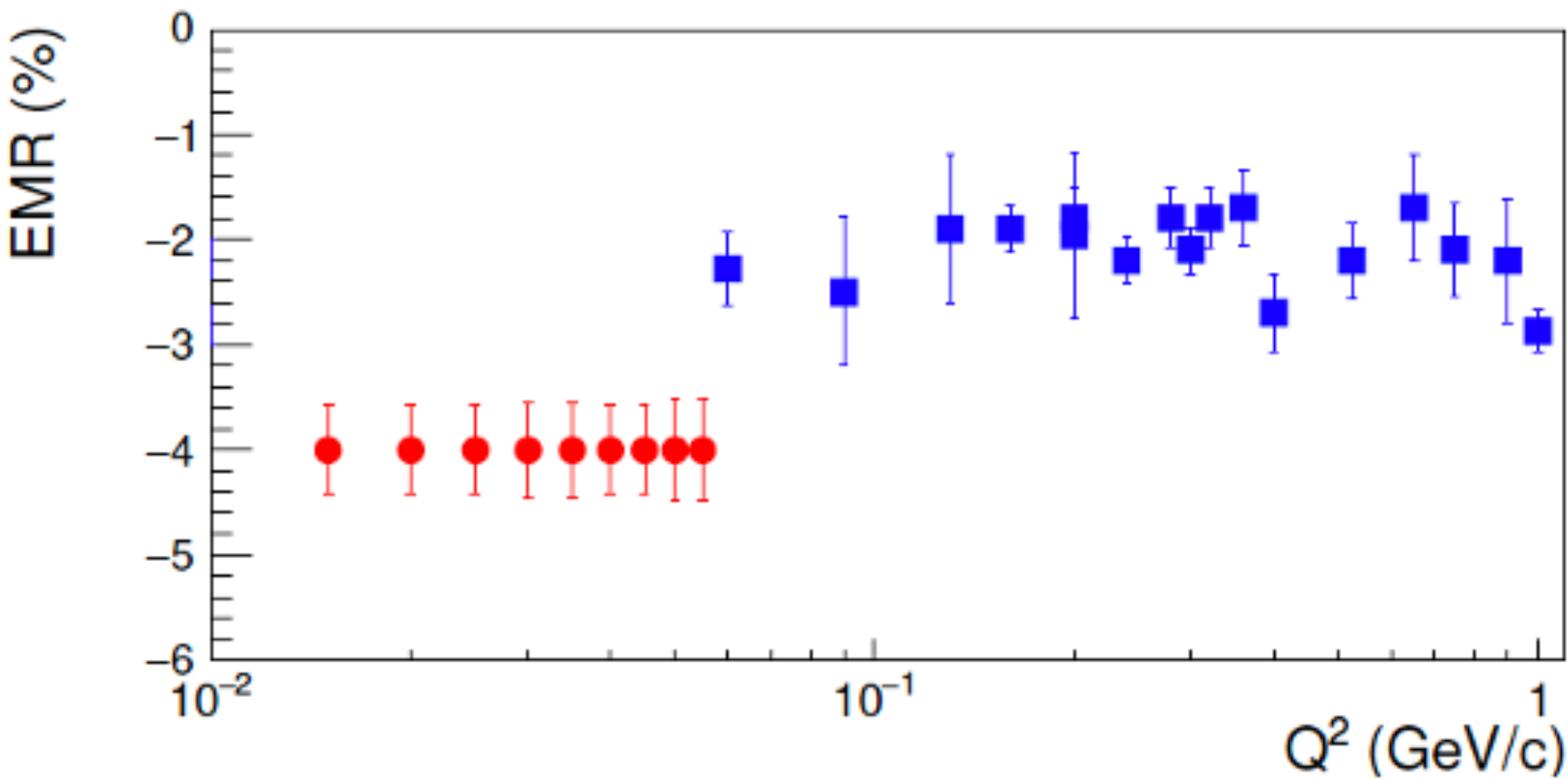
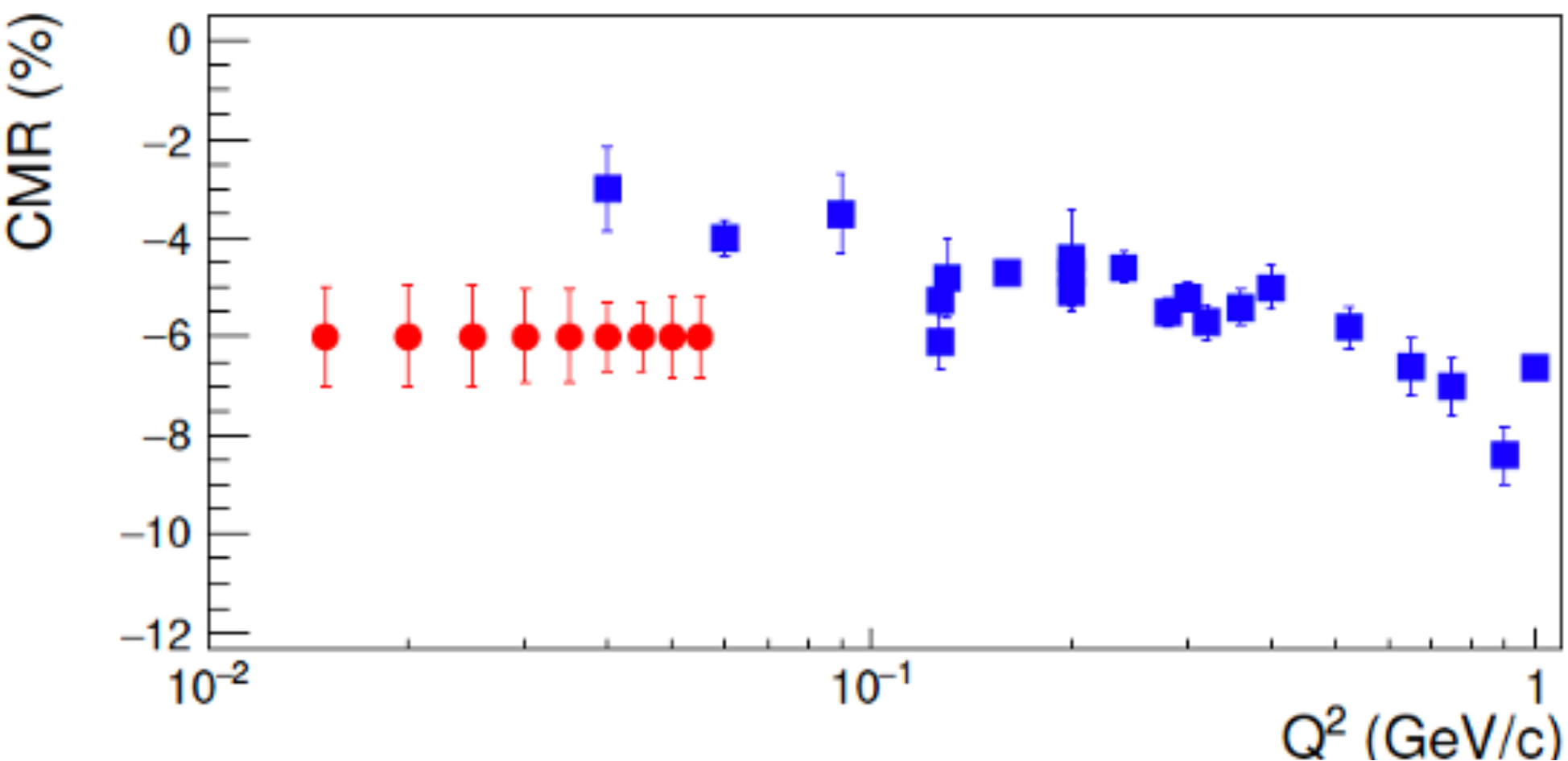


Projected CMR and EMR measurements

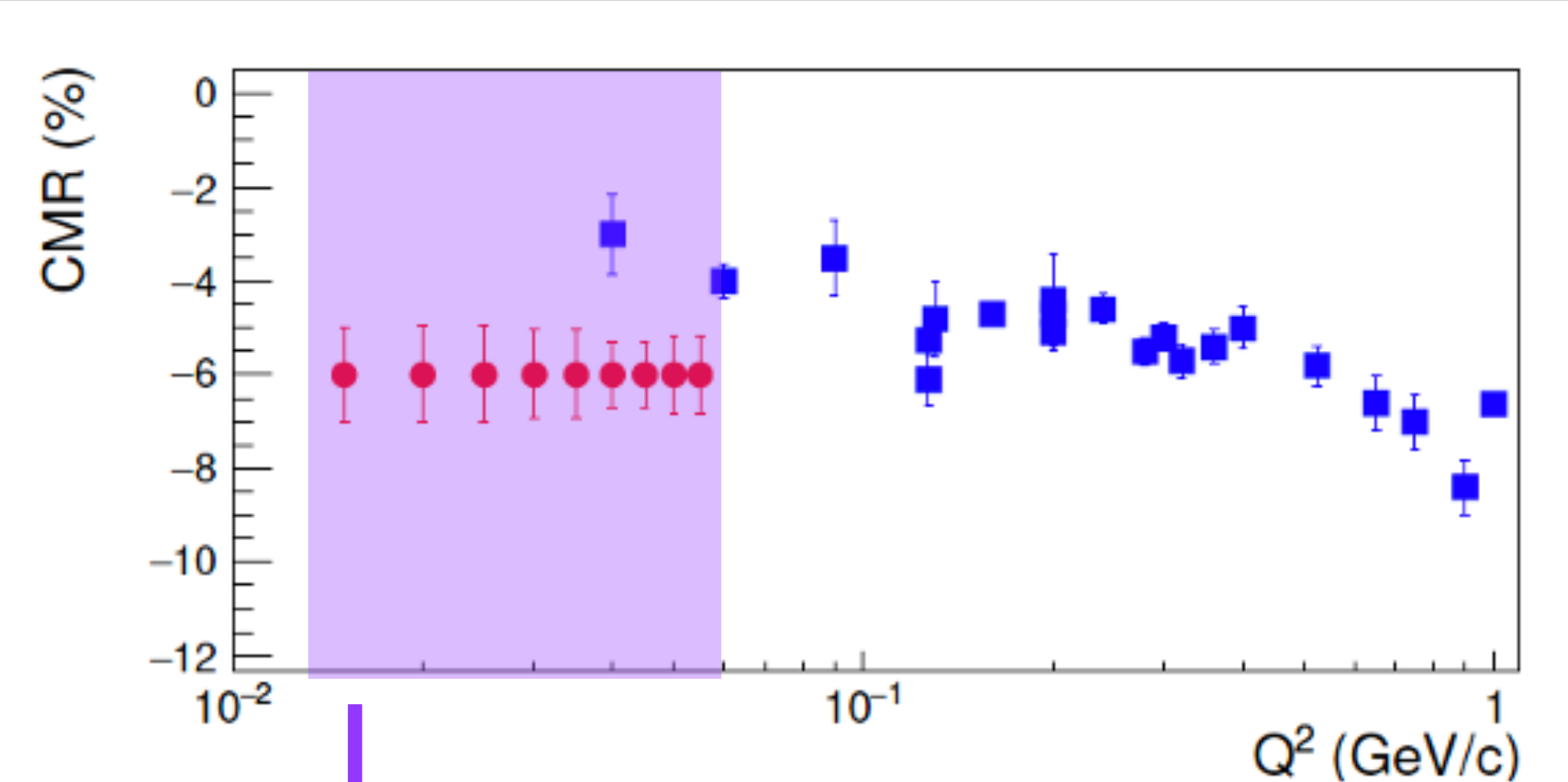
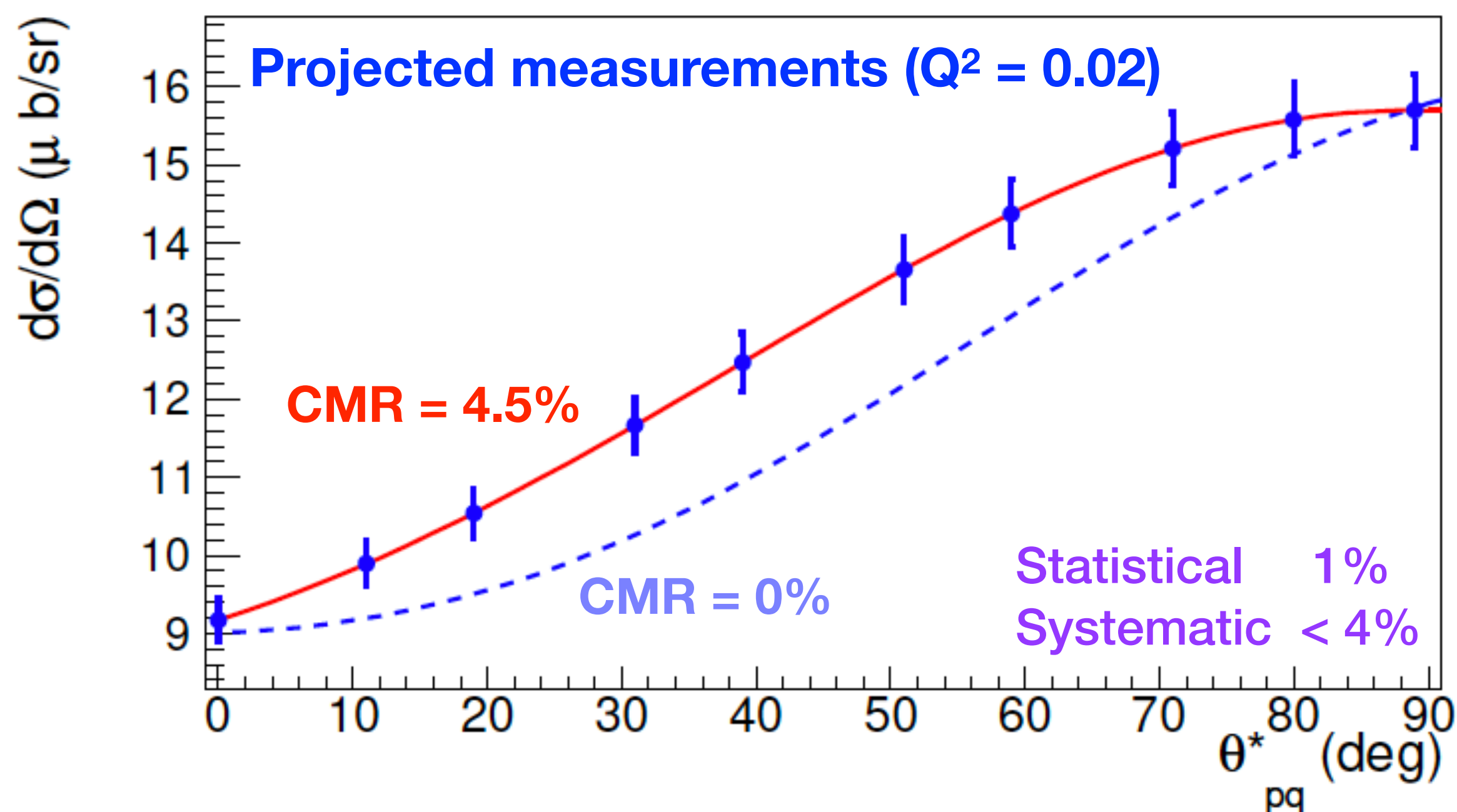


Resolution	2% - 3%
Acceptance	1%
Scattering angle	0.4% - 0.6%
Beam energy	0.7% - 1.2%
Beam charge	1%
Target density	0.5%
Detector efficiencies	0.5%
Target cell background	0.5%
Target length	0.5%
Dead-time corrections	0.5%
Total	2.8% - 3.8%

- High precision in very low Q^2 region that is sparsely populated
- Region where pion-cloud effects are expected to be prominent

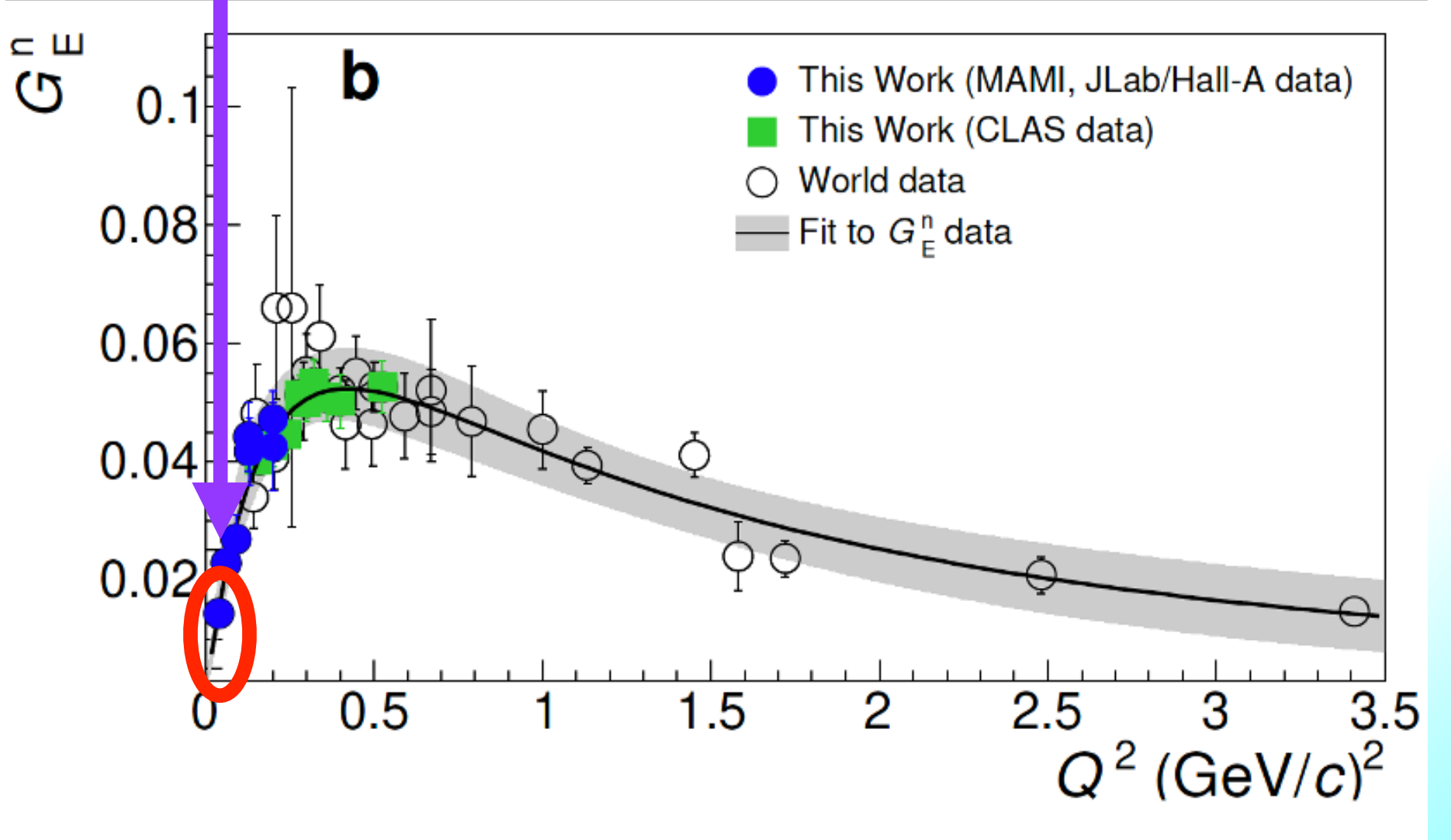


Projected CMR and EMR measurements

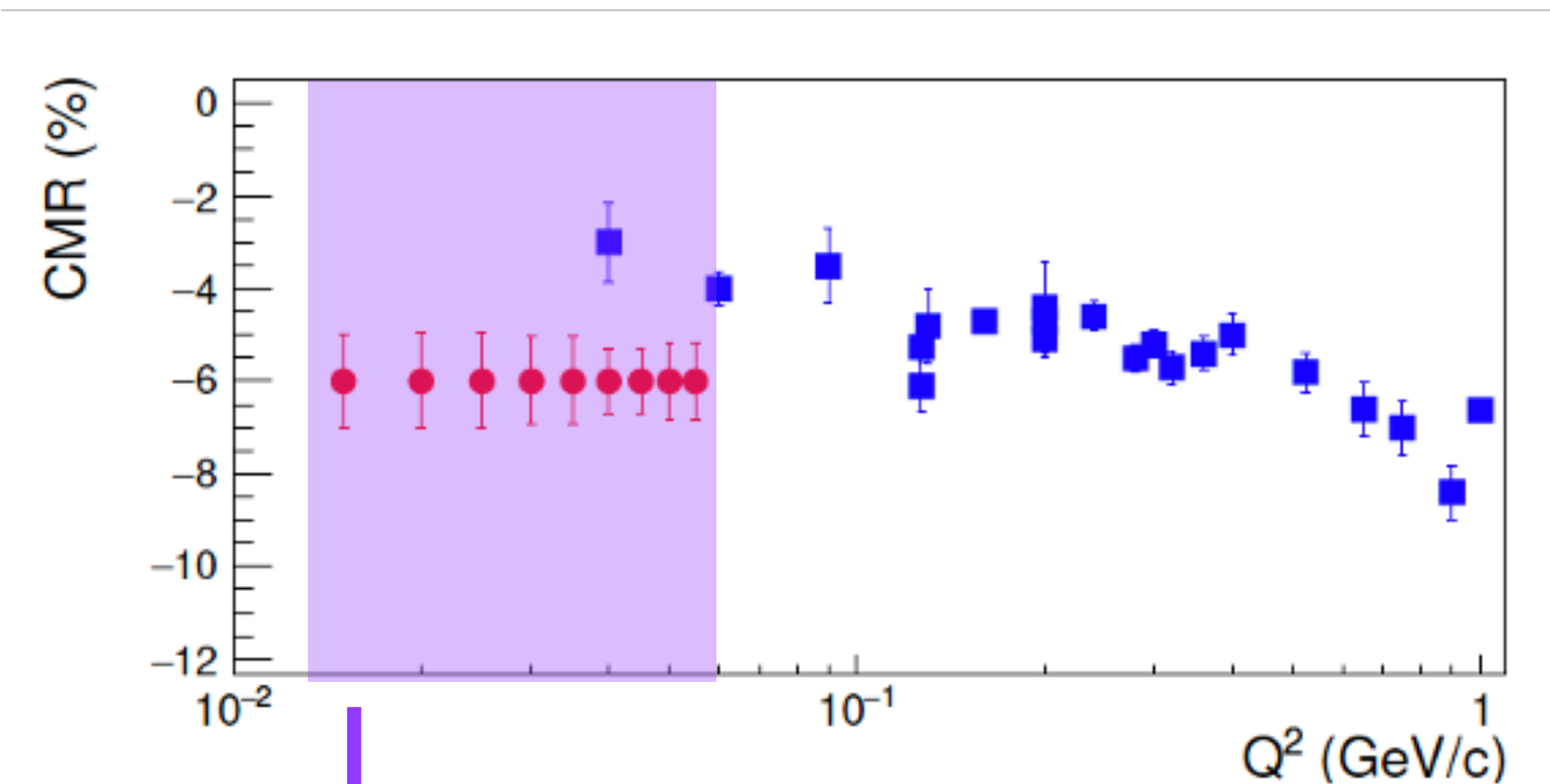
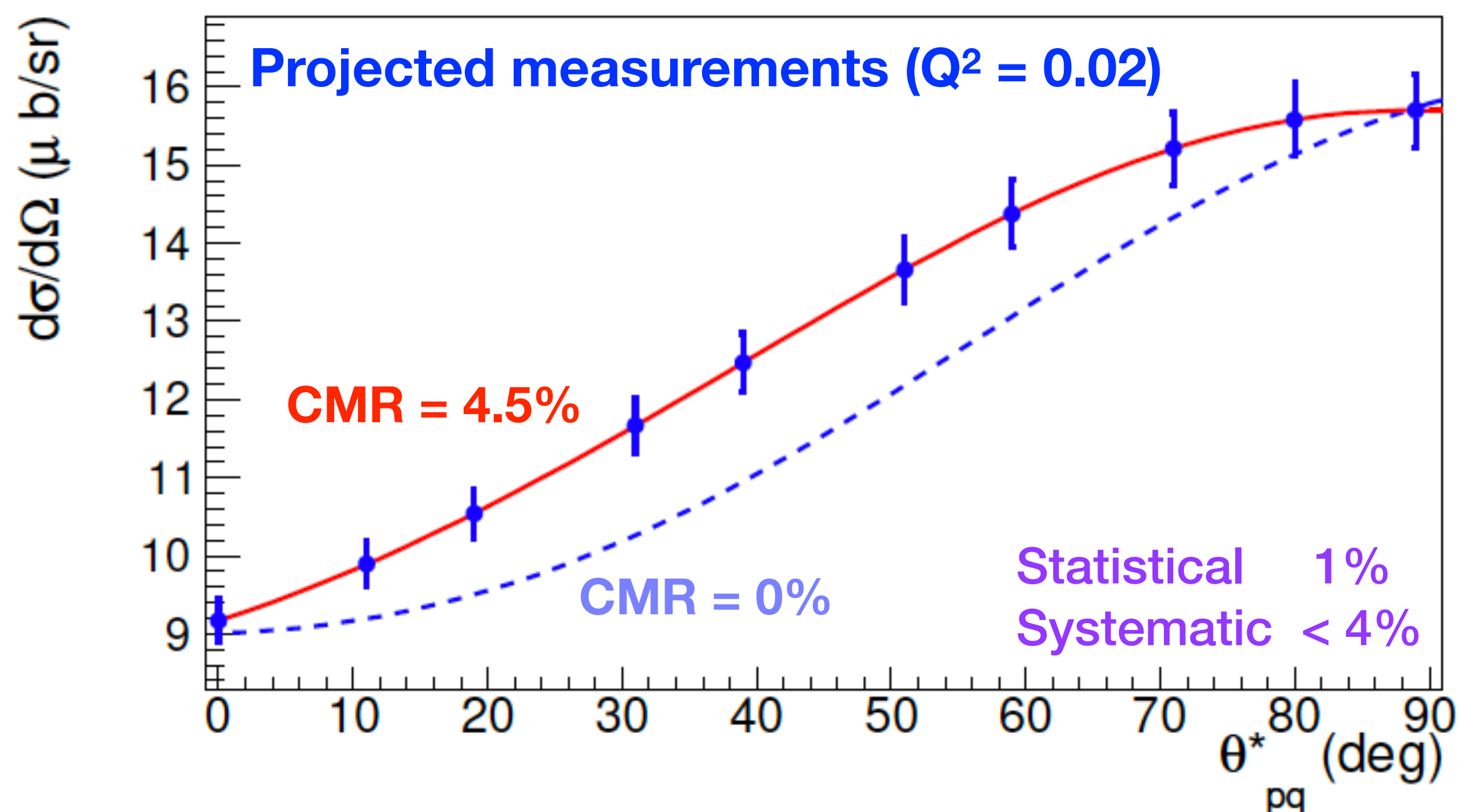


Resolution	2% - 3%
Acceptance	1%
Scattering angle	0.4% - 0.6%
Beam energy	0.7% - 1.2%
Beam charge	1%
Target density	0.5%
Detector efficiencies	0.5%
Target cell background	0.5%
Target length	0.5%
Dead-time corrections	0.5%
Total	2.8% - 3.8%

Proposed to PAC49:
Extraction of Neutron
Charge Radius

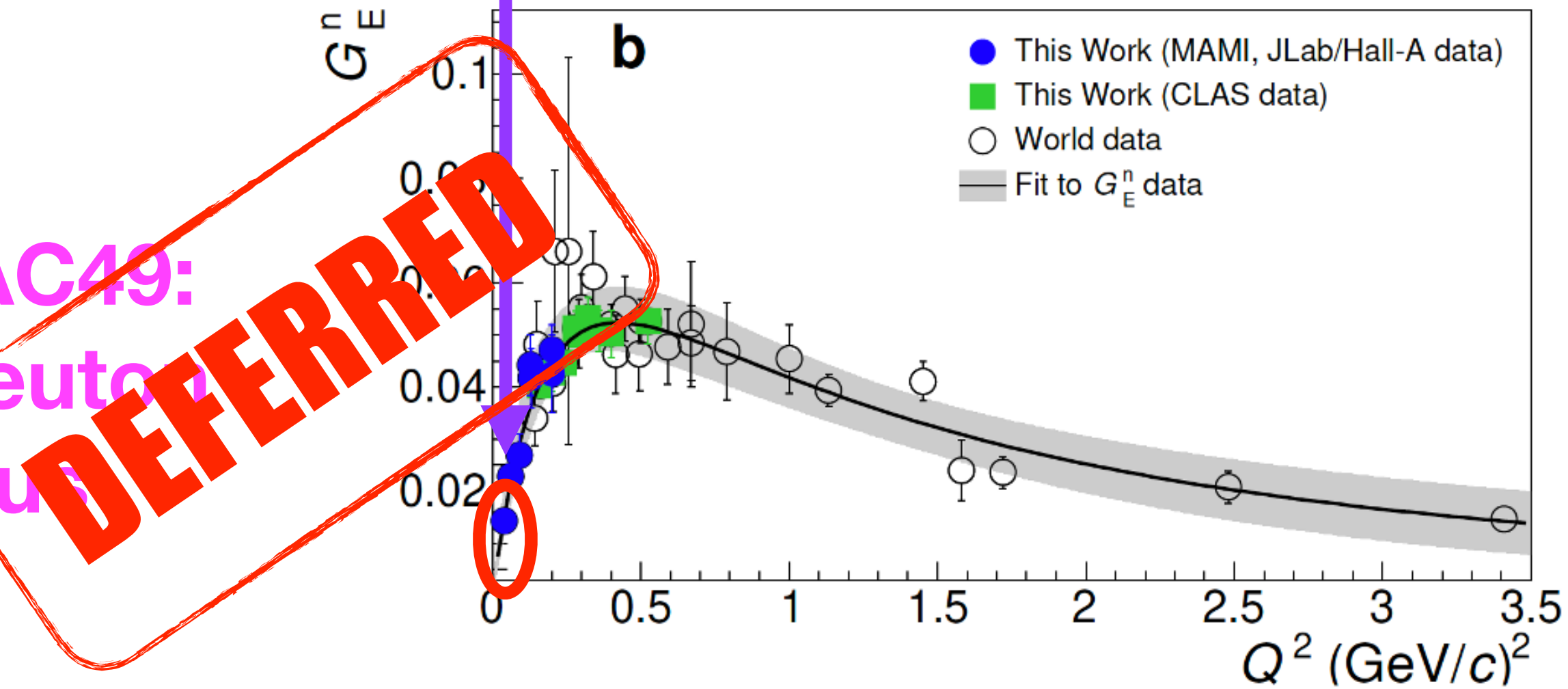


Projected CMR and EMR measurements

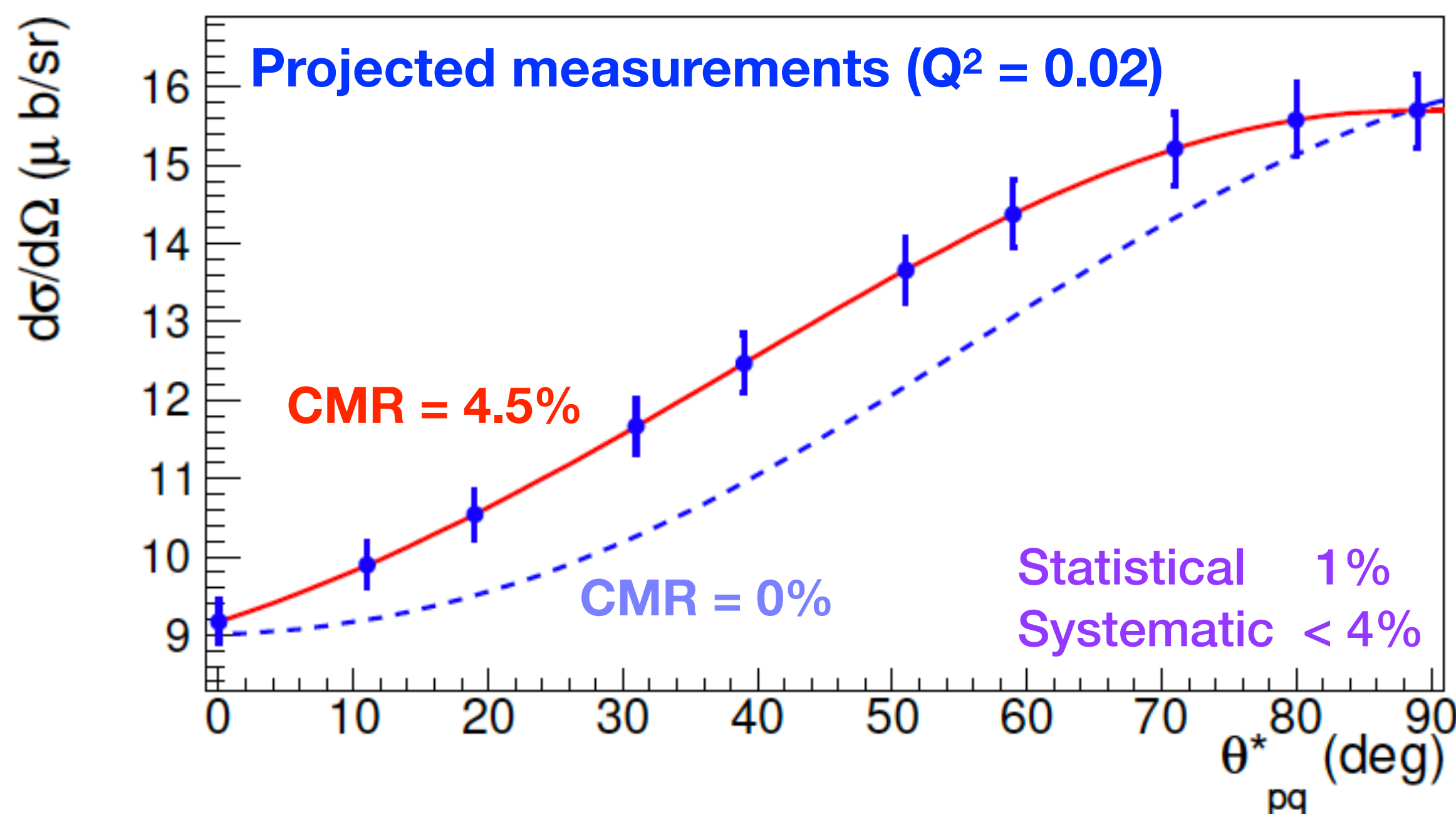


Resolution	2% - 3%
Acceptance	1%
Scattering angle	0.4% - 0.6%
Beam energy	0.7% - 1.2%
Beam charge	1%
Target density	0.5%
Detector efficiencies	0.5%
Target cell background	0.5%
Target length	0.5%
Dead-time corrections	0.5%
Total	2.8% - 3.8%

Proposed to PAC49:
Extraction of Neutron
Charge Radius

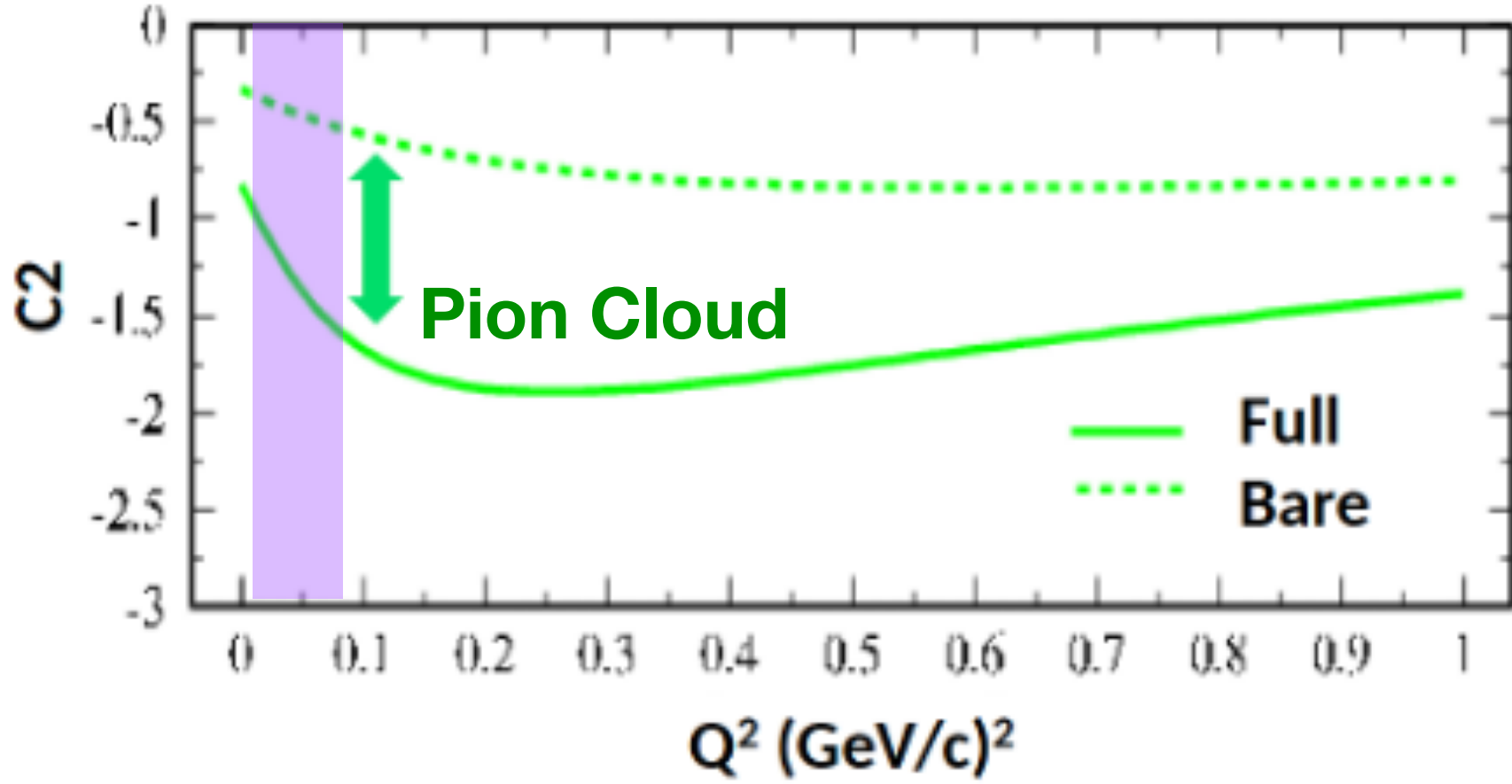
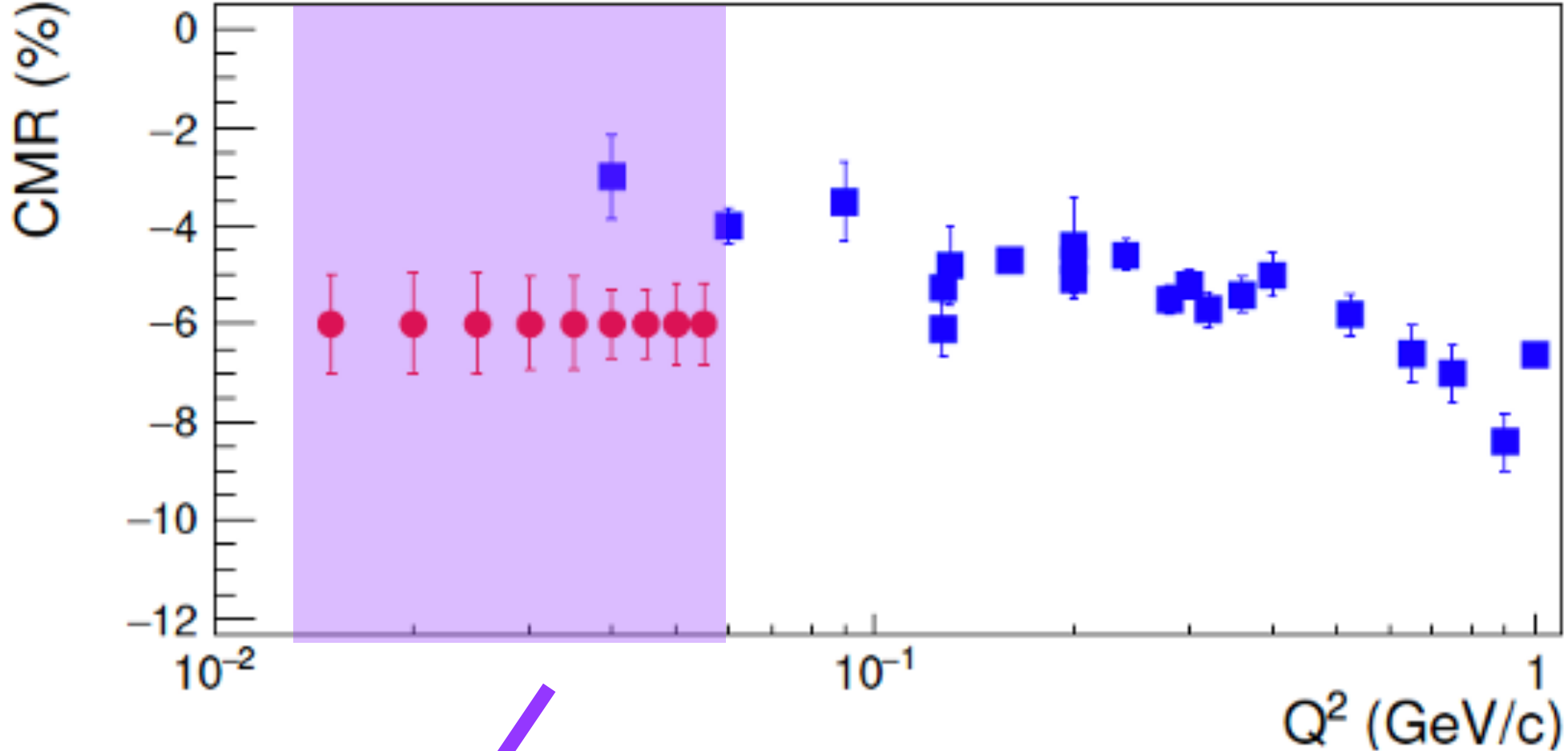


Projected CMR and EMR measurements

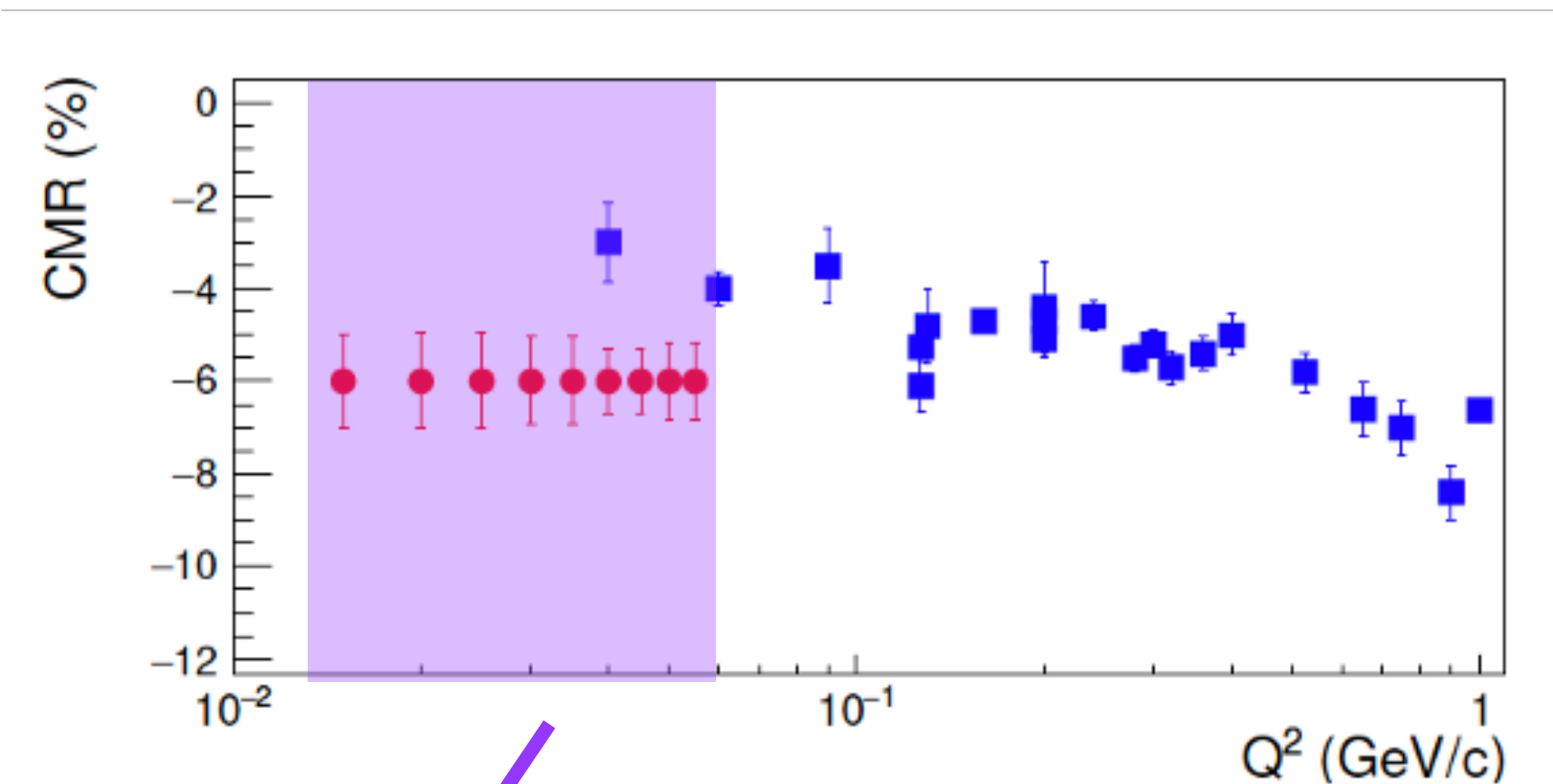
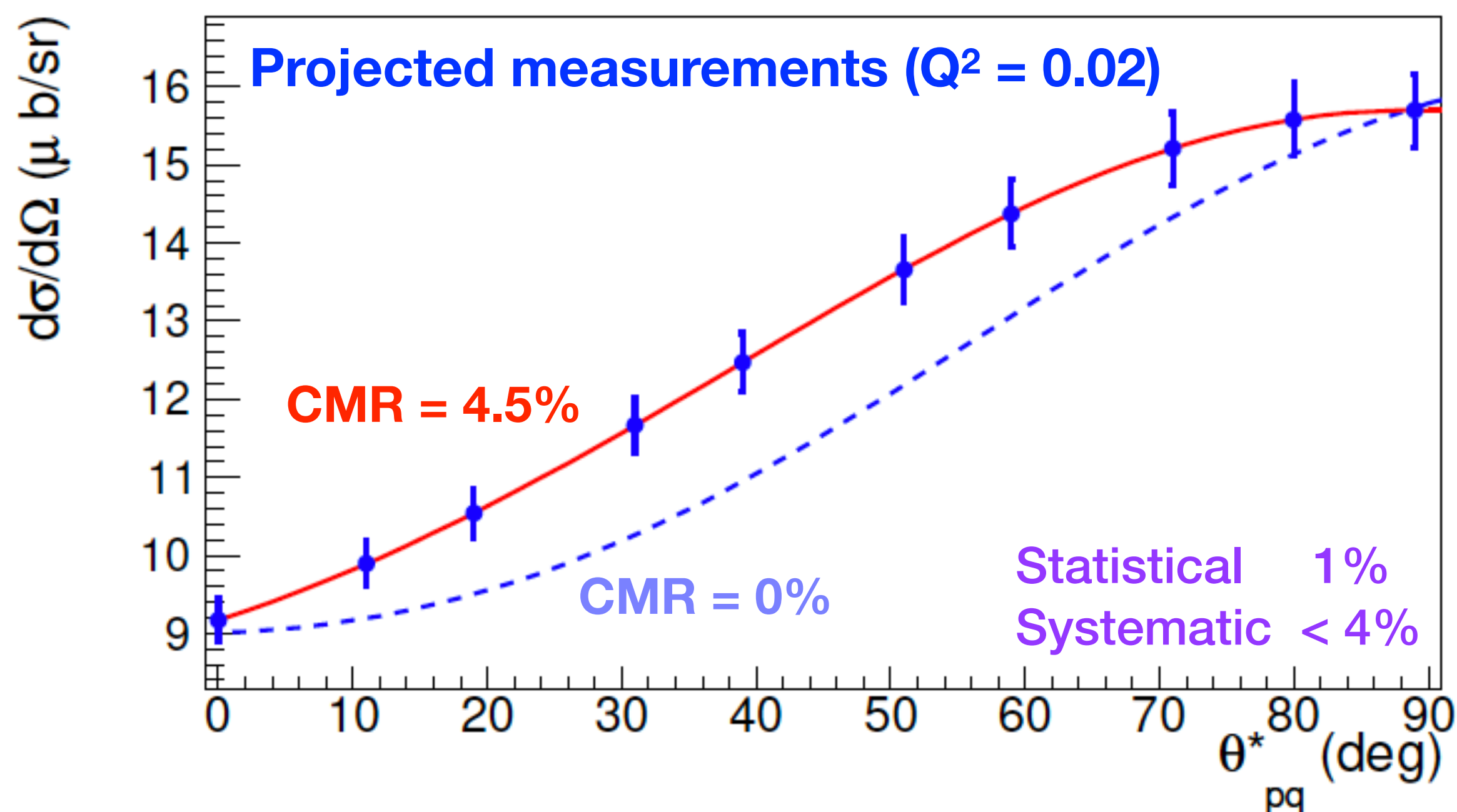


Resolution	2% - 3%
Acceptance	1%
Scattering angle	0.4% - 0.6%
Beam energy	0.7% - 1.2%
Beam charge	1%
Target density	0.5%
Detector efficiencies	0.5%
Target cell background	0.5%
Target length	0.5%
Dead-time corrections	0.5%
Total	2.8% - 3.8%

**Proposed to PAC50:
Extraction of TFFs at
low Q^2**



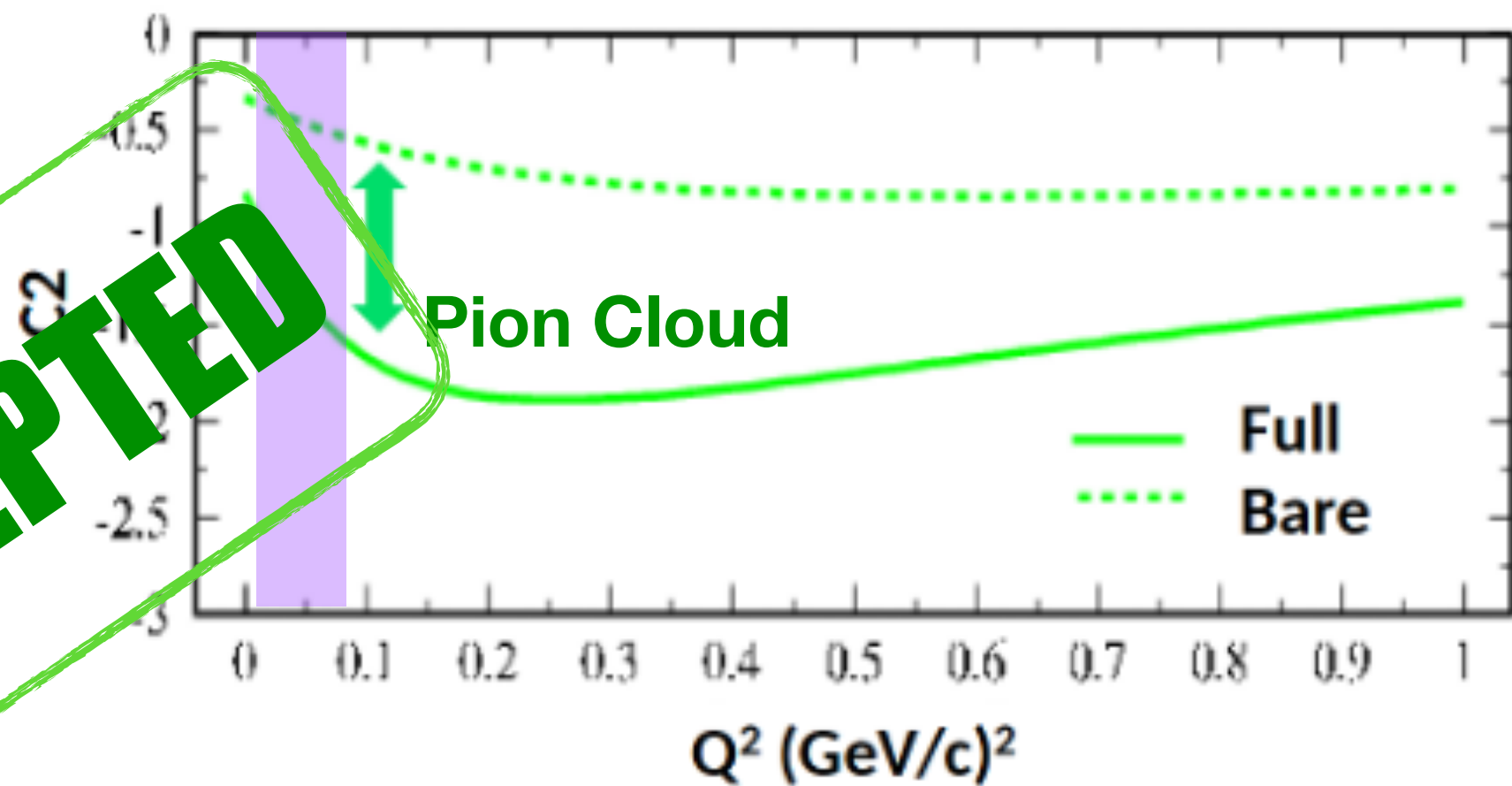
Projected CMR and EMR measurements



Resolution	2% - 3%
Acceptance	1%
Scattering angle	0.4% - 0.6%
Beam energy	0.7% - 1.2%
Beam charge	1%
Target density	0.5%
Detector efficiencies	0.5%
Target cell background	0.5%
Target length	0.5%
Dead-time corrections	0.5%
Total	2.8% - 3.8%

Proposed to PAC50:
Extraction of TFFs at
low Q^2

ACCEPTED



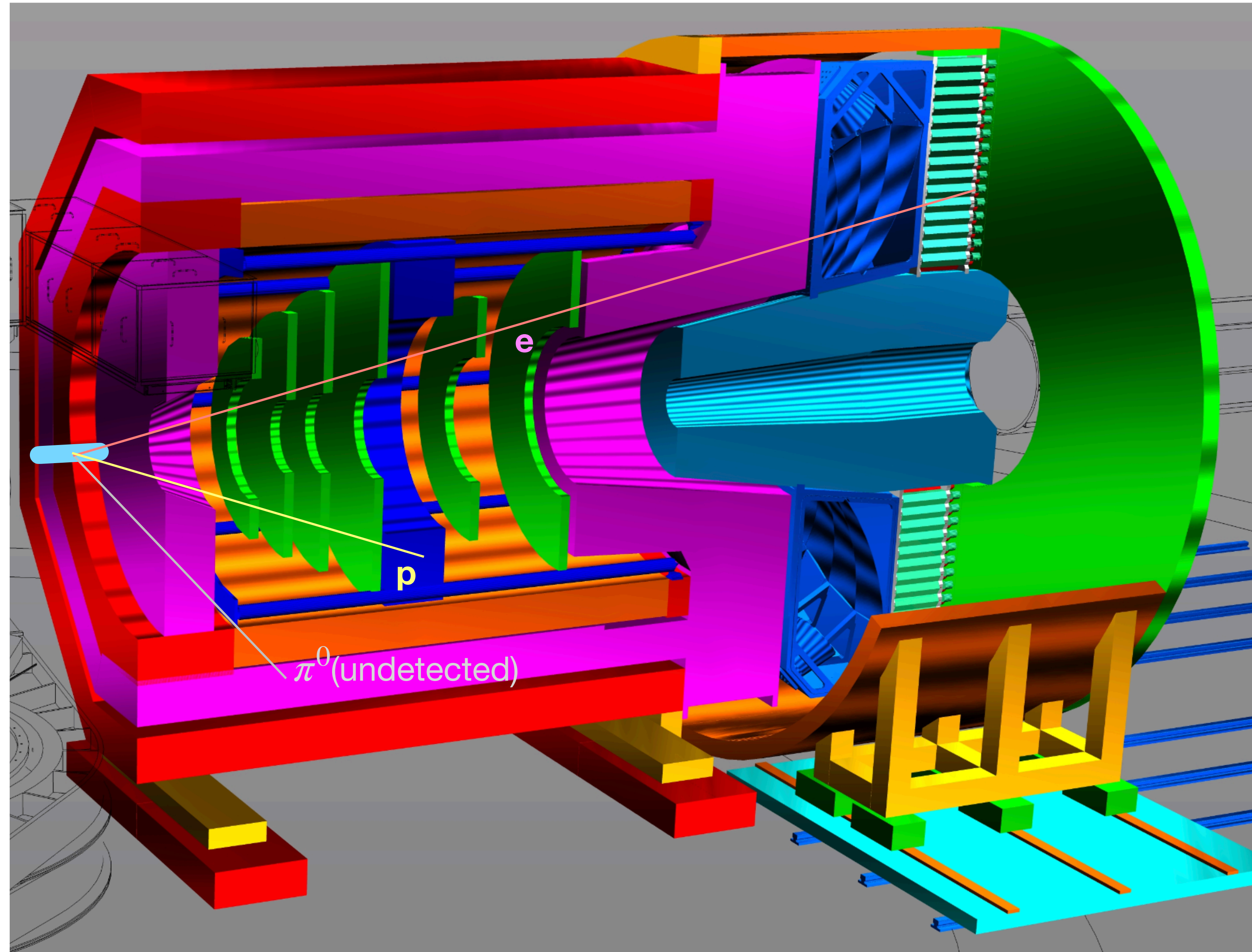
11 days, to run sometime in the “near” future.

Future Analyses at JLab

- CLAS12 has single-pion production coverage up to $Q^2 = 12 \text{ GeV}^2$ over a large range of W .
 - Program focused on large range Nucleon excitation resonances.
 - Specific sensitivity of expected data to EMR and CMR extraction is unclear.
 - How does low-luminosity affect rates at large Q^2 ?
- SoLID:
 - Can detect azimuthal 2π with high luminosity:
 - Limited somewhat by polar angle acceptance and resolution

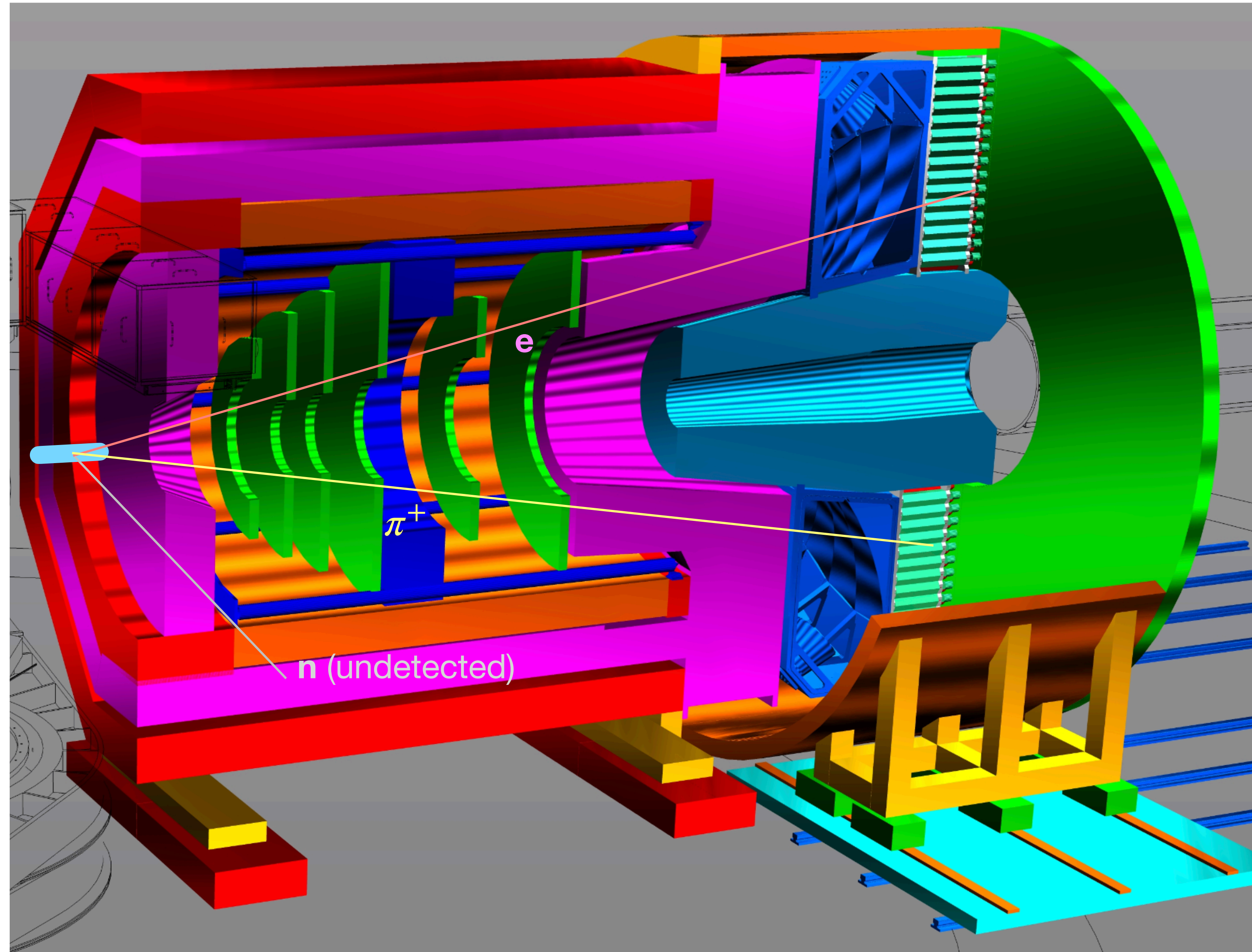
TFFs with SoLID at JLab (J/psi Set-up)

- 15 cm LH2 target
- 11.0 GeV beam Energy
- Luminosity = $10^{37} \text{ N cm}^{-2} \text{ s}^{-1}$
- 4 possible kinematics:
 - $p - \pi^0$
 - Electron detected w small angle
 - Electron detected w large angle
 - $n - \pi^+$
 - Electron detected w small angle
 - Electron detected w large angle



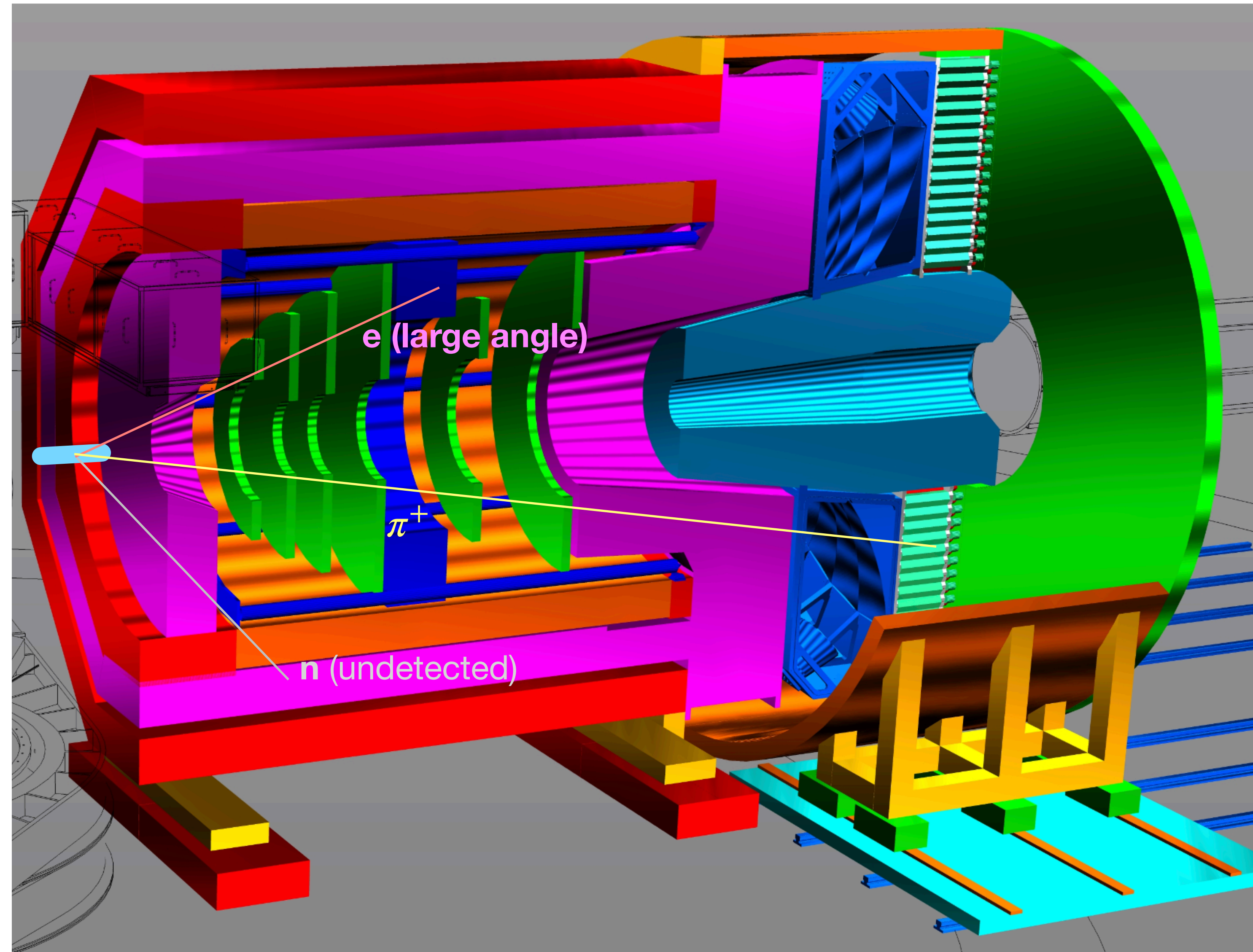
TFFs with SoLID at JLab (J/psi Set-up)

- 15 cm LH2 target
- 11.0 GeV beam Energy
- Luminosity = $10^{37} \text{ N cm}^{-2} \text{ s}^{-1}$
- 4 possible kinematics:
 - $p - \pi^0$
 - Electron detected w small angle
 - Electron detected w large angle
 - $n - \pi^+$
 - Electron detected w small angle
 - Electron detected w large angle



TFFs with SoLID at JLab (J/psi Set-up)

- 15 cm LH2 target
- 11.0 GeV beam Energy
- Luminosity = $10^{37} \text{ N cm}^{-2} \text{ s}^{-1}$
- 4 possible kinematics:
 - $p - \pi^0$
 - Electron detected w small angle
 - Electron detected w large angle
 - $n - \pi^+$
 - Electron detected w small angle
 - Electron detected w large angle



TFFs with SoLID at JLab (J/psi Set-up)

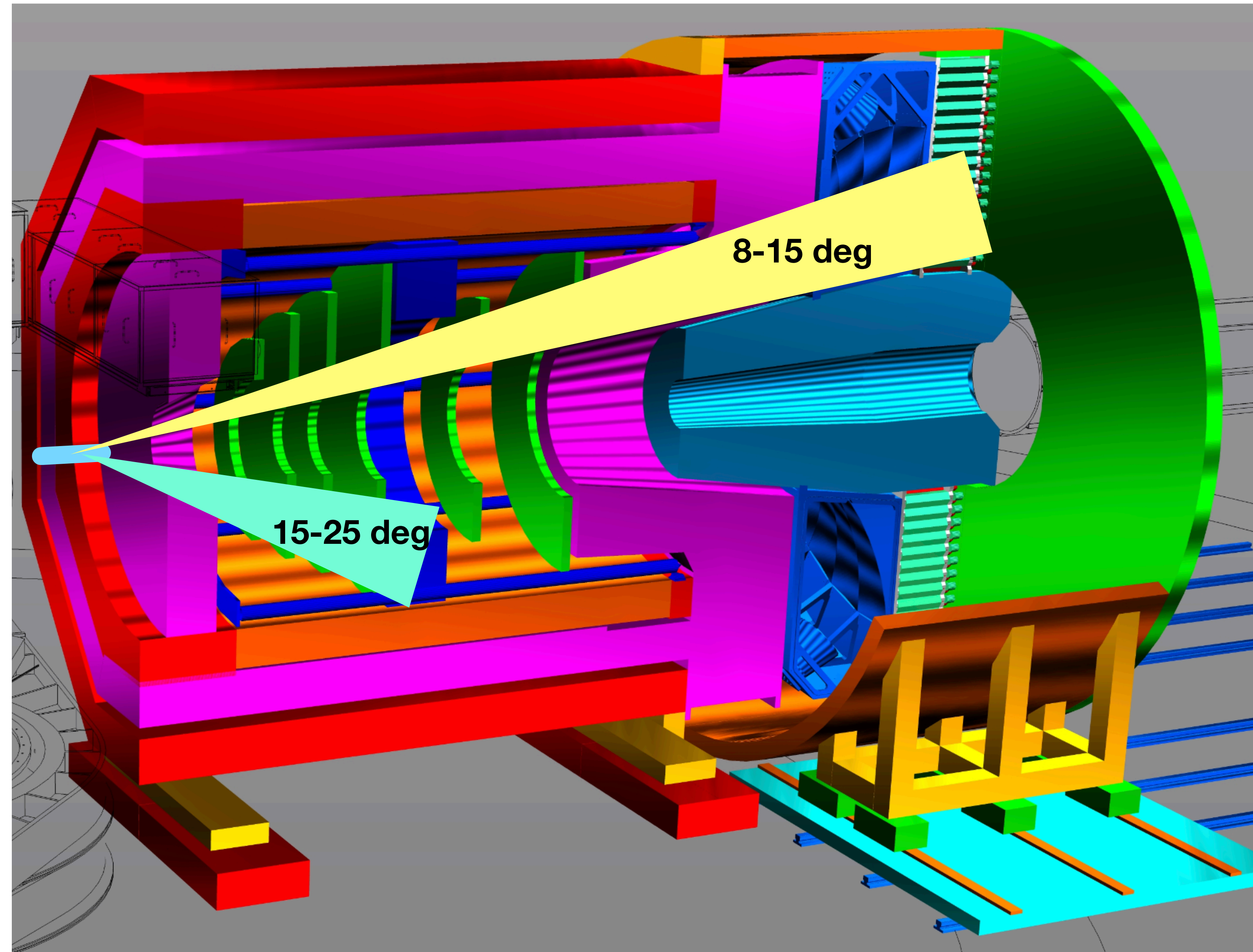
- Small angle electrons vs large angle electrons:

- Advantages for small angle:

- Better resolutions
- LGC for PID
- Standard Trigger Setup
- Better systematics

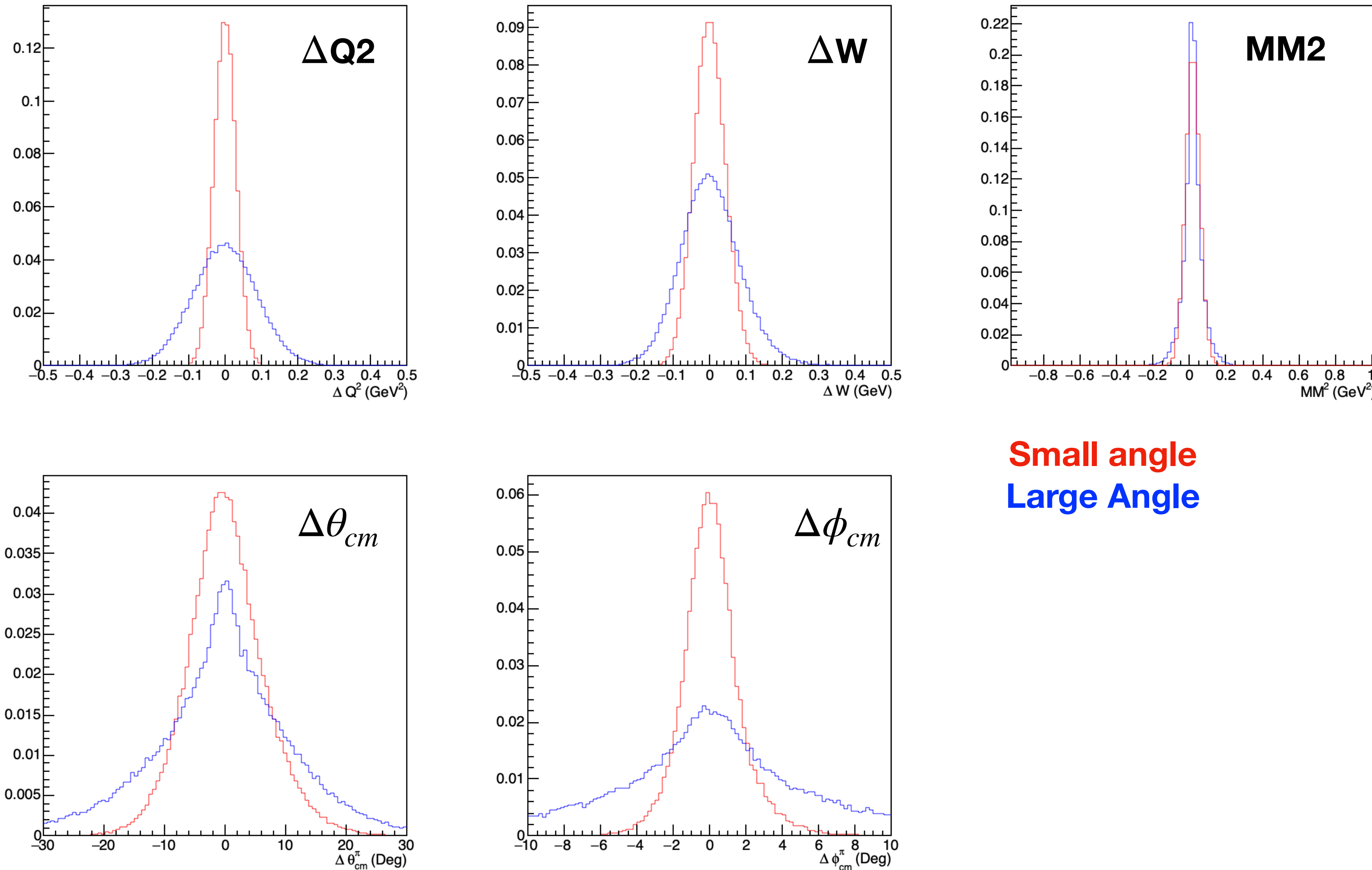
- Advantages for large angle:

- Higher Q2 reach
- Better θ_{cm} and ϕ_{cm} coverage



TFFs with SoLID at JLab (J/psi Set-up)

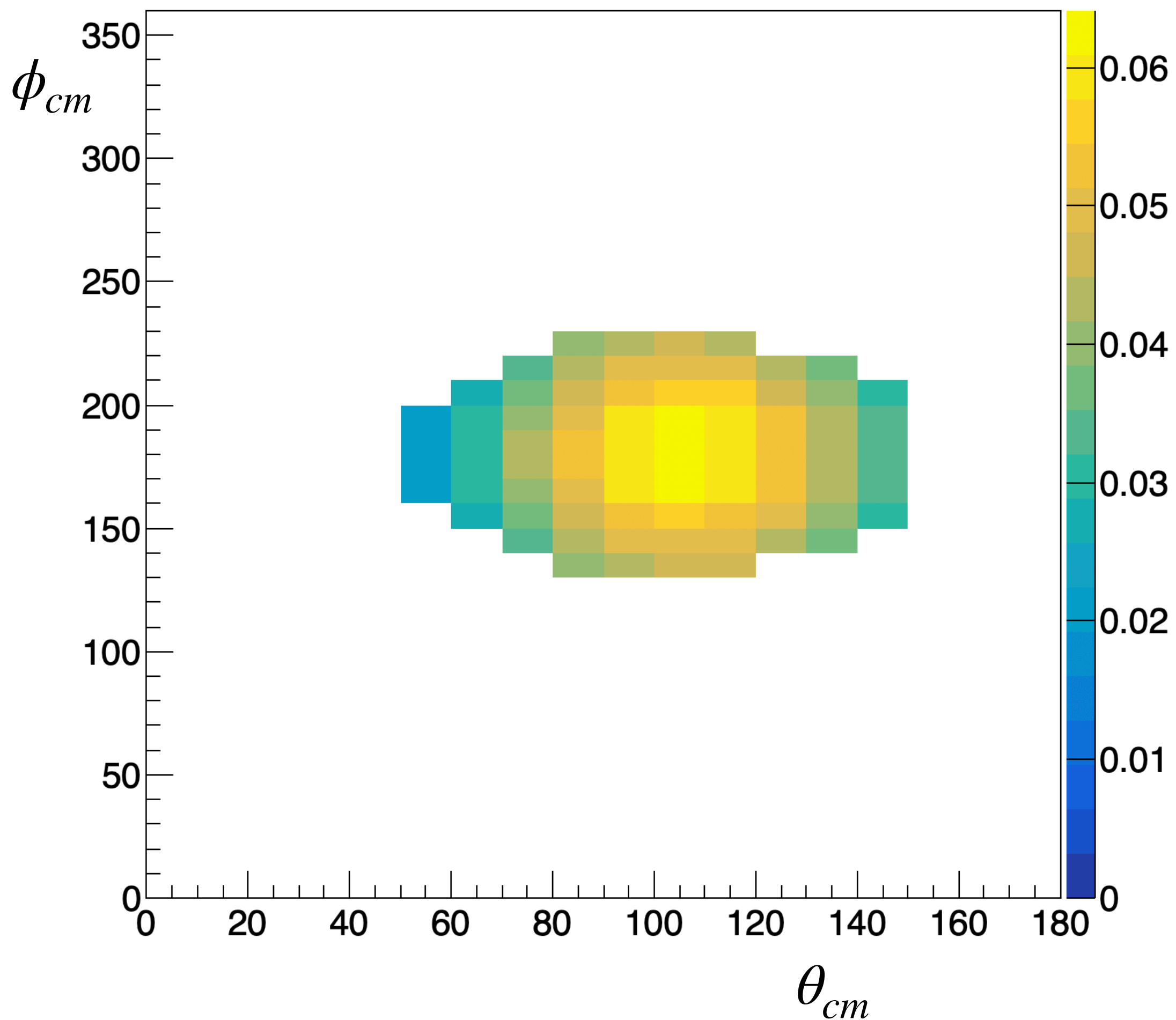
- Resolutions of large angle vs small angle electron detection (Tracking only)



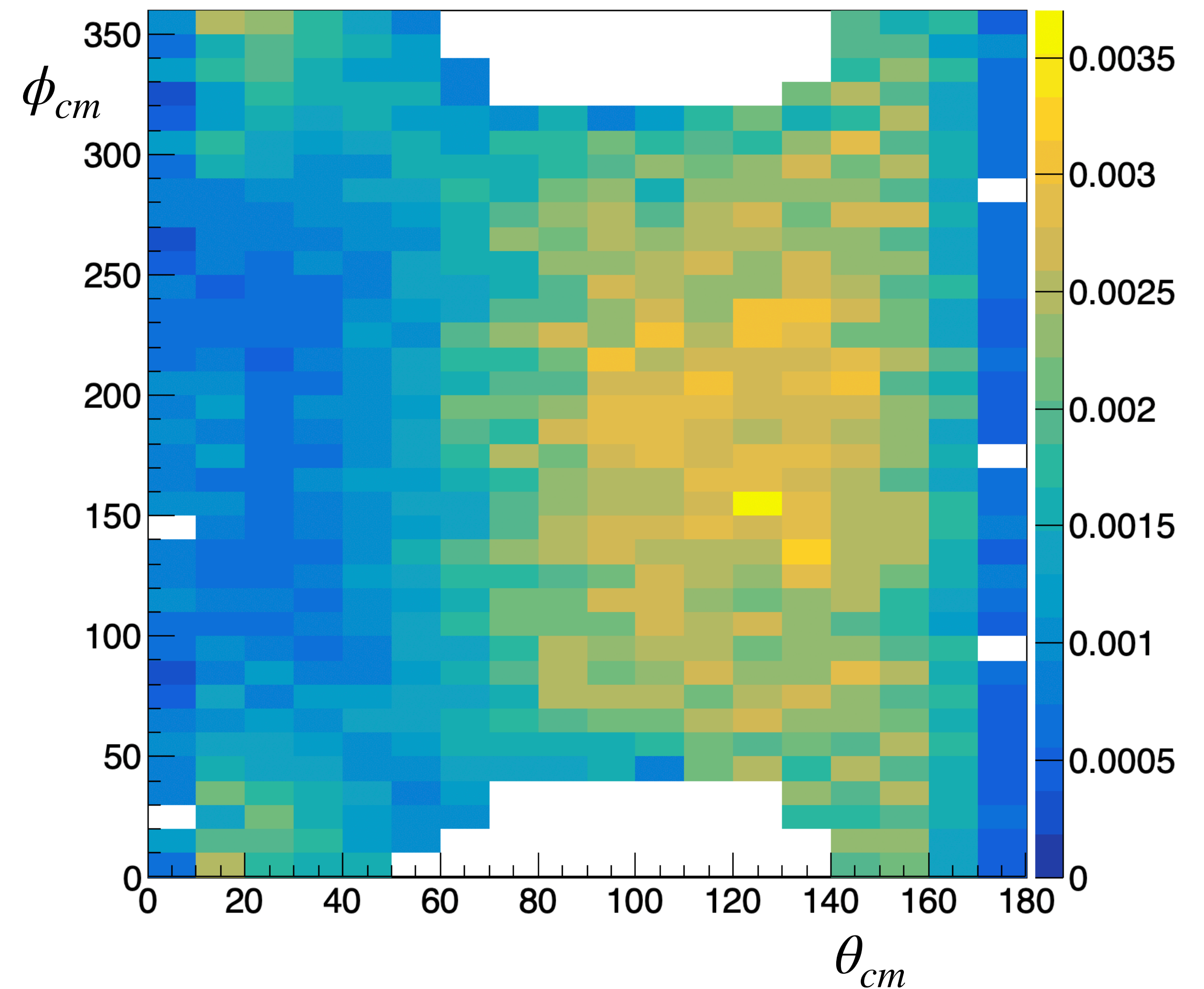
TFFs with SoLID at JLab (J/psi Set-up)

○ θ_{cm} and ϕ_{cm} coverage

Small angle electrons: Q2 = 5.7 GeV

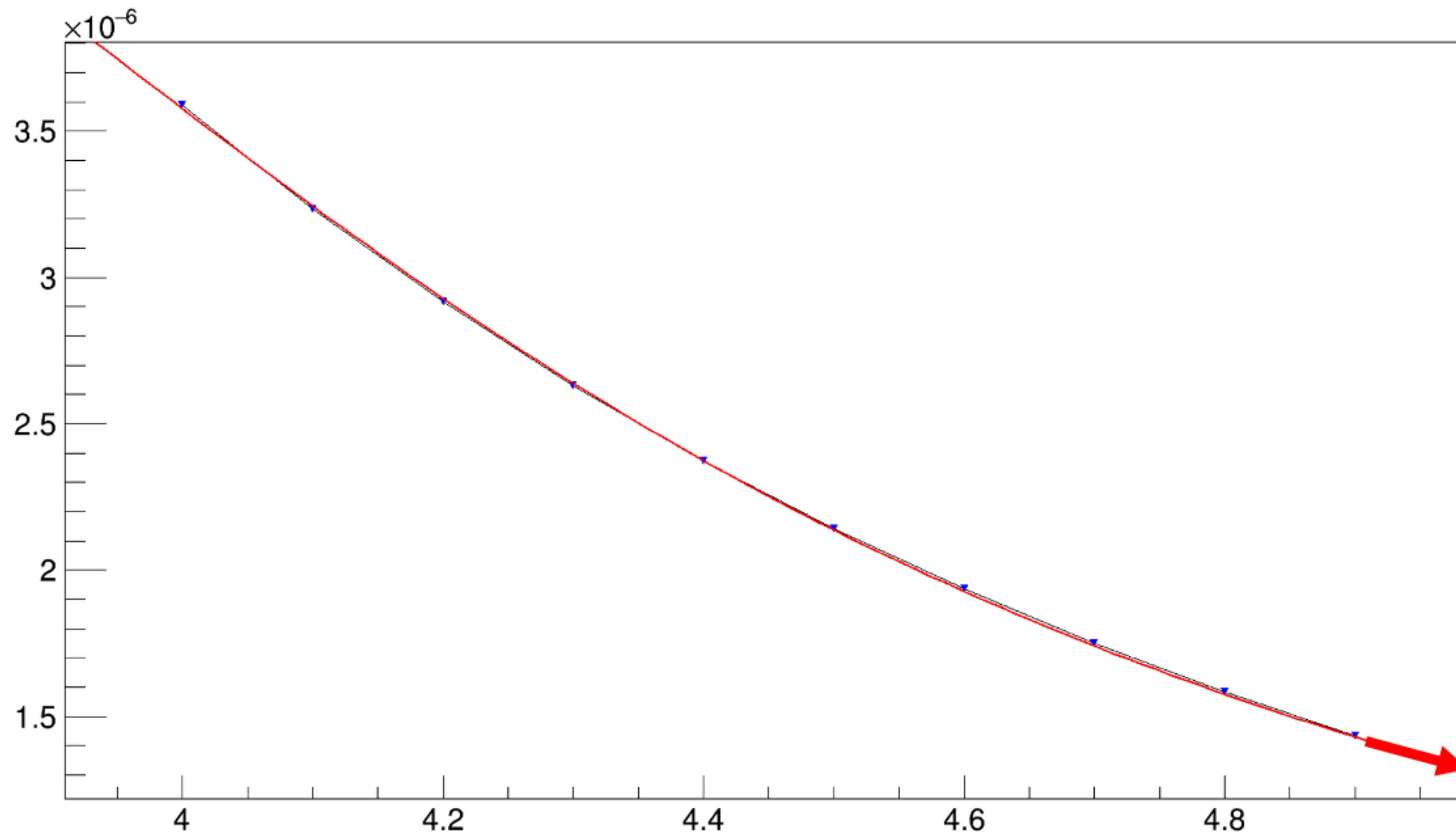


Large angle electrons: Q2 = 8.0 GeV



Cross-Section Extrapolations

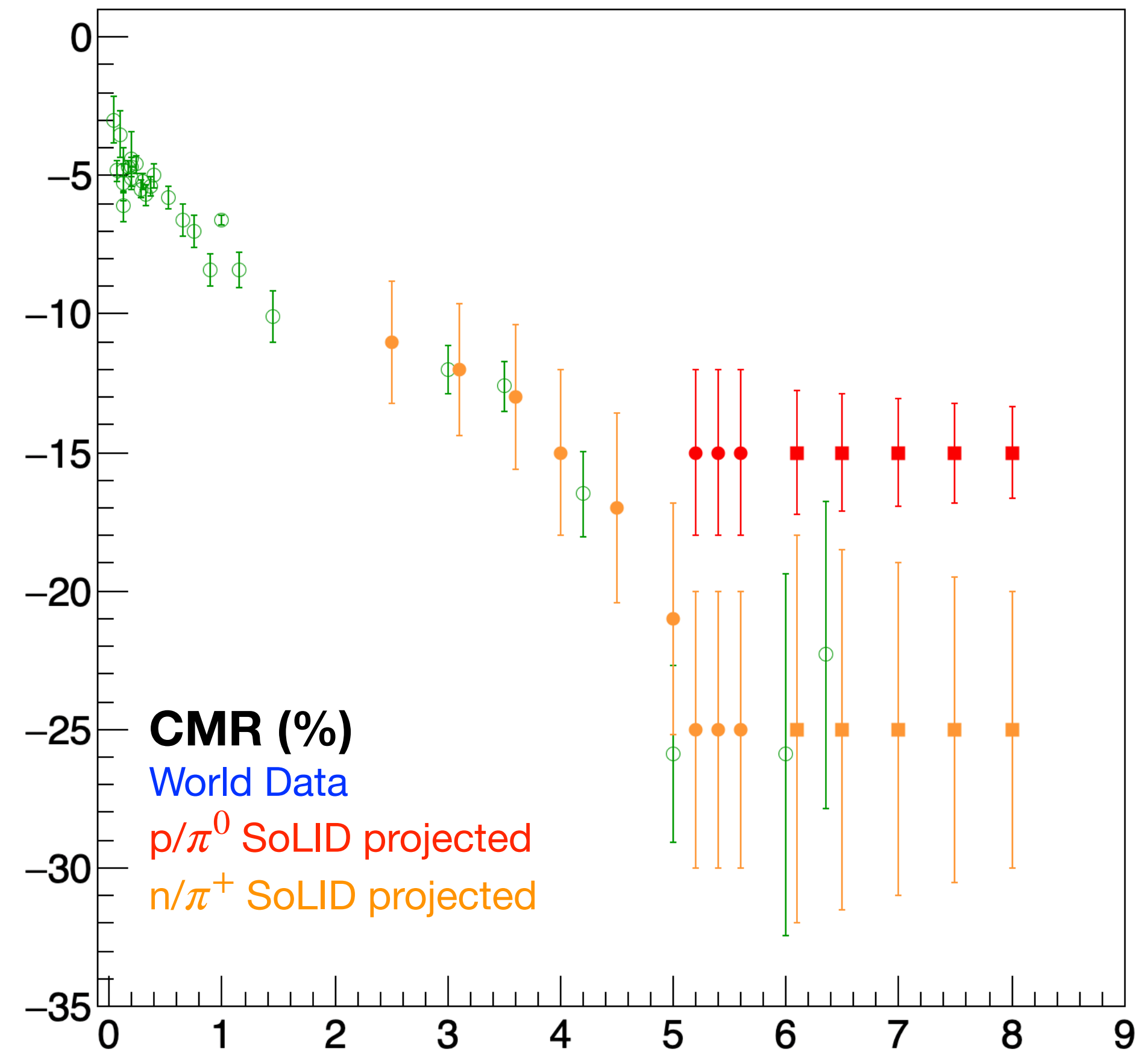
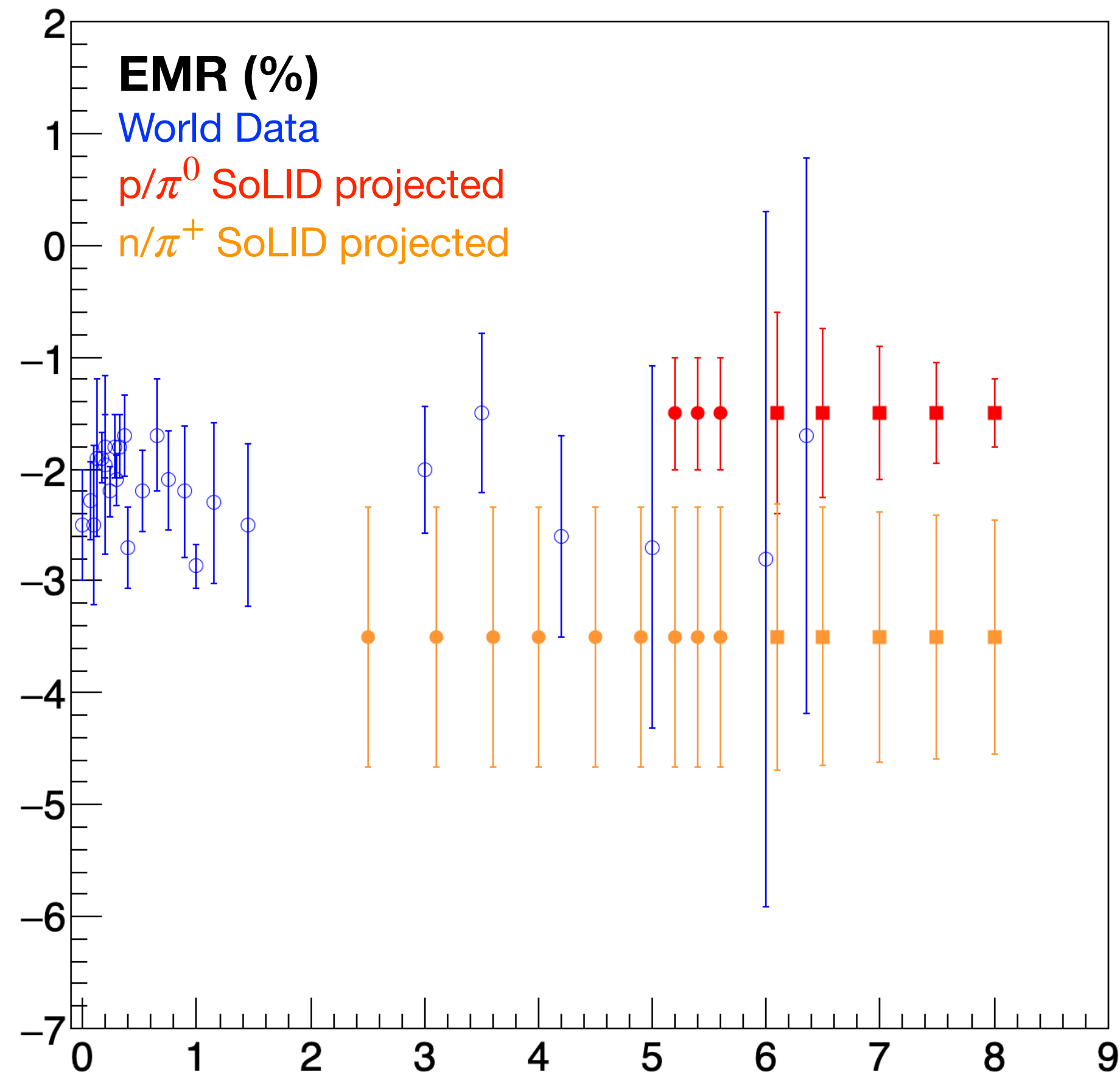
- MAID used for rate estimations, but only provides calculations up to $Q^2 = 5.0$
 - For $Q^2 > 5.0$
 - Fix W , θ_{cm} , π_{cm}
 - Allow beam and scattered energy to scale to obtain cross-sections below $Q^2 = 5.0$
 - Fit trend and extrapolate to higher Q^2 :



Where MAID and SAID disagree at $Q^2 = 5$, take more conservative cross-section in estimates

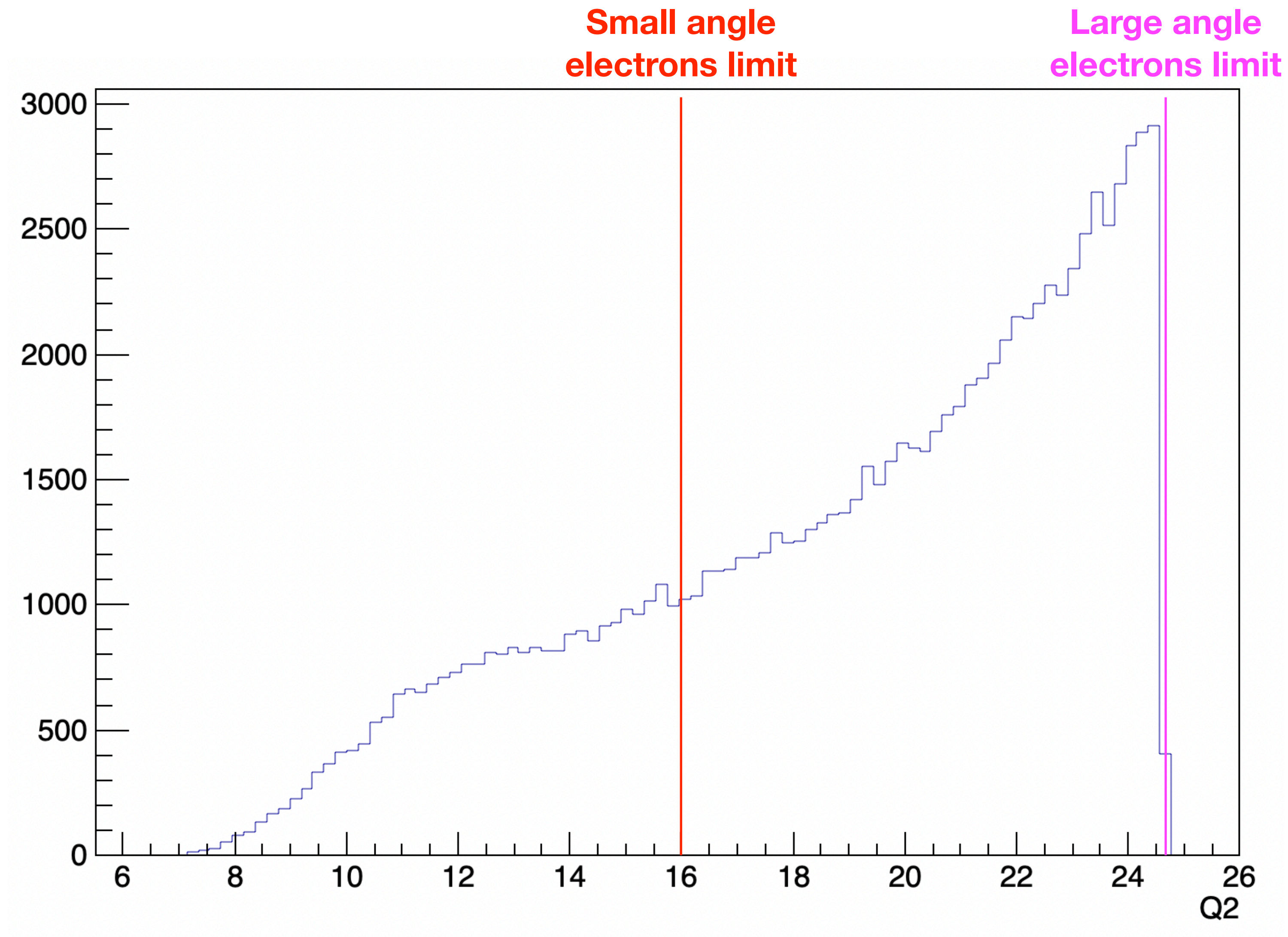
TFFs with SoLID at JLab (J/psi Set-up)

Projections



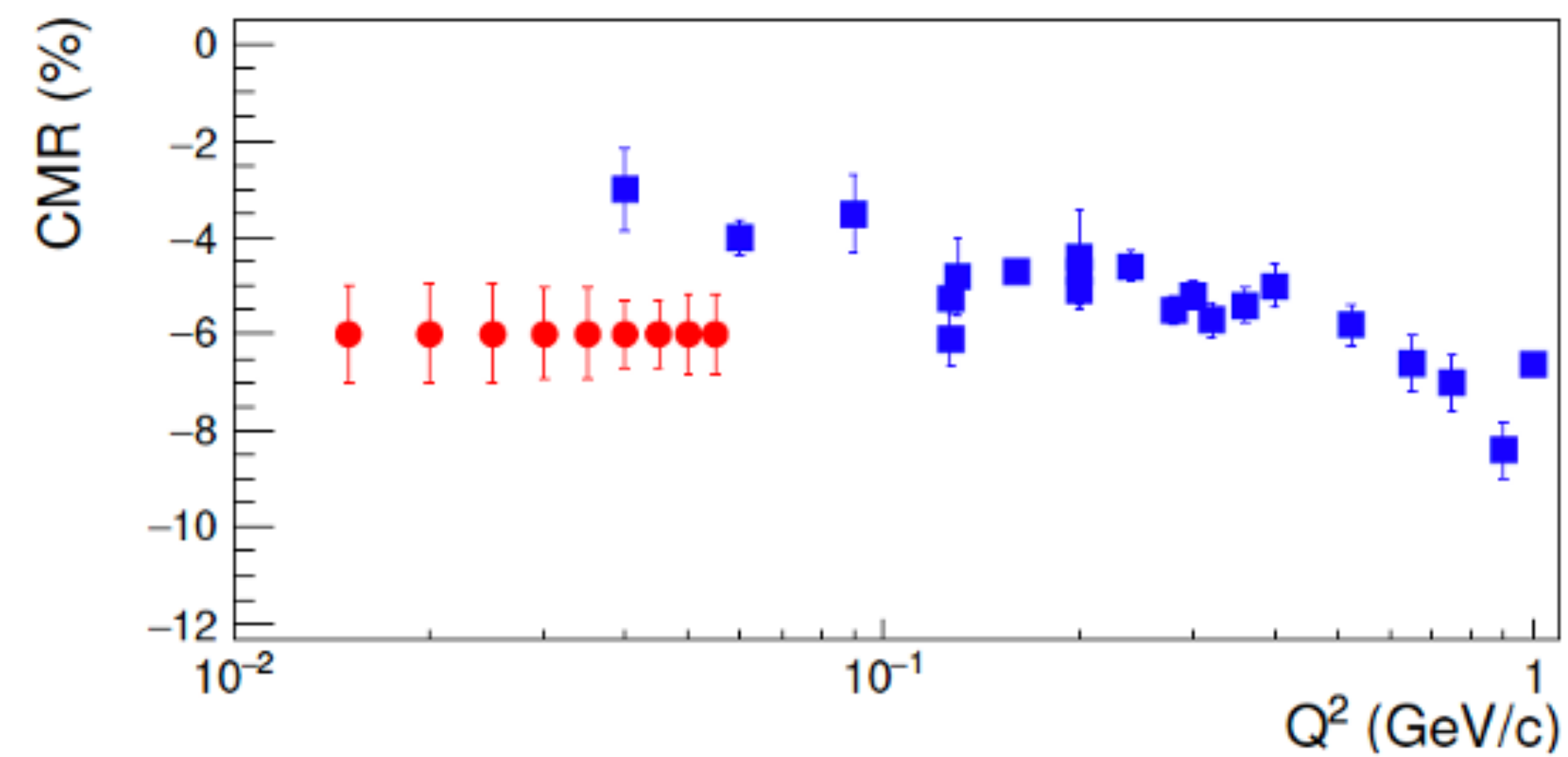
TFFs with SoLID at JLab @ 20 GeV

● Q2 reach



Summary

- The $N \rightarrow \Delta$ TFFs represent a central element of the nucleon dynamics & has been an important part of Jefferson Lab's experimental program (Halls A, B & C)
 - Newly approved experiment will extend these measurements in the low Q^2 region:
 - Test bed for ChEFT calculations
 - High precision benchmark data for the Lattice QCD calculations
 - New constraints and input to the theoretical models
 - Insight to the mesonic-cloud dynamics within a region where they are dominant and rapidly changing
 - Insight to the origin of non-spherical components in the nucleon wave-function
 - Will test if the QCD prediction that CMR & EMR converge as $Q^2 \rightarrow 0$
- $N \rightarrow \Delta$ TFFs enter as an input in scientific problems that extend from hadronic to neutrino physics, and will advance our understanding of the baryon structure & beyond
- At SoLID:
 - We can extend world data for high Q^2 and test pQCD predictions while running parasitic with J/psi



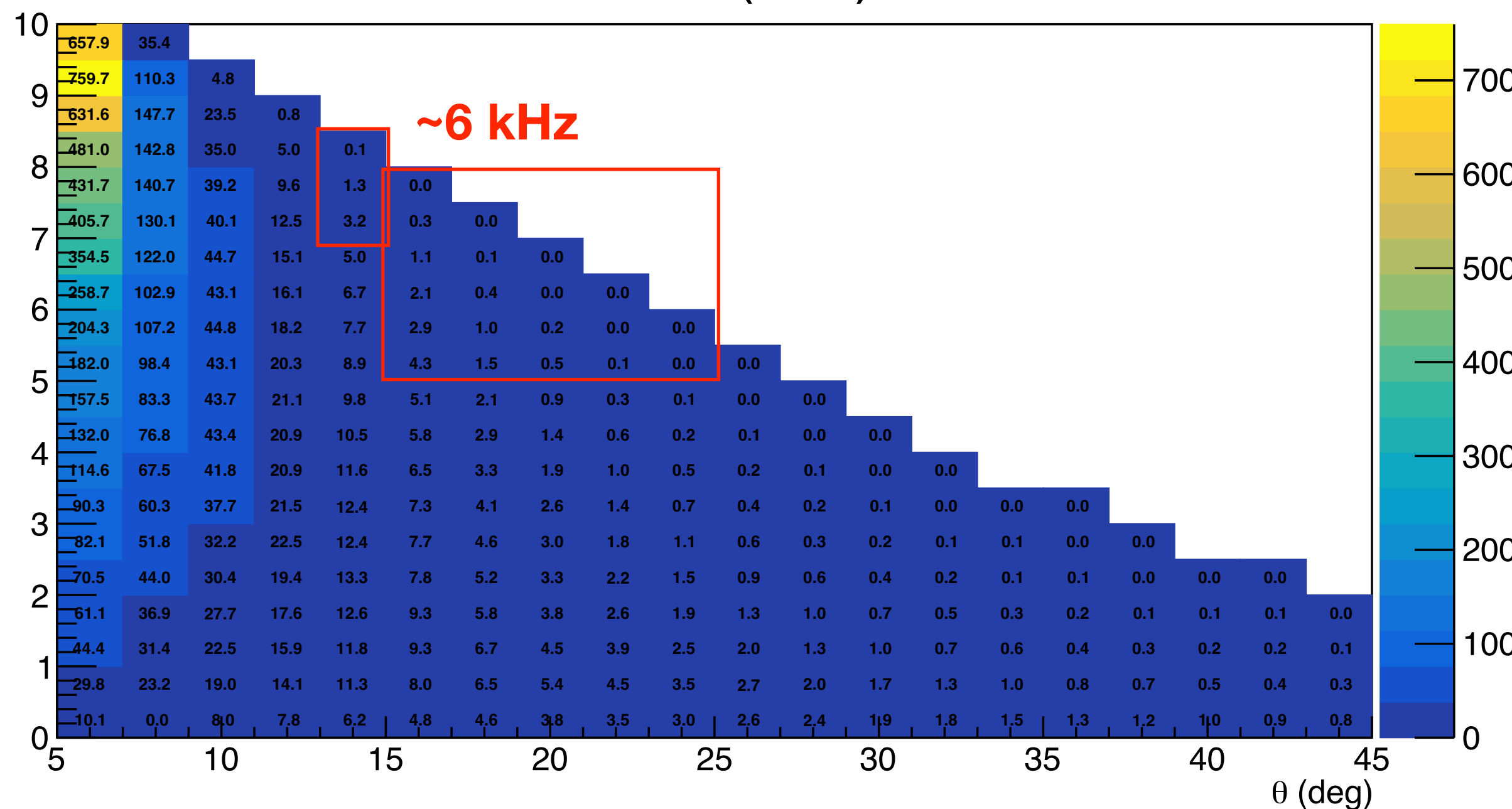
Thank you!

Backup Slides

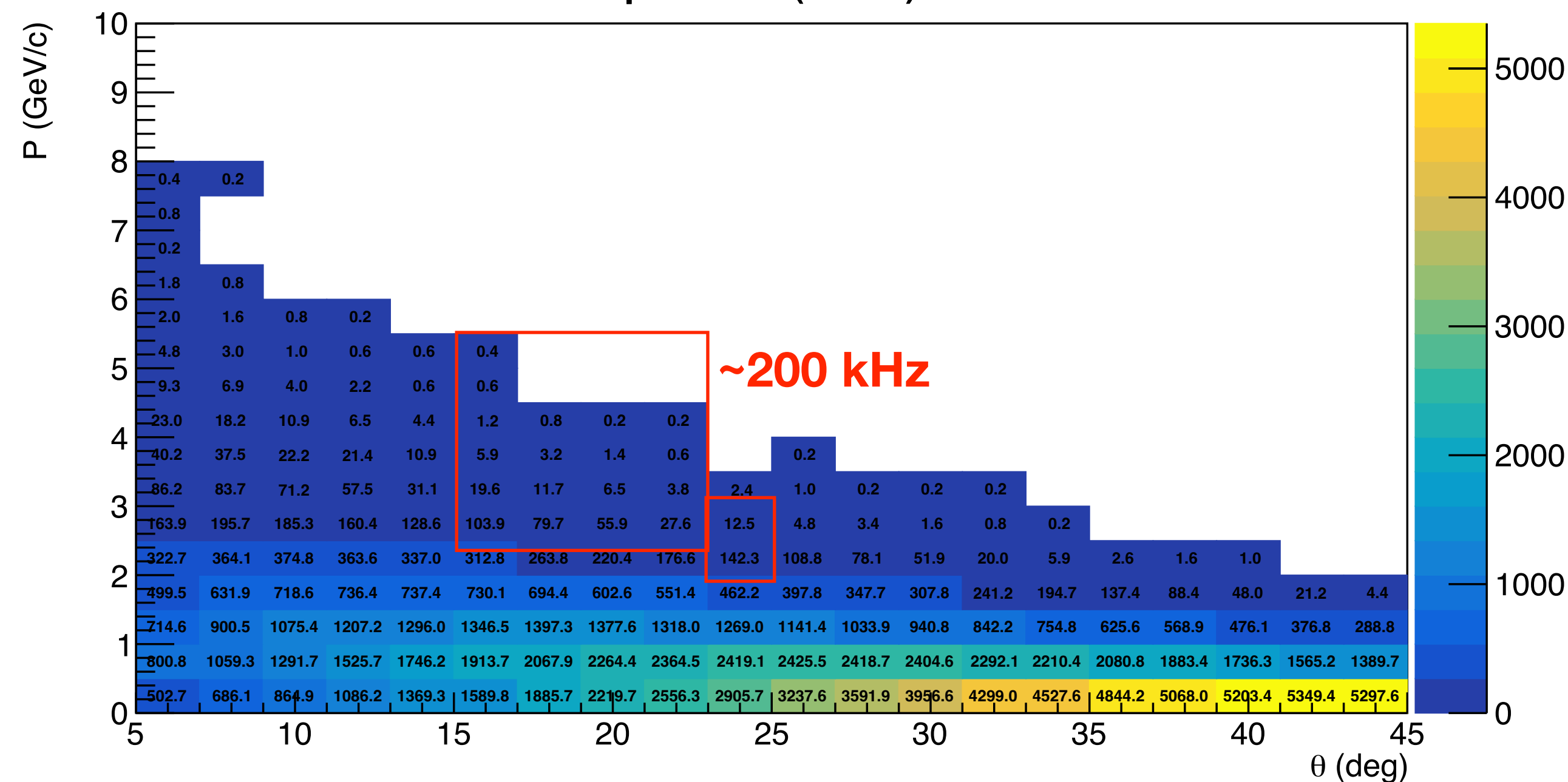
Singles Rates

J/psi Configuration

e^- rate (kHz)



p rate (kHz)

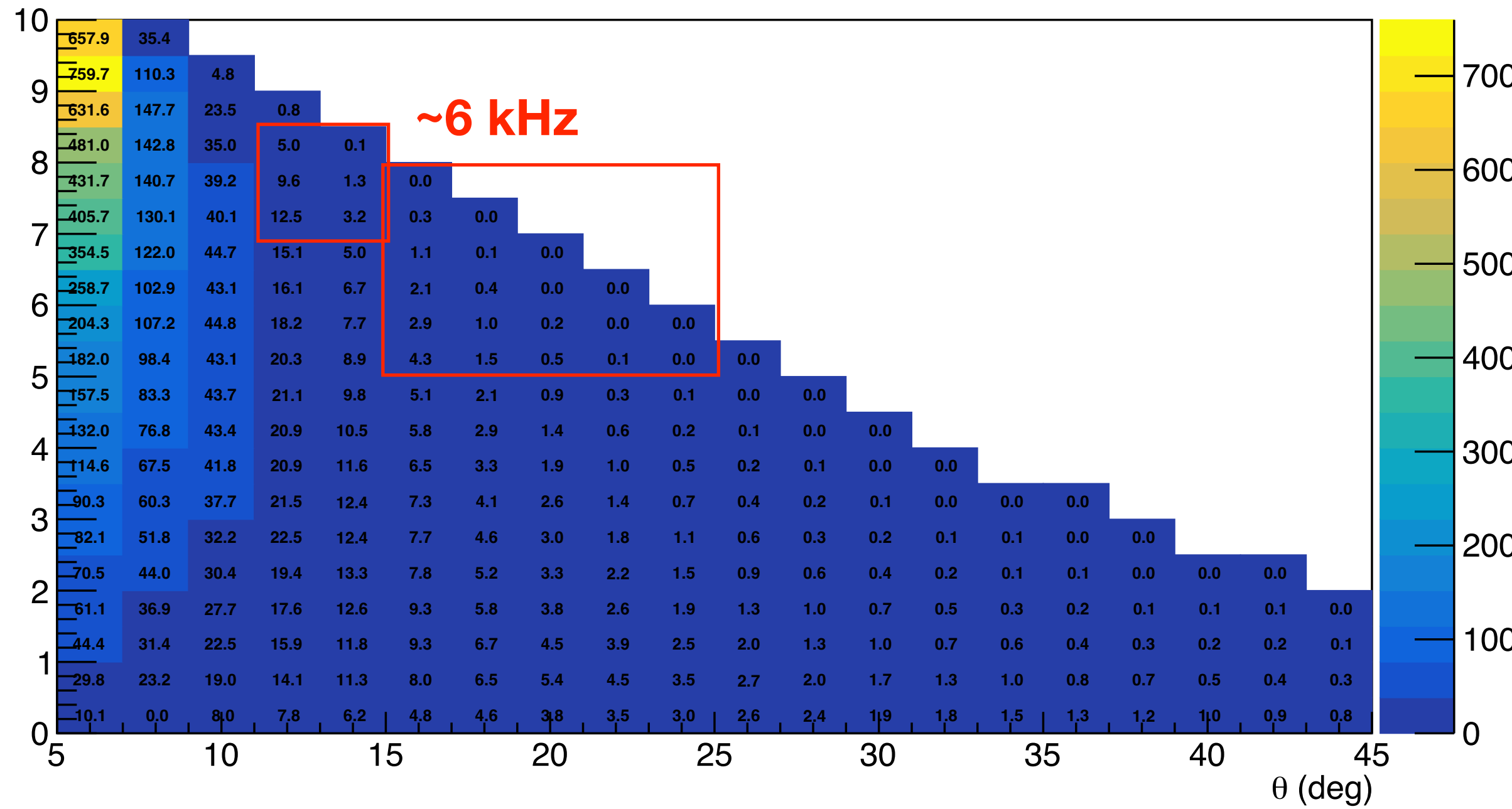


Maximum accidental rate with 100 ns trigger ~ 100 Hz BEFORE subdivision into theta/phi COM bins and missing mass cuts

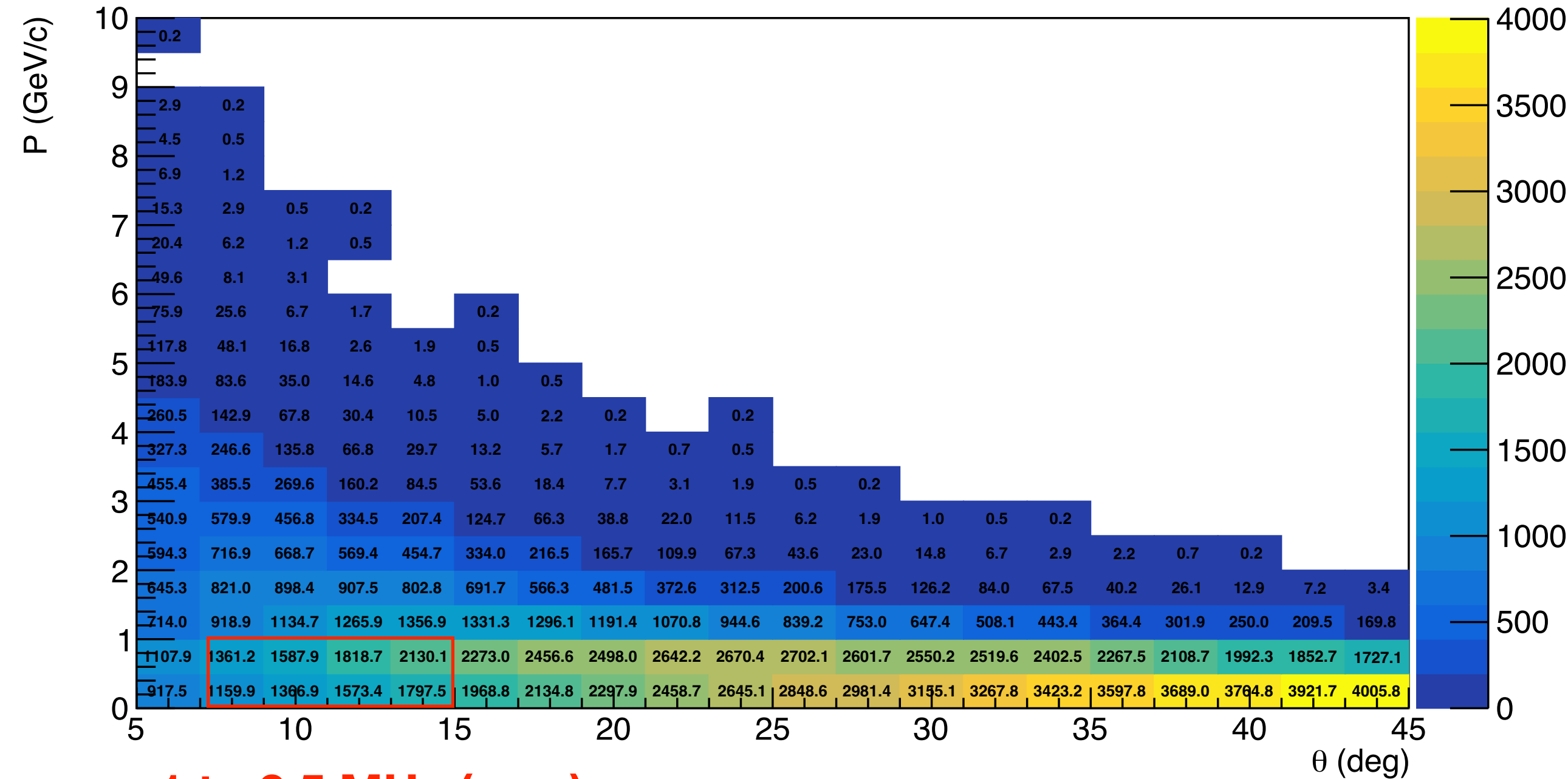
Singles Rates

J/psi Configuration

e^- rate (kHz)



π^+ rate (kHz)



Maximum accidental rate with 100 ns trigger ~ 1.5 kHz BEFORE subdivision into theta/phi COM bins and missing mass